GENETIC AND MOLECULAR CONTROL OF OOCYTE FUNCTION

By

Ashley L. Severance

A DISSERTATION

Submitted to
Michigan State University
in partial fulfillment of the requirements
for the degree of

Genetics-Doctor of Philosophy

2018

ABSTRACT

GENETIC AND MOLECULAR CONTROL OF OOCYTE FUNCTION

By

Ashley L. Severance

A high-quality oocyte will successfully accomplish three critical tasks: segregate chromosomes, reprogram its own genome and that of the incoming sperm to an embryonic state, and support the metabolism and early development of the embryo. This dissertation focuses on two critical determinants of oocyte quality, maintenance of the meiotic spindle and mRNA regulation during meiotic maturation. Chapter 3 of this dissertation focuses on the role of the translational repressor, EIF4EBP1, at the meiotic spindles. I show that blocking EIF4EBP1 phosphorylation, which is normally permissive of translation, disrupts the first meiotic spindle, and that inhibiting Polo-like kinase 1 (PLK1) affects EIF4EBP1 phosphorylation and spindle formation at both meiotic divisions. This exciting result suggests PLK1 as an important regulatory focus for controlling EIF4EBP1 and mRNA translation locally at the spindle, to enable the supply of essential proteins during meiotic maturation. Chapter 4 of this dissertation builds on the theme of understanding maternal mRNA regulation by characterizing the dynamic changes in the pool of mRNAs during oocyte maturation and addresses how this varies with oocyte quality. By comparing maturation changes in the transcriptome between two inbred strains (C57BL/6J and DBA/2J) and F1 hybrids between the two strains (BDF1), I discover differences in maternal mRNA regulation associated with superior BDF1 oocyte characteristics (i.e., oocyte hybrid vigor). This includes differences in regulating mRNAs related to mitochondrial physiology and histone production. I also show that many of the differences

between the three genotypes arise during maturation and thus in the absence of transcription, indicating differences in regulating mRNA degradation. Overall, a combination of processes underlies the differential regulation of maternal mRNA in BDF1 oocytes compared to parental strains. A small amount of transgressive gene expression is seen, but the most prominent mechanisms responsible for differential mRNA regulation in BDF1 oocytes include “blending” (F1 expression levels intermediate between parental expression levels) and additive dominance. Interestingly, up to 25% of the mRNAs differ significantly between genotypes at the MII stage. This includes many proposed markers of oocyte quality, for which mRNAs differential expression between strains exceeded what was reported for differences associated with oocyte quality. Because all three genotypes are fertile, this suggests that single markers may not be reliable indicators of oocyte quality. Overall, these results clearly show that the oocyte utilizes complex regulatory mechanisms at both the meiotic spindles and throughout the ooplasm. This dissertation opens the door for many potential future directions to probe further into understanding these oocyte-specific adaptations. In the future, this research along with other studies could be useful to develop therapies to improve fertility outcomes in both agricultural species and in humans.

For the hero, Hercules.

()()
(‘.’)
( )

ACKNOWLEDGEMENTS

First, I would like to thank my graduate mentor, Dr. Keith E. Latham for letting me join his lab. I have grown more in these past five years under his mentorship that I would have even imagined possible. I would also like to thank my committee members Drs., Jason Knott, Chen Chen, and Kris Chan for their feedback and encouragement throughout the duration of my research. I would like to give a special thank you to our postdoc, Meghan Ruebel, for being a great mentor, mentee, and editing parts of this dissertation. Thank you to all the other Latham Lab members, past and present, who have helped shaped my work. Thank you to Dr. Jennifer Schisa being my mentor during my Master's and encouraging me to pursue my PhD.

I would like to show appreciation to all of my funding sources during my PhD. Specifically, thank you to the Biomolecular Sciences Program at Michigan State University for my assistantship my first year, the Genetics program for my teaching assistantship during my second year, and the National Institute of Health for providing funding to the Latham Lab. I would also like to thank the Reproductive and Developmental Science Program at Michigan State University for appointing me to the RDSP T32 training grant for two years.

Finally, I would like to thank my family and friends for supporting my pursuit of science and believing in me. Thank you to my mom for being patient with a daughter that (apparently) wanted to be in school forever. Thank you to my little brother, John, graduating before me and motivating me to finish. Thank you to my other half, Paulo, for your love and support during my PhD and beyond. Thank you to the best rabbit in the world and my hero, Hercules.

TABLE OF CONTENTS

LIST OF TABLES

LIST OF FIGURES

CHAPTER 1

Introduction

Oocytes are extraordinary. This one cell must accomplish three oocyte-specific vital tasks: deliver a haploid maternal genome, reprogram both parental genomes after fertilization, and support early embryonic development. The oocyte accomplishes all of these essential processes after transcriptional silencing, indicating unique specialization for post-transcriptional control, particularly regulation of mRNA translation and degradation. My dissertation focuses on understanding the control of mRNA translation at the spindle during oocyte meiosis, and the dynamic regulation of maternal mRNA during oocyte maturation.

1.1 Why study the oocyte?

Oocytes follow a unique developmental path. They emerge from primordial germ cells after they colonize the fetal gonad and participate in the formation of ovarian follicles. Oocytes remain arrested in first meiotic prophase for up to decades, depending on species, and must retain the ability to resume and complete meiosis and give rise to a viable embryo. The oocyte undergoes two highly asymmetrical divisions to reduce the chromosome number to haploid while maintaining the largest ooplasmic volume possible. In addition, the oocyte reprograms the both parental genomes and supports early embryonic development until zygotic genome activation. These events are all accomplished during a period of transcriptional quiescence, highlighting the great importance of post-transcriptional regulation in the oocyte. The unique developmental path and specific tasks coupled with great importance of the oocyte to

reproduction heighten the importance of understanding oocyte biology. The ultimate goal of oocyte research is to understand what makes a good egg good, what makes a bad egg bad; i.e., what molecular factors and processes establish oocyte and embryo developmental potential.

1.2 The saga of oocyte meiosis

Although the process of meiotic chromosome segregation is not unique to the oocyte, there are several unique features to oocyte meiosis. This includes two separate oocyte-specific arrest points and asymmetric divisions. Oocytes first arrest in prophase of meiosis I for a prolonged time, which can be years or even decades, depending on the species. Oocytes arrest a second time during metaphase of meiosis II while awaiting fertilization. Oocytes spindles differ greatly from mitotic spindle in that they have several unique modifications to achieve highly asymmetric cell divisions (see Chapter 2). These modifications have allowed the oocyte to increase in overall size during evolution. After fertilization, the oocyte is briefly triploid and must accurately segregate half of the remaining oocyte sister chromatids quickly into the second polar body, to ensure a euploid genome in the embryo.

The spindle is a complex structure that requires many components to form and function correctly. Localized mRNA translation is one possible means of providing these components. EIF4EBP1 is a regulator of cap-dependent translation. When hypophosphorylated, EIF4EBP1 binds to EIF4E and represses cap-dependent translation by blocking formation of the cap-dependent translation initiation complex. In other cells and cellular contexts, this repression is relieved when several upstream kinases phosphorylate specific sites in EIF4EBP1, changing EIF4EBP1 conformation to release it from EIF4E. Phosphorylated EIF4EBP1 is present on mouse

oocyte meiotic spindles (Romasko, Amarnath, Midic, & Latham, 2013), but the importance of this phosphorylation and the upstream kinase responsible have been unknown. The first part of my dissertation revealed two novel discoveries: blocking EIF4EBP1 phosphorylation disrupts the spindle at meiosis I and II and PLK1 is the principal kinase mediating this phosphorylation at both stages. In other cells, PLK1 is responsive to insulin stimulation or is altered during cellular senescence (H. J. Kim, Cho, & Kim, 2013; Shirakawa et al., 2017), both of which are factors that could impact oocyte quality. Overall, the responsiveness of PLK1 to exogenous factors, the effects of these factors on oocyte quality, and the effects of PLK1 inhibition on the spindle, implicate PLK1 as a novel regulatory nexus connecting these exogenous factors to oocyte meiotic spindle formation and function. Future studies providing a greater understanding of the roles of PLK1 and EIF4EBP1 at the oocyte meiotic spindle may offer unique possibilities for therapies to protect oocytes and preserve female fertility.

1.3 The importance of maternal mRNA regulation in the oocyte

The oocyte matures, supports early embryo development, and reprograms maternal and paternal chromatin to an embryonic state during a period of transcriptional quiescence, making post-transcriptional regulation critical to oocyte function. These important cellular processes are temporally regulated to maintain oocyte quality and the developmental potential of the future embryo. To accomplish this, the oocyte regulates the stability, translation, and degradation of the mRNAs in the ooplasm during meiotic maturation. The oocyte uses mRNA regulation to control the expression timing and localization of the encoded proteins. Oocyte mRNAs present at fertilization support changing embryo needs, and are thus crucial

determinants of embryo developmental potential. Since the mRNA population is so important to the oocyte and future embryo, many mRNAs have been identified as putative markers of oocyte quality. But, until we understand how much variation exists naturally between healthy oocytes, the value of any single proposed marker may be in doubt. Furthermore, understanding characteristics of a superior quality oocyte will provide important insights into possible ways to improve the health of other oocytes.

The second half of my dissertation is focused on comparing the oocyte transcriptome during meiotic maturation in two hybrid strains, B57BL/5 and DBA/2, and their F1 offspring (BDF1). Oocytes from BDF1 females display superior phenotypic characteristics including better performance in somatic cell nuclear transfer, in vitro maturation, and better tolerance of in vitro embryo culture. This oocyte 'hybrid vigor' offers a unique opportunity to understand the factors, processes, and pathways that contribute to making a superior oocyte. My work revealed a vast number of differentially expressed genes (DEGs) between the three genotypes and within stage and throughout meiotic maturation, and implicate specific mechanism that may underlie hybrid vigor. After evaluating transgressive gene expression, dominance factors, and intermediate levels of mRNA expression as possible sources of oocyte hybrid vigor, I conclude that the latter two are the main mechanisms responsible. Additionally, I report a key set of mRNAs that are regulated similarly across strains during maturation. These mRNAs could be a useful source of potential biomarkers of oocyte quality that do not vary widely with genotype, and that may be shared across species. This work highlights the dynamic nature of mRNA regulation during oocyte maturation, and suggests that different genotypes may utilize distinct modes of mRNA regulation to achieve fertility. Through the combined study of a

spindle-associated translation regulator, and genetic variation in oocyte transcriptome dynamics, my research provides new insight into the genetic and molecular control of mammalian oocyte function.

CHAPTER 2

Meeting the meiotic challenge: specializations in mammalian oocyte spindle formation

Citation:

Severance, A., Latham, K. Meeting the meiotic challenge: Specializations in mammalian oocyte spindle formation. Molecular Reproduction and Development. March 2018. doi: 10.1002/mrd.22967.

2.1 Abstract

Oocytes uniquely accumulate cytoplasmic constituents to support early embryogenesis. This unique specialization is accompanied by acquisition of a large size and by execution of asymmetric meiotic divisions that preserve precious ooplasm through the expulsion of minimal size polar bodies. While often taken for granted, these basic features of oogenesis necessitate unique specializations of the meiotic apparatus. These include a chromatin-sourced RanGTP gradient that restricts spindle size by defining a spatial domain where meiotic spindles form, acentriolar centrosomes that rely on microtubule organizing centers to form spindle poles, and an actin-based mechanism for asymmetric spindle positioning. Additionally, localized protein synthesis to support spindle formation is achieved in the spindle forming region, whilst protein synthesis is reduced elsewhere in the ooplasm. This is achieved through enrichment of spindle-related mRNAs in the spindle forming region combined with local PLK1-mediated phosphorylation and inactivation of the translational repressor EIF4EBP1. This allows PLK1 to function as an important regulatory nexus through endogenous and exogenous signals can impact spindle formation and function, and highlights the important role that PLK1 may have in maintaining oocyte quality and fertility.

2.2 Introduction

The oocyte is a remarkable cell with two universal roles in reproduction: correct segregation of chromosomes during two successive rounds of meiosis and sustaining viability of the early embryo until transcriptional activation. In order to provide the large macromolecular endowment to the embryo, oocytes manifest enlarged sizes compared to most somatic cells

and undergo asymmetric meiotic divisions that minimize loss of precious ooplasm into polar bodies destined to degenerate. These two properties have major consequences for how oocytes must control spindle formation and function, and specialized mechanisms have arisen for this. This review summarizes these mechanisms and how they relate to understanding the impact of endogenous and exogenous factors on oocyte quality and female mammalian fertility.

Modifications in the use and control of the oocyte cytoskeleton are key components to the specialized meiotic mechanisms of oocytes. Asymmetrical meiotic divisions in oocytes are enabled by modifications of both the microfilament and microtubule components of the cytoskeleton. A modified actin microfilament network positions both first and second meiotic spindles asymmetrically in the oocyte. Additionally, the oocyte regulates microtubule nucleation to restrict spindle size and define the region of the ooplasm where the spindle forms. A chromatin-generated RanGTP gradient organizes microtubules in association with the chromosomes, defining the spatial domain of spindle formation. In some species, another oocyte-specific spindle forming adaptation is the use microtubule organizing centers (MTOCs) to nucleate microtubules at acentriolar spindle poles. This removes the requirement to tether centrioles to opposite sides of the cell cortex, and works with the RanGTP gradient to allow the oocyte to restrict spindle size and position it asymmetrically.

Along with asymmetrical spindle localization comes the need for oocytes to provide spindle-associated proteins to the region where the spindle is forming. A novel hypothesis to account for this is that the oocyte enriches a subset of maternal mRNAs that encode spindle-associated proteins at the spindle-forming region. The key translation inhibitor, EIF4EBP1,

undergoes a dynamic pattern of phosphorylation at the spindle, consistent with localized release of translational inhibition to allow local production of spindle-associated proteins, even while translation diminishes elsewhere in the cell.

It is reasonable to posit that these mechanisms must be robust and work together to ensure successful meiotic progression and chromosome segregation, including successfully completing the first meiotic division followed by rapid progression to the second metaphase with a stable spindle being maintained during MII metaphase arrest. This coordination creates a point where endogenous signals can regulate meiosis, and exogenous insults can disrupt it. Understanding the remarkable solutions that oocytes use to ensure successful spindle formation and function is thus crucial for understanding how a variety of physiology and health-related issues impact oocyte quality and female fertility.

2.3 Define the spindle: spindle position and size restriction by RanGTP and MTOCs

Asymmetrical spindle positioning and oocyte size creates the need for specialized mechanisms of generating a high-quality meiotic spindle in proximity to the condensing chromosomes. This review discusses oocyte specializations to microtubule dynamics with respect to the RanGTP gradient and MTOC functions during meiotic spindle formation.

The RanGTP gradient in oocytes is similar to the RanGTP gradient that forms in mitotic cells, but in oocytes, the RanGTP gradient directs oocyte-specific spindle size restrictions necessary for asymmetric spindle localization, and differences between MI and MII spindle responses to RanGTP gradient perturbations indicate further oocyte-specific differences that remain poorly understood. RanGTP gradient formation begins at the condensed chromatin, and

from there, defines the ooplasmic region where the spindle forms (Kalab, Solc, & Motlik, 2011). The RanGTP gradient also plays a critical role in activating spindle-related microtubule factors (discussed more below) needed during meiotic spindle formation in the absence of centrioles, which oocytes lack.

RanGTP gradient formation is regulated at the condensed chromosomes where the Ran guanosine exchange factor Regulator of Chromosome Condensation 1 (RCC1) binds (J. Dumont et al., 2007a). RCC1 is the guanine nucleotide exchange factor for Ras-Related Nuclear Protein (Ran) that facilitates the exchange of RanGDP for RanGTP. This creates a high concentration of RanGTP at the chromatin, which diffuses away to form a RanGTP gradient (Figure 2.1) (Bischoff & Ponstingl, 1991). During meiotic spindle formation, RanGTP helps nucleate and stabilize microtubules (Kalab et al., 2011). RanGTP induces spindle formation by binding to the inhibitory proteins, Importin-α and -β, and mediating the release of the Importin-bound spindle assembly factors such as TPX2 and NuMA (Gruss et al., 2001; Nachury et al., 2001; Weaver & Walczak, 2015; Wiese et al., 2001). RanGTP regulates over 22 spindle assembly factors during mitosis (Walczak & Heald, 2008). Many of these are also likely regulated by RanGTP during meiosis, but the importance of these spindle assembly factors remains poorly understood in the oocyte (Cavazza & Vernos, 2015). Spindle assembly factors participate in microtubule nucleation, microtubule stabilization, microtubule end protection, transport along microtubules, spindle pole microtubule focusing, γ-tubulin localization, microtubule bundling, microtubule elongation, etc. (Cavazza & Vernos, 2015; Walczak & Heald, 2008). As RanGTP diffuses away, the cytoplasmic RanGAP induces RanGTPase activity, which converts RanGTP back to RanGDP, effectively creating the sink for the RanGTP gradient, and defining where the spindle forms

(Bischoff, Klebe, Kretschmer, Wittinghofer, & Ponstingl, 1994). *Xenopus laevis* egg extract experiments demonstrate that the competence of the RanGTP gradient to stabilize microtubules and support spindle formation rapidly declines over a distance of 20µm from the chromatin (Athale et al., 2008). This acute spatial diminishment in RanGTP concentration is particularly important in the large oocyte, where spindle size must be carefully restricted.

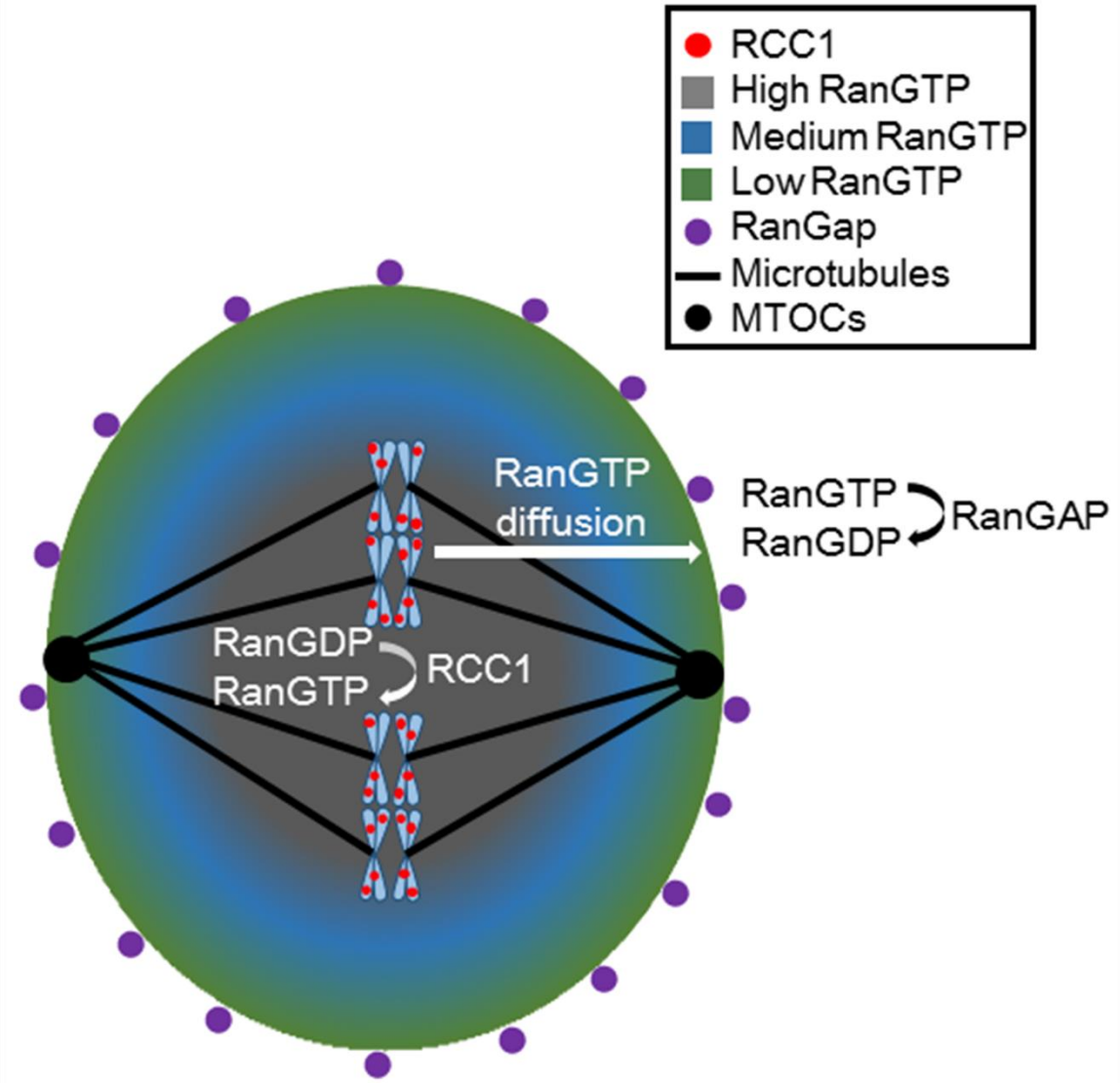

Figure 2.1 RanGTP gradient around MI spindle. At the chromosomes, RCC1 converts RanGDP to RanGTP and diffusion of RanGTP forms the RanGTP gradient. In the cytoplasm, RanGAP converts RanGTP back to RanGDP, setting the boundary for the RanGTP gradient and

In the oocyte, both the MI and MII spindles have a RanGTP gradient but each has varying susceptibility to RanGTP gradient perturbation (J. Dumont et al., 2007a). Loss of the RanGTP gradient from the MI spindle does not impair spindle migration but results in a longer

MI spindle, which leads to extrusion of a larger polar body (J. Dumont et al., 2007a; Schuh & Ellenberg, 2007). During MI spindle movement to the oocyte cortex, the RanGTP gradient persists and is maintained around the migrating spindle (J. Dumont et al., 2007a). In both *Xenopus laevis* and mouse oocytes, MII spindle formation is severely compromised or no clear MII structure forms with loss of the RanGTP gradient (J. Dumont et al., 2007a). However, like the MI spindle, MII spindles forming after loss of the RanGTP gradient do not display defects in spindle localization. In human oocytes, RanGTP gradient inhibition during meiosis I severely impairs microtubule nucleation and MI spindle formation (Holubcova, Blayney, Elder, & Schuh, 2015). The effects of RanGTP gradient loss on human MII spindle formation remains unexplored, and given the different RanGTP MI and MII susceptibilities observed in other species, this exciting inquiry should be completed for human MII spindles. Overall, these studies demonstrate that the RanGTP gradient does not have a role in the spindle migration for either meiotic spindle, but is critical for regulating spindle size. The mechanisms responsible for the different responses of the MI and MII spindles to RanGTP gradient perturbation remain unknown.

It is important to note that there exists a second chromatin-mediated spindle assembly pathway utilized in oocytes called the chromosome passenger complex (CPC) (Bennabi, Terret, & Verlhac, 2016). In *Xenopus* egg extracts, the chromosome passenger complex appears to support microtubule nucleation independently of the RanGTP gradient (Kelly et al., 2007; Sampath et al., 2004). The chromosome passenger complex localizes to the kinetochore-microtubules attachments during meiosis I and II and consists of the Aurora B/C kinase (AURKC, oocyte specific), inner centromere protein (INCENP), Survivin, and Borealin (J. Dumont & Desai,

2012; Ruchaud, Carmena, & Earnshaw, 2007). The chromosome passenger complex promotes microtubule growth from kinetochores because Aurora B phosphorylates and thereby deactivates MCAK and stathmin, microtubule destabilizing proteins (Prosser & Pelletier, 2017). The functional role of the chromosome passenger complex during spindle formation in other organisms remains poorly described.

Mammalian oocytes do not use canonical centrosomes with centrioles during meiotic spindle formation. They instead have oocyte-specific structures called MTOCs that split and coalesce during meiosis to form foci, from which microtubules nucleate (Schuh & Ellenberg, 2007). Oocytes also lack astral microtubules, which in mitotic cells emanate from centrioles during centralized localization of the mitotic spindle (Bennabi et al., 2016). The specialized oocyte MTOC system contributes to the asymmetric localization of the meiotic spindle, and formation of a smaller spindle than would be possible with centrioles anchored to opposite sides of the oocyte cortex. During cell division in other cell types, centrosomes (with centrioles) initially migrate to the opposite sides of the nucleus before nuclear envelope breakdown (NEBD) and microtubules simultaneously grow from these centrosomes toward the chromosomes and cell cortex to form the spindle and anchor the centrosomes to opposite sides of the cell (Tanenbaum & Medema, 2010). In mouse oocytes, MTOC fragmentation near the chromatin is critical to form a smaller meiotic spindle that is not initially tethered to the oocyte cortex (Clift & Schuh, 2015). Before germinal vesicle breakdown (GVBD), oocytes possess approximately three MTOCs in close proximity to the chromosomes. These fragment to form up to 26 smaller MTOCs in a Polo-Like Kinase 1 (PLK1)-dependent mechanism (Clift & Schuh, 2015) (Figure 2.2). Next, Bicaudal D Homolog 2 (BICD2)-anchored dynein elongates the fragmented

MTOCs to wrap around the germinal vesicle (Clift & Schuh, 2015). After GVBD, Kinesin Family Member 11 (KIF11) further fragments the stretched MTOCs. Then, the fragmented MTOCs coalesce into two foci on opposite sides of the chromosome cluster, initiating bipolar spindle formation (Clift & Schuh, 2015). Newly polymerized microtubules in the meiotic spindle are bundled and stabilized by clathrin heavy chain (CLTC) protein during meiotic maturation (Z. Han et al., 2010; Holzenspies et al., 2010). Conflicting results exist in the literature as to whether human oocytes use MTOCs to nucleate microtubules during meiotic spindle formation. Several studies have reported the presence of MTOCs in human oocytes (Battaglia, Goodwin, Klein, & Soules, 1996; Battaglia, Klein, & Soules, 1996; Pickering, Johnson, Braude, & Houliston, 1988). But, this idea has been challenged by a large human oocyte study that detected no γ-tubulin or pericentrin positive MTOCs in human oocytes (Holubcova et al., 2015). Determining whether human oocytes possess MTOCs, and the similarity of their protein makeup could indicate which model organism(s) most closely model microtubule dynamics of the human meiotic spindle.

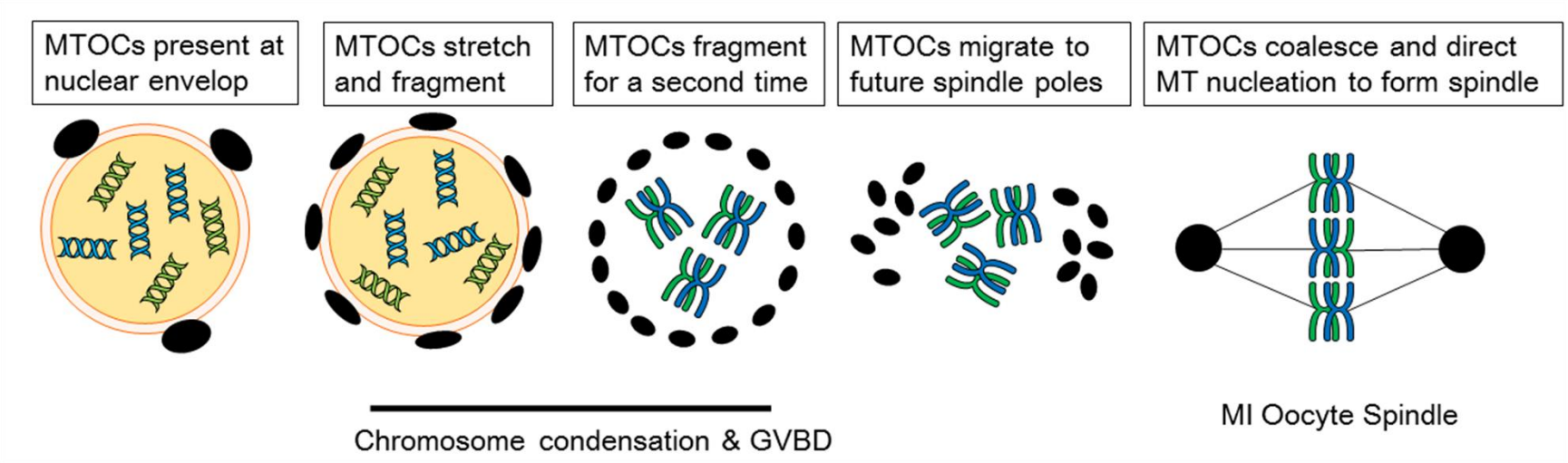

Figure 2.2 Oocyte Microtubule Organizing Centers (MTOCs) fragment, migrate, and coalesce to direct meiotic spindle formation. GV oocytes possess few MTOCs that are localized to the nuclear envelope. These MTOCs fragment and stretch around the GV. After germinal vesicle breakdown (GVBD), the MTOCs fragment a second time, and then, migrate to opposite sides of the chromosomes, where the spindle poles will form. Lastly, the MTOCs coalesce to form the spindle poles and direct microtubule nucleation and spindle formation.

2.4 Move the spindle: actin-mediated spindle migration

In addition to having restricted sizes, both meiotic spindles must be asymmetrically positioned in the oocyte by being translocated (MI) or formed (MII) near the oocyte cortex on one side of the oocyte. This asymmetrical localization ensures maximum retention of the ooplasmic endowment during polar body extrusion. It is enabled by an oocyte-specific modification of the actin cytoskeleton. The MI spindle forms slightly off-centered in the middle of the oocyte (Maro & Verlhac, 2002; Verlhac, Lefebvre, Guillaud, Rassinier, & Maro, 2000). Shortly before first polar body extrusion, the MI spindle is moved by actin to the cell cortex (Verlhac et al., 2000). Coordinated nucleation within two fractions of F-actin, cytoplasmic and cortical, allows the MI spindle to translocate from the center of the cell to the cortex (Figure 2.3). The cytoplasmic fraction of F-actin is nucleated by Formin-2 and Spire1/2, whereas, the cortical F-actin fraction thickens under the control of Arp2/3 (Almonacid, Terret, & Verlhac, 2014; Chaigne et al., 2013; Leader et al., 2002; Pfender, Kuznetsov, Pleiser, Kerkhoff, & Schuh, 2011; Schuh & Ellenberg, 2008; Yi et al., 2013). These two actin fractions connect the cortex to the spindle and result in greater density of F-actin extending from the cell cortex to the closer spindle pole. These F-actin attachments to each spindle pole results in greater Myosin II-mediated pulling forces on one spindle pole and this determines the direction in which the spindle will migrate to reach the cortex (Chaigne et al., 2015; Schuh & Ellenberg, 2008). Upon arrival at the oocyte cortex, the MI spindle is already oriented perpendicular to the oocyte cortex, and therefore, no rotation need occur prior to first polar body extrusion.

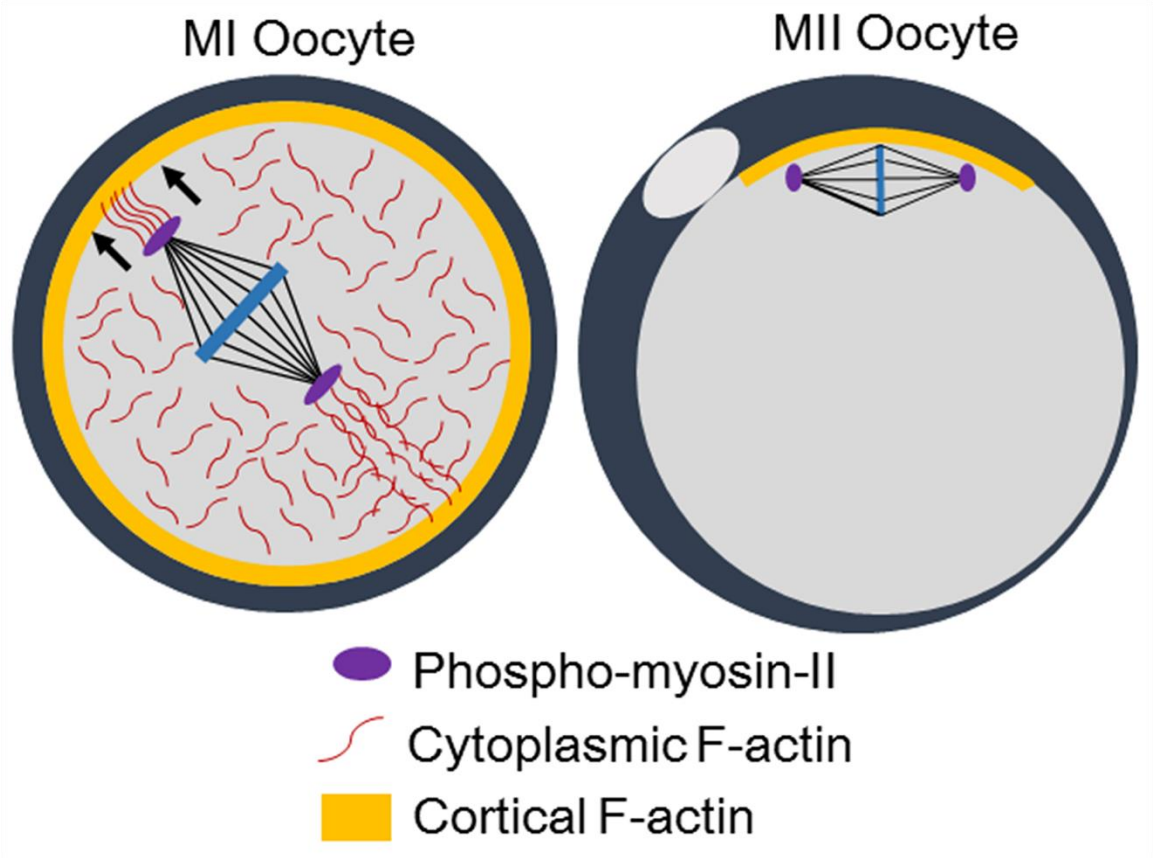

Figure 2.3 The actin cytoskeleton controls MI spindle migration and MII spindle tethering to the oocyte cortex. MI oocyte: MI spindle forms slightly off-centered. The different spindle pole-to-cortex distances result in unequal phospho-myosin-II pulling forces on actin and the spindle migrates towards the cortex in the direction of the closer spindle pole. MII oocyte: The small MII spindle forms in close proximity to the cortex where first polar body extrusion occurred. The actin cytoskeleton tethers it tightly to the oocyte cortex.

In contrast to the MI spindle, the oocyte MII spindle forms at the oocyte cortex near the location at which first polar body extrusion occurred. In mice, the MII spindle forms parallel to the cortex and is anchored there by the cortical actin cytoskeleton, which is partially regulated by a locally high RacGTP concentration (Zhu et al., 2003). RacGTP enrichment at the cortex is initiated during MI and is further promoted during MII by the proximity of the chromatin to the oocyte cortex (Halet & Carroll, 2007). In humans, the MII spindle forms in close proximity to the

cortex, but the spindle angle appears not important, because MII oocytes with different initial spindle angles have equal developmental competence (Moon et al., 2003). As with the MI spindle, MII spindle localization is also carefully controlled by the pulling action of Myosin II and actin nucleation by the Arp2/3 complex but MII also uses the cortically enriched Ezrin/Radixin/Moesin (ERM) family of proteins to assist in anchoring the MII spindle to the oocyte cortex (Larson et al., 2010; Yi et al., 2011). One additional role of the cortical microfilament network in mouse oocytes is that it rotates the cortex-anchored MII spindle 90^{o} immediately after fertilization, bringing the spindle perpendicular to the cortex. This is is necessary for second polar body extrusion (Zhu et al., 2003). RhoA, a small GTPase, is required to organize the microfilament network for spindle rotation (Zhong, Huo, Liang, Chen, & Sun, 2005). The calcium/CaM/CaMKII pathway is also critical to MII spindle rotation, although the exact role it plays in spindle rotation remains elusive (Ai et al., 2008).

2.5 Supply the spindle: role of localized translation in meiotic spindle formation

The oocyte is a large cell, and with that size comes a need to ensure protein availability at specific subcellular locations to support specialized functions. Additionally, protein synthetic activity can vary with subcellular location. The oocyte manifests several specialized features to provide proteins required for spindle formation and function.

After a prolonged period of meiotic arrest, oocyte growth, and acquisition of meiotic competence, oocytes respond to an ovulatory stimulus by undergoing GVBD, progression through the first meiotic division, and a prolonged arrest at the second metaphase. After fertilization, the second meiotic division is completed and embryos initiate development.

Oocytes are transcriptionally silent from prior to GVBD until some number of hours and cleavage divisions after fertilization, according to species (Bouniol-Baly et al., 1999; De La Fuente & Eppig, 2001). The transition from non-surrounded to surrounded nucleolus configurations signifies transcriptional silencing driven by chromatin modifications (Debey et al., 1993). At the molecular level, histone deacetylation is key for meiotic spindle formation by allowing spindle forming factors to associate with the nucleosomes (Balboula, Stein, Schultz, & Schindler, 2014; Gu, Wang, & Sun, 2010). The lack of new transcripts available to the oocyte highlights the critical importance of mRNA stability, polyadenylation, selective and timed translation, and degradation to provide for the overall control of cell functions and production of proteins at specific times. Maturation-promoting factor (MPF; a complex of CDK1/CDC20 and Cyclin b) is activated upon meiotic resumption and phosphorylates cytoplasmic polyadenylation element binding protein (CPEB), triggering CPEB degradation and its release from mRNAs, which thereby become accessible for polyadenylation and translation (Sha et al., 2017). Other cis-regulatory elements provide positive and negative control of translation in oocytes and early embryos (Potireddy, Midic, Liang, Obradovic, & Latham, 2010a). Some maternal mRNAs possess an internal ribosome entry site (IRES) and can be translated without the need for polyadenylation (Hellen & Sarnow, 2001). The crucial roles of these translational control mechanisms in the temporal control of development, including during mammalian oocyte maturation and early development mechanisms for spatial regulation of mRNA translation in mammalian systems, have not been thoroughly studied.

Localized mRNAs function as crucial developmental determinants in diverse species such as amphibians, insects, and nematodes. The importance of localized mRNAs as determinants in

mammalian oocytes is still unclear but generally is not considered to be as essential as in these other organisms (Becalska & Gavis, 2009; Ciemerych, Mesnard, & Zernicka-Goetz, 2000; Shulman, Benton, & St Johnston, 2000). But, mRNA localization to the spindle forming region does exist in oocytes, and may be key for spindle formation and function, in mammals and other species such as amphibians. One study reported that mRNAs are localized to mitotic spindle microtubules (Blower, Feric, Weis, & Heald, 2007), and mitotic-spindle proteomics revealed over 400 spindle-enriched proteins remaining after removal of DNA-associated proteins (Bonner et al., 2011; Sauer et al., 2005). CPEB-mediated translational control is reported as important for mitotic spindle integrity (Groisman et al., 2000). For oocytes, cDNA array analysis reveals mRNAs enriched in the spindle forming region including the *Mis18a* mRNA; MIS18 protein is also confirmed to be enriched on the MII spindle (Romasko et al., 2013). In addition, the presence of phospho-S6 kinase, a marker of active translation, on the meiotic spindle poles indicates active translation at the meiotic spindle (Blower et al., 2007; Romasko et al., 2013). These observations are consistent with the hypothesis that mRNAs encoding spindle-associated proteins are localized to the spindle region and may be translated to support spindle formation and function. An alternate hypothesis that mRNA localization to the spindle facilitates equal cytoplasmic segregation is less relevant to oocytes as compared to mitotic cells, because ensuring ooplasm segregation to the polar body would be counter-productive. If mRNAs enriched at the meiotic spindle provide for local production of required proteins, it is expected that translation of those mRNAs could be regulated, and could provide for an additional means of coordination of spindle formation, function and meiotic progression with other cellular events and processes.

One means of regulating spindle-enriched mRNAs involves local regulation of the translation inhibitor eukaryotic translation initiation factor 4E binding protein, EIF4EBP1. EIF4EBP1 is a 12kDa regulatory protein that, when hypophosphorylated, binds to EIF4E and blocks formation of the translation pre-initiation complex by preventing the EIF4E and EIF4G interaction (T. A. Lin et al., 1994; Pause, Belsham, et al., 1994a). Unphosphorylated EIF4EBP1 binds with a higher affinity to the same region of EIF4E as EIF4G, preventing EIF4E-EIF4G interaction at the 5' mRNA m7G cap, thereby inhibiting cap-dependent translation (Hughes et al., 1999). The phosphorylation of five residues in EIF4EBP1 (T37, T45, S64, S69, and S111), which are positioned on either side of the binding domain (residues 53-59), alter its EIF4EBP1 affinity for EIF4E (Fletcher et al., 1998). In some cell types, a hierarchy of EIF4EBP1 phosphorylation events occurring in a specific temporal sequence controls the release of EIF4EBP1 from EIF4E. EIF4EBP1 phosphorylation has been studied in interphase cells in response to insulin stimulation or nutrient deprivation (Acosta-Jaquez et al., 2009; Gingras et al., 1999), and in mitotic cells (Heesom, Gampel, Mellor, & Denton, 2001). The order of site phosphorylation and the upstream kinase(s) mediating the phosphorylation events varies with cell-type, cell-cycle stage, and cell-stimulation state. During insulin stimulation or nutrient restriction, for example, MTOR (mammalian target of rapamycin) phosphorylates EIF4EBP1 first at T36 and T45, and then CDK1 phosphorylates EIF4EBP1 at T69 and S64, enabling release of eIF4E from EIF4EBP1 (Acosta-Jaquez et al., 2009; Gingras et al., 1999; Heesom et al., 2001). Also in response to insulin stimulation, ATM (ataxia telangiectasia mutated) phosphorylates EIF4EBP1 at S111 (D. Q. Yang & Kastan, 2000). PLK1 and CDK1 are implicated as the primary kinases that phosphorylate EIF4EBP1 in synchronized mitotic cell lines. During mitosis, CDK1,

not mTOR, phosphorylates EIF4EBP1 T36 and T45, followed by T69 and S64 (Heesom et al., 2001; M. Shuda et al., 2015). PLK1 phosphorylates human EIF4EBP1 at S112 (human residues are number one higher than mouse) at the mitotic spindle poles (Shang et al., 2012). The effects of phosphorylation at some of these phosphorylation sites (e.g., EIF4EBP1-S111) have not been fully explored.

During meiotic maturation in the oocyte, the rate of protein synthesis decreases (Schultz, LaMarca, & Wassarman, 1978b), so that a localized increase in production of particular proteins requires a mechanism to promote mRNA translation locally. In contrast to CPEB-mediated regulation, there is a strong temporally and spatially dynamic pattern of EIF4EBP1 phosphorylation at the both stages of meiotic spindles in mouse oocytes (Romasko et al., 2013; Severance & Latham, 2017). This suggests an important role for EIF4EBP1 in meiotic spindle formation and function related to its only known function of translational control (Romasko et al., 2013; Severance & Latham, 2017; Susor et al., 2015a). An initial study reported that treatment with 4EGI, which binds EIF4E to inhibit IEF4G binding and enhances EIF4EBP1 binding, results in an increase in the percentage of MI oocytes with lagging chromosomes and abnormal MI spindle formation (Susor et al., 2015a). A second study confirmed the finding that that 4EGI treatment results in a greater number of lagging chromosomes during MI spindle formation but also shows that 4EGI treatment results in a decrease in the average β-tubulin fluorescence intensity on the MI spindle (Severance & Latham, 2017). This indicates that EIF4EBP1 phosphorylation is important during formation and organization of the oocyte MI spindle. A series of studies employing kinase inhibitors identified the key kinases controlling EIF4EBP1 phosphorylation at mouse oocyte spindle poles. Inhibition with mTOR, ATM, and PLK1

reveals that PLK1 is the principal mediator of EIF4EBP1-P-S64 and -S111 phosphorylation at MI and MII meiotic spindles. PLK1 is only known to phosphorylate EIF4EBP1 at S111. Phosphorylation on S64 is most likely mediated indirectly by PLK1 through interactions with CDK1. CDK1 could not be directly studied in oocytes using this approach, because it is essential for GVBD during MI and maintenance of the meiotic arrest at MII (W. I. Jang, Lin, Lee, Namgoong, & Kim, 2014; Phillips et al., 2002; Saskova et al., 2008). The only other kinase which phosphorylates EIF4EBP1 at S64 (mTOR) was minimally involved, as mTOR inhibition had little effect on EIF4EBP1 phosphorylation or spindle structure. Interestingly, PLK1 and CDK1 are also the primary regulators of EIF4EBP1 phosphorylation during mitosis, indicating a role for PLK1 and CDK1 that is shared between both mitotic and meiotic divisions. It remains unknown if the PLK1 and CDK1 achieve this by maintaining the phosphorylation of EIF4EBP1 molecules that are stably tethered to the spindle, or continually phosphorylate EIF4EBP1 subsequent to protein turnover. The importance of EIF4EBP1 phosphorylation is incorporated into an overall model showing the importance of localized translation at the meiotic spindle (Figure 2.4).

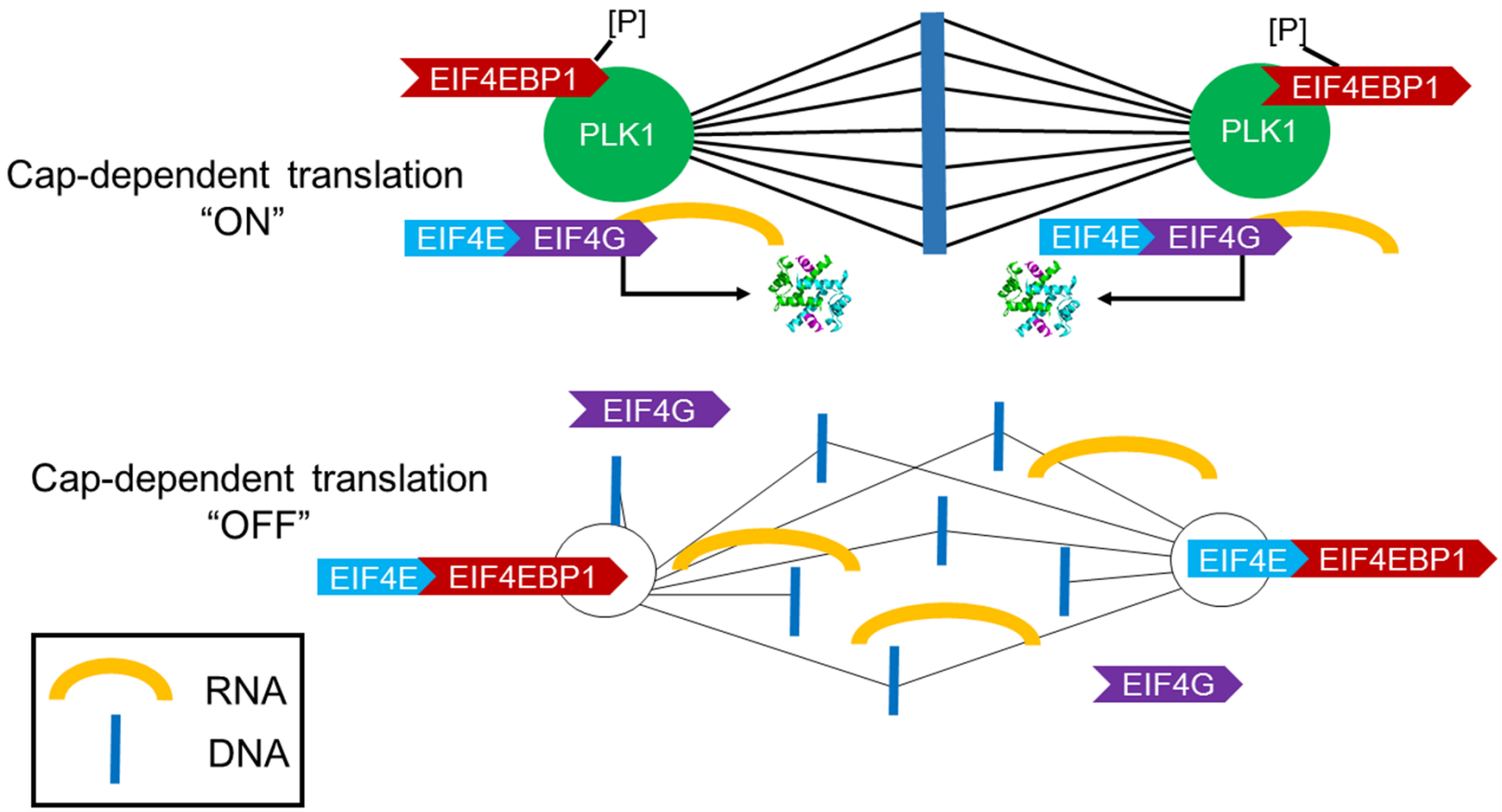

Figure 2.4 Model of cap-dependent translation regulation at the meiotic spindle. Top: PLK1 maintains EIF4EBP1 phosphorylation at the meiotic spindle poles, preventing or releasing EIF4EBP1 binding to EIF4E. Therefore, EIF4E and EIF4G are bound, forming the cap-dependent initiation complex and activate translation of mRNAs enriched at the meiotic spindle. Bottom: When PLK1 is lost from the spindle, EIF4EBP1 phosphorylation is also lost. EIF4EBP1 binds to EIF4E in place of EIF4G and cap-dependent translation is blocked. The poor supply of essential proteins to the spindle structure causes a variety of spindle defects on both meiotic spindles. These defects include a decrease in β-tubulin intensity on the MI spindle, and this is illustrated in the bottom figure as thinner black lines. Chromosome congression defects shown were only noted on MI spindles.

2.6 Meiotic spindle susceptibility to exogenous and endogenous insults

Not only is PLK1 an important regulator of meiotic MI and MII spindle formation, but it is also highly responsive to exogenous and endogenous signals. Although first discovered as an important cell cycle regulator, PLK1 regulates the DNA damage response system in cells and can halt the cell cycle while DNA damage is repaired (L. Wang, Guo, Fisher, Liu, & Peng, 2015). Insulin stimulation increases PLK1 levels in pancreatic islet cells, and this response is blunted in diabetic patients (Shirakawa et al., 2017). In obese non-diabetic mice, *Plk1* and other genes are upregulated to mediate β-cell mass expansion, a mechanism used by obese animals as a means to compensate for insulin resistance and prevent diabetes (Davis et al., 2010).

The role of PLK1 in responding to exogenous and endogenous signals is of particular interest in the oocyte, as many of the stimuli to which PLK1 is responsive, such as insulin, also adversely affect oocyte quality and fertility (Shirakawa et al., 2017). Both maternal diabetes and obesity negatively affect oocyte quality by disrupting metabolism, redox state, and meiotic spindle formation, and can lead to early miscarriage and congenital defects (Farrell, Neale, & Cundy, 2002; Greene, 1999; Reynolds, Boudoures, Chi, Wang, & Moley, 2015; Q. Wang et al., 2009). Expressed throughout meiotic progression, PLK1 promotes meiotic progression and is needed for high-quality meiotic spindle formation (Pahlavan et al., 2000; Solc et al., 2015a). Overall, the important role of PLK1 in oocyte meiosis, its responsiveness to exogenous and endogenous signals, and the known adverse effects of these signals on meiotic spindle formation and oocyte quality implicate PLK1 as an important point of regulation coupling downstream oocyte quality to upstream signals.

2.7 Concluding remarks

The oocyte must artfully balance the need to reduce faithfully chromosome number to haploidy while maintaining the maximum amount of ooplasm to support embryogenesis. To achieve this, the oocyte modifies in multiple ways the mechanisms that create and regulate the spindles of both meiotic divisions, providing for asymmetric localization and size restriction (Severson, von Dassow, & Bowerman, 2016). Additional oocyte-specific mechanisms also arise to support spindle formation and function with localized mRNAs and localized protein synthesis. These modifications ensure correct spindle formation and chromosome segregation in a manner that is compatible with large size and macromolecular endowment of the oocyte. While this system usually results in haploid oocytes with plentiful ooplasm, it is highly prone to errors, and the rates of aneuploidy in oocytes can be high even in young, healthy females (Hunt & Hassold, 2008). The incident of aneuploidy increases further during sub-optimal fertility conditions, such as poor maternal health. The causes of chromosome segregation defects in mammalian oocytes have been difficult to discern, but data reviewed here implicate PLK1 as a critical regulatory nexus connecting these exogenous and endogenous signals to the spindle formation, maintenance, and function in the oocyte. Among other potential roles, PLK1 regulates localized translation of spindle-enriched mRNAs by phosphorylating and thereby inhibiting the translational repressor EIF4EBP1. A careful exploration of PLK1 downstream targets and the signaling pathways that are activated in response to maternal health problems, such as obesity or diabetes, could provide new approaches to enhancing oocyte quality and fertility and reducing aneuploidy in these affected patients.

CHAPTER 3

PLK1 regulates spindle association of phosphorylated eukaryotic translation initiation factor 4E binding protein and spindle function in mouse oocytes

Citation

Severance, A.L., Latham, K.E. PLK1 regulates spindle association of phosphorylated eukaryotic translation initiation factor 4E binding protein, and spindle function in mouse oocytes. American Journal of Physiology-Cell Physiology. August 2017. https://doi.org/10.1152/ajpcell.00075.2017.

3.1 Abstract

Oocyte meiotic spindles are associated with spindle-enriched mRNAs, phosphorylated ribosome protein S6, and phosphorylated variants of the key translational regulator EIF4EBP1, consistent with translational control of localized mRNAs by EIF4EBP1 in facilitating spindle formation and stability. Using specific kinase inhibitors, we determined which kinases regulate phosphorylation status of EIF4EBP1 associated with meiotic spindles in mouse oocytes, and effects of kinase inhibition on chromosome congression and spindle formation. Neither ATM nor mTOR inhibition significantly affected phosphorylation status of spindle-associated EIF4EBP1 at the phosphorylation sites examined. Spindle-associated phospho-EIF4EBP1, spindle formation, and chromosome congression were strongly disrupted by PLK1 inhibition at both MI and MII. In addition, direct inhibition of EIF4EBP1 via 4EGI led to spindle defects at MI, indicating a direct role for EIF4EBP1 phosphorylation in meiotic spindle formation. PLK1 also regulated microtubule dynamics throughout the ooplasm, indicating likely coordination between spindle dynamics and broader ooplasm cytoskeletal dynamics. Because diverse upstream signaling pathways converge on PLK1, these results implicate PLK1 as a major regulatory nexus coupling endogenous and exogenous signals via EIF4EBP1 to the regulation of spindle formation and stability.

3.2 Introduction

Oocytes accumulate a large store of maternal mRNA, much of which is stored in an inactive form and then translationally recruited in a temporally regulated manner to produce different proteins at different times once oocyte transcription has ceased (Latham, Garrels, Chang, & Solter, 1991; Potireddy, Amarnath, & Latham, 2013; Potireddy, Midic, Liang, Obradovic, & Latham, 2010b). In some species, spatial localization of mRNA also contributes to localized production of proteins that direct embryo cell fate specification (Zhou & King, 2004). Mammalian oocytes, however, are not known to localize mRNAs for translation. One exception is at the oocyte spindle, around which certain mRNAs are enriched at second meiotic metaphase (MII) (Romasko et al., 2013). An RNA-rich domain and translational hotspots are also seen around the chromosomes after nuclear envelope breakdown following the resumption of meiosis (Susor et al., 2015b). *Xenopus* oocyte spindles are also enriched for mRNAs, including mRNAs that encode proteins known important to spindle formation and function (Blower et al., 2007).

In addition to RNAs, proteins and phosphorylated variants of proteins are enriched at spindles (Romasko et al., 2013). Phosphorylated ribosomal protein S6, a marker of active mRNA translation, is present around condensing chromosomes and on MII spindles in mouse oocytes (Romasko et al., 2013). Phosphorylated variants of eukaryotic translation initiation factor 4E binding protein one (EIF4EBP1), a global inhibitor of cap-dependent RNA translation that is inactivation by phosphorylation, are enriched on oocyte spindles in a temporally and spatially dynamic manner (Romasko et al., 2013).

Because EIF4EBP1 binding to EIF4E and repressing cap-dependent mRNA translation (Clark et al., 1996) is the only known function of EIF4EBP1, and because EIF4EBP1 phosphorylation releases EIF4E to allow formation of the cap-dependent translation initiation complex, the above observations have been interpreted collectively to indicate ongoing translational control of spindle-associated mRNAs by EIF4EBP1 phosphorylation to facilitate spindle formation and stability (Romasko et al., 2013). Consistent with this model, injecting GV oocytes with a dominant negative EIF4EBP1 variant causes spindle defects at the MII stage (Jansova et al., 2017). This provides a powerful means by which spindle formation and function could be controlled by and coordinated with cell cycle progression and other exogenous and endogenous signals, and by which disruptions in the regulation could lead to aneuploidy. Understanding the mechanisms that regulate EIF4EBP1 phosphorylation at the spindle should thus reveal key insight into mechanisms that enable the formation and ovulation of high quality oocytes.

In somatic cells, EIF4EBP1 phosphorylation is regulated by several upstream kinases in conjunction with cell cycle progression, hormone stimulation, and nutrient deprivation. Phosphorylation of EIF4EBP1 at four sites increases in response to insulin stimulation and at least two of these sites are phosphorylated by the mechanistic target of rapamycin (mTOR) (Gingras et al., 1999; Heesom, Avison, Diggle, & Denton, 1998). Also during insulin stimulation, the Ataxia telangiectasia mutated (ATM) kinase phosphorylates EIF4EBP1 at S111 (D. Q. Yang & Kastan, 2000). The Polo-Like kinase 1, (PLK1), phosphorylates EIF4EBP1 at S111 on the mitotic spindle in human HepG2 cells (Shang et al., 2012). Cyclin-dependent kinase 1 (CDK1) phosphorylates EIF4EBP1 at up to four sites during mitosis (Heesom et al., 2001; M. Shuda et

al., 2015). As mTOR, ATM, CDK1, and PLK1 are all present in the oocyte during meiosis, they are candidates to contribute to EIF4EBP1 phosphorylation. Furthermore, these kinases are detected directly on oocyte meiotic spindles (Du et al., 2015; Jansova et al., 2017; Kogasaka, Hoshino, Hiradate, Tanemura, & Sato, 2013; Lin, 2015). mTOR inhibition during MI disrupts spindle migration, formation of the actin cap, and formation of the spindle structure (Susor et al., 2015b). ATM is expressed throughout oocyte maturation but has not been shown to phosphorylate EIF4EBP1 during this time (Lin, 2015). In porcine oocytes, ATM inhibition inhibits GVBD or PB1 (first polar body extrusion) (Lin, 2015). ATM-/- oocytes display meiotic failure and are infertile due to meiosis I arrest (Xu et al., 1996). CDK1 regulates meiotic resumption, kinetochore-microtubule spindle attachments, meiosis II metaphase, and polar body extrusion (Adhikari et al., 2012; Davydenko, Schultz, & Lampson, 2013; Masui & Markert, 1971; Pomerantz et al., 2012). PLK1 becomes active immediately before GVBD and its inhibition disrupts GVBD, bi-polar meiotic spindle formation, microtubule organizing center formation, chromosome segregation, and chromosome condensation (Pahlavan et al., 2000; Solc et al., 2015b; Tong et al., 2002).

To identify the specific kinases regulating EIF4EBP1 phosphorylation in association with oocyte meiotic spindle formation, we examined the roles of individual upstream kinases in EIF4EBP1 phosphorylation at the meiotic spindle during the first and second meiotic division of mouse oocytes. We find that PLK1 is the only upstream kinase tested that regulates EIF4EBP1 phosphorylation at the spindle and that loss of the PLK1-mediated EIF4EBP1 phosphorylation disrupts normal spindle formation and function. Additional roles for PLK1 are seen for microtubule polymerization. Inhibition of EIF4EBP1 phosphorylation at the spindle reduces

abundance of the key structural protein β-Tubulin on the MI spindle, consistent with a role for EIF4EBP1 phosphorylation in oocyte spindle formation. Collectively, these observations reveal PLK1 as a key regulatory nexus of mammalian oocyte spindle formation, stability, and function, operating through EIF4EBP1 and presumably its attendant control over the production of spindle-associated proteins.

3.3 Glossary of abbreviations

4EGI: EIF4EBP1 inhibitor

ATM: Ataxia telangiectasia mutated

BI2536: PLK1 inhibitor

CDK1: Cyclin-dependent kinase 1

COCs: Cumulus-oocyte complexes

EIF4EBP1: Eukaryotic translation initiation factor 4E binding protein

GV: Germinal vesicle

GVBD: Germinal vesicle breakdown

IBMX: 3-Isobutyl-1-methylxanthine

IFCM: Immunofluorescence confocal microscopy

KU55933: ATM inhibitor

MI: Metaphase I, forms in oocyte during meiosis I

MII: Metaphase II, forms in oocytes during meiosis II

MEF: Mouse embryonic fibroblast

MTOC: Microtubules organizing center

mTOR: Mechanistic target of rapamycin

Ooplasm: Cytoplasm within oocyte

PLK1: Polo-like kinase I

Torin 1: mTOR inhibitor

3.4 Materials and Methods

3.4.1 Oocyte isolation and culture

(B6D2)F1 females were obtained from Jackson Laboratories at 7 weeks age and used from 8 to 12 weeks age. Germinal vesicle (GV) stage oocytes were collected from ovaries of females 46-48 h after intraperitoneal injection with 5 IU of equine chorionic gonadotropin (eCG) (EMD Millipore: 367222). Ovaries were transferred to room temperature HEPES-buffered M2 media with 0.225M 3-Isobutyl-1-methylxanthine (IBMX) (Sigma: I7018), and cumulus-oocyte complexes (COCs) were released. Only GV stage oocytes with multiple rows of cumulus cells completely surrounding the oocyte were used. Denuded, abnormal, and dying oocytes were discarded. GV stage oocytes were cultured for 1 h in MEMα (ThermoFisher: 12561072)

with 20% fetal bovine serum (ThermoFisher: 16000044) and 0.225 M IBMX in 5% O_2 and 5%CO_2 that had been preequilibrated in a humidified atmosphere for at least 1 h. Attached cumulus cells were removed by pipetting using a narrow bore pipet with a 100 µm outer diameter. For in vitro maturation (IVM), GV stage COCs were released from IBMX treatment by washing and culturing in MEMα with 20% FBS. *In vivo* matured MII stage oocytes were collected from females superovulated with 5 IU eCG followed 48 h later by 5 IU of human chorionic gonadotropin (hCG) (Sigma-Aldrich; C1063), at 14-16 h post-hCG injection. MII stage COCs were released in M2 medium, and cumulus cells removed using hyaluronidase at 300 µg/ml (Sigma: H4272), and oocytes were cultured in potassium simplex optimized medium (KSOM) (Ho, Wigglesworth, Eppig, & Schultz, 1995; Lawitts & Biggers, 1993) in a humidified atmosphere as above. For each experimental replicate, GV or MII oocytes were collected from 5 BDF1 mice, pooled, and randomly assigned to either DMSO or inhibitor treatment groups; therefore, each replicate represents 5 independent mice. All BDF1 mice in this study were from the same source and are genetically identical. All studies were approved by the Michigan State University Institutional Animal Care and Use Committee, consistent with National Institutes of Health (NIH) Guide for the Care of Use of Laboratory Animal, and with the Association for Assessment and Accreditation of Laboratory Animal Care (AAALAC) accreditation.

3.4.2 Inhibitor treatments

The PLK1 inhibitor BI2536 (Selleckchem: S1109) was applied at a concentration of 500 nM, as in previous studies that showed effective PLK1 inhibition in mouse oocytes (Baran, Solc,

Kovarikova, Rehak, & Sutovsky, 2013; Clift & Schuh, 2015; Solc et al., 2015b). The ATM inhibitor KU55933 (Selleckchem: S1092) was applied at a concentration of 10 µM, a concentration used previously in mouse embryos and porcine oocytes (Mu, Jin, Farnham, Li, & O'Neill, 2011; H. Wang et al., 2015). The mTOR inhibitor, Torin 1 (Selleckchem: S2827), was applied at 1 µM, an effective concentration in mouse oocytes (A. Yamamoto, Mizushima, & Tsukamoto, 2014). The EIF4EBP1 inhibitor 4EGI was applied at 100 µM as described for mouse oocytes (Susor et al., 2015b). All inhibitors except 4EGI were diluted in MEMα with 20% fetal bovine serum at a 1:1000 concentration. Vehicle treated control received DMSO at a concentration of 1:1000. 4EGI was diluted 1:250 in the same medium, and DMSO controls were treated with DMSO at 1:250. GV stage oocytes were washed though several droplets of media to remove IBMX, and then treated for 7 h to permit progression to metaphase I and an opportunity for spindle formation. For MII oocytes, inhibitors were diluted in KSOM medium and oocytes were rinsed through several droplets. MII oocytes were treated for 3 h. The efficacy of the Torin 1 and KU55933 treatments were also verified in MEFs to ensure inhibitor treatment was successfully inhibiting mTOR and ATM respectively. To validate Torin 1 activity, (B6D2)F1 mouse embryonic fibroblasts were treated with 1µM Torin 1 or 1:1000 DMSO vehicle for 1 h, and stained using oocyte immunofluorescence protocol (data not shown). To validate KU55933 activity, (B6D2)F1 mouse embryonic fibroblasts were pre-treated with 10 µM KU55933 or 1:1000 DMSO for 3 h and then treated with 10 µM KU55933 only, 50 µM etoposide only, or 10 µm KU55933 and 50 µM etoposide simultaneously, and stained using oocyte immunofluorescence protocol (data not shown).

3.4.3 Oocyte fixation and immunofluorescence

For fixation, zonae pellucidae were removed by treating in acidified Tyrode's buffer (Tyrode, 1910) for approximately 30 sec followed by immediate washing through M2 media for 1 min. To remove any bovine serum albumin (BSA), oocytes were rinsed briefly through 0.4% polyvinyl alcohol (PVA)/PBS before fixation in 4% paraformaldehyde/PBS (pH 7.0; Sigma-Aldrich: P6148). Fixed oocytes were rinsed with 0.4% PVA/PBS and either stored in 0.4% PVA/PBS at 4^{o} or processed immediately.

Immunofluorescence detection of target proteins was performed in NUNC 4-well dishes (Sigma Aldrich: 179830) using 750 µl of each solution. With the exception of overnight incubation with primary antibody, all steps were performed at room temperature. Oocytes were permeabilized for 30 min in PBS containing 0.1% Triton X-100 (Fisher Scientific: BP151) and then moved to blocking buffer [PBS with 0.1% BSA (Sigma-Aldrich: A9418), 0.01% Tween-20 (Sigma-Aldrich: P9416), and 0.02% (Sigma-Aldrich: S8032)] for 1 h. Primary and secondary antibodies were diluted in blocking buffer. Primary antibodies included: phospho-S64-EIF4EBP1 (Cell Signaling: 9451S, diluted 1:50), phospho-S111-EIF4EBP1 (Abgent: AP3473a, diluted 1:50), PLK1 (Sigma: SAB1404220, diluted 1:100), β-tubulin (Santa Cruz: sc-9935, diluted 1:200), Nuclear Mitotic Apparatus Protein 1 (NuMA) (Santa Cruz: sc-51164, diluted 1:500), and pan-EIF4EBP1 (Cell Signaling: 9452, diluted 1:50). Torin 1 and KU55933 treated MEFs were stained for phospho-235/236-S6-Kinase (Cell Signaling: 4858P, diluted 1:100) and phospho-S15-p53 (Cell Signaling: 9286, diluted 1:400). Specificity of the polyclonal phospho-S64-EIF4EBP1 antibody has been established in earlier studies (Ellederova et al., 2006; Fonseca et al., 2011; Gingras et al., 2001; Ma et al., 2009; X. Wang, Li, Parra, Beugnet, & Proud, 2003). Specificities of

the PLK1, β-tubulin, NuMA, phospho-235/236-S6-kinase, and phospho-S15-P53, and pan-EIF4EBP1 antibodies have all been previously validated by Western blotting (Chiang, Duncan, Schindler, Schultz, & Lampson, 2010; Gladding et al., 2014; Lopez-Mateo, Villaronga, Llanos, & Belandia, 2012; Si, Verma, Lampson, Cai, & Robertson, 2008; Till et al., 2015; Yuan et al., 2009). Phospho-S111-EIF4EBP1 (Abgent) has been used extensively by our lab in the past (Romasko et al., 2013) and was further validated using a second, independent phospho-S111-EIF4EBP1 antibody (MyBioSource MBS9210664). Specificities of the primary antibodies were also confirmed by replicating staining patterns using another primary antibody from a different vendor (data not shown). Oocytes were incubated in primary antibodies overnight at 4^{o}C. Oocytes were then washed three times in blocking buffer for 10 min each wash, and incubated in secondary antibodies for 1 h at room temperature. Secondary antibodies included: donkey anti-rabbit-Alexa 594 (Abcam: ab150076, diluted 1:300), donkey anti-goat-Alexa 594 (Abcam: ab150132, diluted 1:300), donkey anti-mouse-Alexa 488 (Abcam: ab150109, diluted 1:500), and donkey anti-goat-Alexa 488 (Abcam: ab150129, diluted 1:1000). Controls lacking primary antibody treatment were tested for each secondary antibody and yielded no detectable spindle signal (data not shown). After secondary antibody incubation, oocytes were washed three times in blocking buffer, mounted on slides in 11 µl Vectashield mounting solution with DAPI (Vector: H-1200), mounted on slides with coverslips, and the coverslip edges sealed with nail polish.

3.4.4 Confocal Microscopy and immunofluorescence image analysis

Immunofluorecence confocal microscopy (IFCM) was performed on an Olympus FluoView FV1000 confocal laser scanning microscope with a 40X 1.25 NA oil objective, using 2X zoom and a 1µm step size. The Olympus software is the Olympus FluoView FV1000 Advanced Software (FV10-ASW), version 4.2. Signal detection was provided through the software using photomultiplier tube detection. For DAPI excitation, the sampled was excited with a 405-nm laser. For Alexa 488 excitation, each sample was excited with a 488-nm laser. For 594 excitation, each sampled was excited with a 543-nm laser. All settings were kept constant within groups. Spindle images were compiled as Z-projections of all slices containing signal at the spindle (5-10 1µM slices). All image analysis was done using ImageJ (Schneider, Rasband, & Eliceiri, 2012).

3.4.5 Spindle and cytoskeleton protein analyses

With 4EGI treatment, lagging chromosomes were quantified at 7 h of IVM, as chromosomes not overlapping with other chromosomes at the metaphase plate of the MI spindle. The number of oocytes with and without lagging chromosomes was compared between control and inhibitor treated groups. Spindles were only analyzed for lagging chromosomes and β-tubulin when oriented perpendicular to the confocal laser, and only if DAPI stain intensity was equal between the treated and vehicle control groups in each experimental run, thereby minimizing potential imaging artifacts resulting from part of the spindle being out of the visualization plane. The intensity of β-tubulin on MI spindles were

measured after immunofluorescence confocal microscopy and image analysis using Image J to measure the average pixel intensity in the region of interest, normalized to average background fluorescence in an adjacent region of same size. Since the MII spindle is stably arrested, a fair comparison can be made between the size of MII spindles and this can be taken into account to calculate total β-tubulin. Therefore, in MII spindle studies, apparent spindle area when viewing the z-stack (henceforth denoted "spindle area") was also measured. For quantification of total β-tubulin intensity at the MII midzone, the average pixel intensity for the region containing the metaphase plate was quantified, normalized to background by dividing the average midzone intensity by the average intensity values for an equal sized region over the nearby ooplasm, and then multiplied by the area. Quantification of total β-tubulin on the MII spindle was done the same way but the area measured contained the entire MII spindle.

Chromosome congression was examined in oocytes treated with BI2536 either during IVM to the MI metaphase stage, or in matured MII oocytes. Spindles were scored as displaying failed chromosome congression (FCC) following BI2536 treatment either if they had apparent metaphase plates, but some chromosomes were outside of the apparent spindle structure, or if they displayed no obvious metaphase plate due to nearly complete failure of chromosome congression. Spindles with lagging chromosomes contained within the image area demarcated by the spindle structure were not scored as having failed chromosome congression. NUMA intensity was quantified by measuring NuMA intensity at the spindle pole regions, normalized to the background by dividing by average intensity values for an equal sized region over the nearby ooplasm, and the averaged together. The association of total EIF4EBP1, phosphorylated EIF4EBP1 variants, and PLK1 with spindles was examined by IFCM. The presence of EIF4EBP1-P-

S64, EIF4EBP1-P-S111, and PLK1 was scored solely as present or absent, except in the case of MIIs treated with Torin 1 or DMSO. Intensity of phospho-EIF4EP1 variants and PLK1 were measured at MII spindle poles in both DMSO and Torin 1 treatments groups and the signal was normalized to the background. Total EIF4EBP1 was examined at spindle poles in 7-12 individual 1 µm confocal sections spanning each entire spindle, and in z-stacks of those sections combined to assess possible changes in at the spindle poles. Microtubule flaring was quantified at MII only and was the presence of microtubules attached to spindle poles at one end but the other end was not oriented towards the spindle. Microtubule hyperpolarization was quantified at MI and MII and was the presence of microtubules present but not attached to the spindle.

3.4.6 Statistical Analysis

Statistical analyses were performed using Prism GraphPad version 7.01 for windows, GraphPad Software, La Jolla California USA, www.graphpad.com. An unpaired t-test or Mann-Whitney U test used as indicated to calculate differences between groups. A difference of $p<0.05$ was considered significant. Error bars shown represent standard deviation (SD).

3.5 Results

3.5.1 Confirmation of role for EIF4EBP1 in spindle formation

Preventing EIF4EBP1 phosphorylation and release of EIF4E to bind EIF4G could disrupt spindle formation and function. Consistent with this, a previous study (Susor et al., 2015b), reported disruption in spindle formation and chromosome congression using the specific

inhibitor, 4EGI, which mimics hypophosphorylated EIF4EBP1 and binds to EIF4E to inhibit formation of cap-dependent initiation complexes (Moerke et al., 2007). To confirm this effect for the system used here, we cultured (B6D2)F1 mouse GV oocytes for 7 h in the presence of 4EGI and imaged MI spindles to assess any defects in β-tubulin and chromosome congression. The total amount of β-tubulin on MI spindles was decreased by an average of 34% (DMSO n=14; 4EGI n=27 oocytes; $p < 0.005$) with the 4EGI treatment, consistent with reduced production of β-tubulin for spindle formation (Figure 3.1A-G). The frequency of lagging chromosomes was increased in the 4EGI treated oocytes by more than four-fold from 14% (n=2/14) in the DMSO control to 54% (n=13/24) with 4EGI treatment (Fig 1H). These results confirm a role for EIF4EBP1 in regulating mRNA translation initiation via EIF4E binding, and the need for release of EIF4EBP1from EIF4E to allow efficient spindle formation and function.

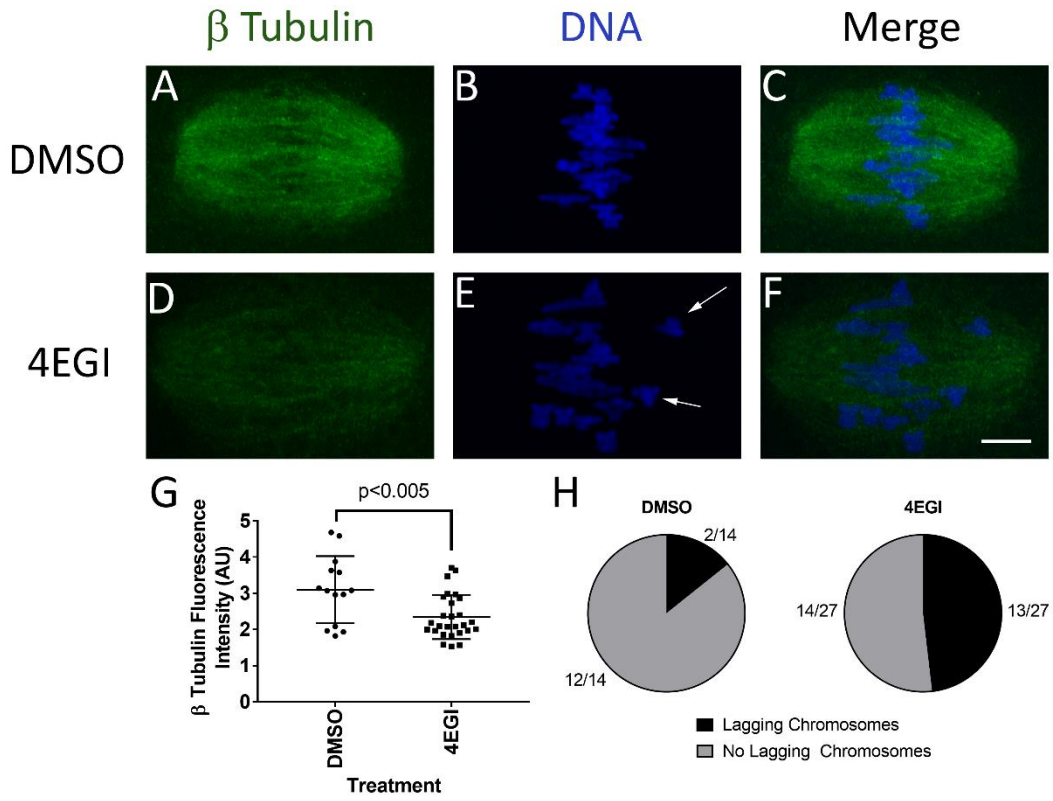

Figure 3.1 Decreased β-Tubulin intensity and lagging chromosomes on mouse oocyte MI Spindle after 7hr 4EGI treatment observed by IFCM. GV oocytes were matured in DMSO or 4EGI for 7 hours in vitro, fixed, and immunostained. (A-C) MI oocytes matured in DMSO vehicle control. (D-F) MI oocytes matured in 4EGI inhibitor. (A,D) β-Tubulin innunoreactive signal. (B,E) DNA observed by fluorescent DAPI staining. (C,F) Merged image in which β-Tubulin is shown in green and DNA is shown in blue. White arrows denote lagging chromosomes. (G) Quantitative analysis of β-Tubulin fluorescence intensity on MI spindle after 4EGI treatment. (p=0.003 using a one-tailed t-test with equal variance, error bars=SD; DMSO n=14, 4EGI n=27) (H) Number of oocytes in each treatment group with lagging chromosomes present was quantified. Oocytes were collected from 5 BDF1 mice, pooled, and randomly assigned to either DMSO or 4EGI treatment groups; this was repeated for two replicates. Bar, 10 µm. GV, germinal vesicle; MI, metaphase I1.

3.5.2 Upstream kinases affecting EIF4EBP1 phosphorylation and formation of the first (MI) meiotic spindle

To understand how EIF4EBP1 is regulated, and thereby couples spindle formation to other events in the cell, it is essential to determine the upstream kinases that control EIF4EBP1 phosphorylation, localization, and activity. EIF4EBP1 phosphorylation events observed in cultured cells and mitotic cell extracts may have little relevance to processes occurring during oocyte meiosis. Additionally, first and second meiotic divisions are markedly different, making it necessary to examine EIF4EBP1 regulation during both divisions. We used a series of highly specific kinase inhibitors to test for involvement of individual upstream kinases in EIF4EBP1 phosphorylation on the first meiotic spindle, and attendant effects on spindle properties and chromosome congression.

Our first target kinase for analysis was PLK1, which earlier studies showed is involved in mitotic and meiotic spindle formation (Clift & Schuh, 2015; van Vugt & Medema, 2005). PLK1 directly phosphorylates EIF4EBP1 at S111 during mitosis on the spindle (Shang et al., 2012). Treatment of oocytes during IVM with BI2536 completely eliminated EIF4EBP1-P-S111 at the spindle poles (n=35 oocytes) (Figure 3.2.1B). Another site, EIF4EBP1-P-S64 is phosphorylated by CDK1, which is activated by PLK1 in oocytes (Heesom et al., 2001; Pahlavan et al., 2000). As with EIF4EBP1-P-S111, spindle-associated EIF4EBP1-P-S64 was completely eliminated with BI2536 treatment (n=31 oocytes) (Figure 3.2.1F). No change in spindle-associated EIF4EBP1-P-S111 or EIF4EBP1-P-S64 was seen in DMSO negative control oocytes (n=47 and n=50 oocytes affected, respectively) (Figure 3.2.1A, 3.2.1E).

BI2536 treatment also resulted in a loss of PLK1 on all MI spindles (n=24), but PLK1 remained present on all MI spindles in DMSO treated controls (n=49) (Figs. 2.1J & I, respectively). The loss of PLK1 from the first meiotic spindle after inhibition indicates successful PLK1 inhibition, as PLK1 must be active in order to be tethered to the spindle structure (K. S. Lee, Grenfell, Yarm, & Erikson, 1998; Lenart et al., 2007).

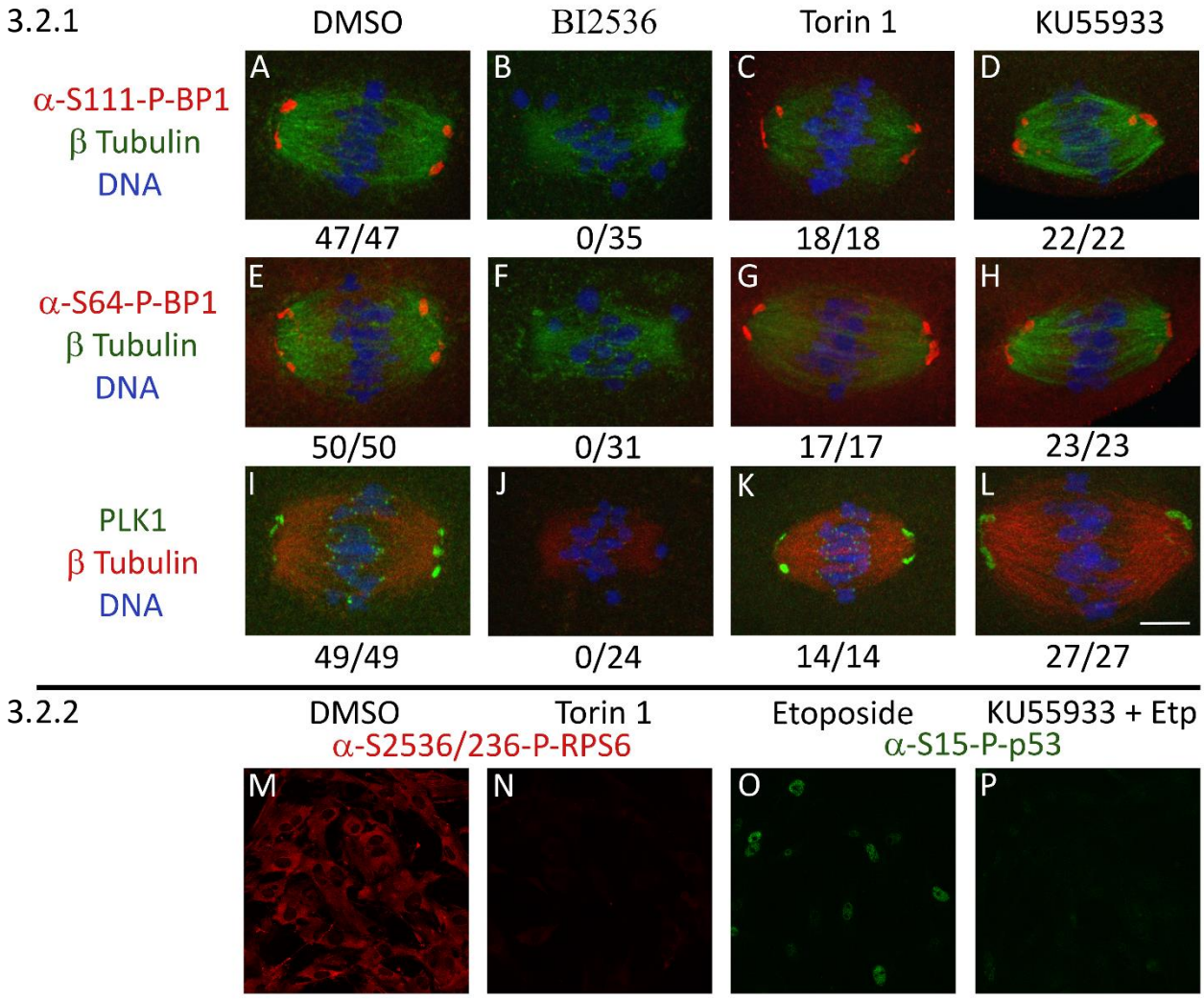

Figure 3.2 Localization of EIF4EBP1-P-S64, -P-S111, and PLK1 signal mouse oocyte MI spindle after DMSO, BI2536, Torin 1, and KU55933 treatment observed by IFCM. **Figure 3.2.1.** GV oocytes were matured in DMSO, BI2536, Torin 1, or KU55933 for 7 hours in vitro, fixed, and immunostained. (A-D) EIF4EBP1-P-S111 spindle localization in MI oocytes matured in DMSO, BI2536, Torin 1, or KU55933. (E-H) EIF4EBP1-P-S64 spindle localization in MI oocytes matured in DMSO, BI2536, Torin 1, or KU55933. (I-L) PLK1 spindle localization MI oocytes matured in DMSO, BI2536, Torin 1, or KU55933. Quantification for number of oocytes with target protein localized to spindle out of total oocytes quantified shown below each images. Oocytes were collected from 5 BDF1 mice, pooled, and randomly assigned to either DMSO or inhibitor treatment groups; this was repeated for a minimum of two replicates. Bar, 10 µm. **Figure 3.2.2.** Shows efficacy of Torin 1 and KU55933 inhibitor as tested in MEFs. GV, germinal vesicle; MI, metaphase I; MEFs, mouse embryonic fibroblast.

BI2536 treatment caused pronounced spindle defects after 7 h of IVM. We observed a complete failure of a bipolar spindle formation in 24.8% of the total MI oocytes quantified (n=34/133), a phenotype not seen in the DMSO treatment group (n=154) (Figure 3.3, Table 3.1). Nearly all (n=98/99) of the remaining spindles displayed failed chromosome congression (FCC). No FCC was seen in the DMSO treatment group (n=154) (Table 3.1). As with the 4EGI treatment, BI2536 treatment also resulted in a significant decrease in average β-tubulin intensity on the MII spindle (Figure 3.4). These results illustrate a strong negative effect of PLK1 inhibition on spindle formation and chromosome congression that is associated with loss of PLK1 from the spindle, loss of spindle-associated PLK1-mediated EIF4EBP1-P-S111 phosphorylation, and loss of spindle-associated PLK1-regulated CDK1-mediated EIF4EBP1-P-S64 phosphorylation.

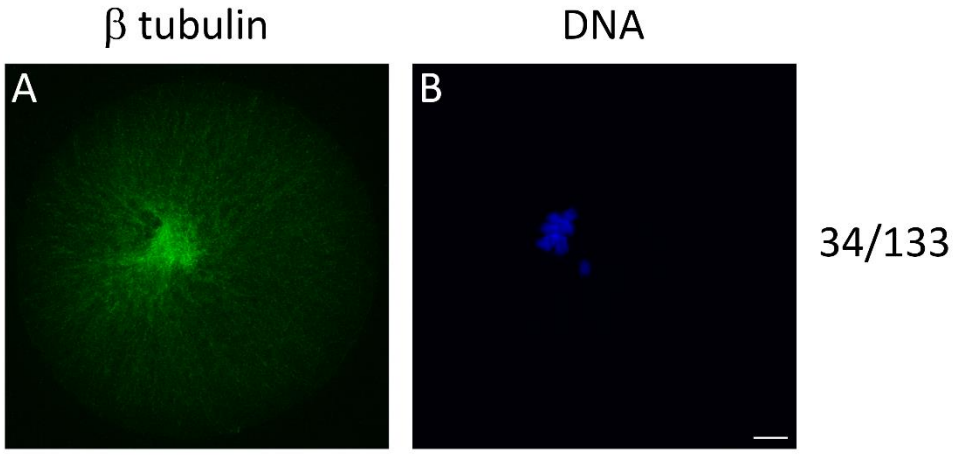

Figure 3.3 Spindle failure phenotype on mouse MI oocyte after 7hr BI2536 treatment during in vitro maturation observed by IFCM. GV oocytes were matured in BI2536 for 7 hours *in vitro*, fixed, and immunostained. (A-B) MI oocytes matured in BI2536. (A) β-Tubulin innunoreactive signal. (B) DNA observed by fluorescent DAPI staining. Quantification of oocytes with no bipolar MI spindle after BI2536 treatment shown on far right. Oocytes were collected from 5 BDF1 mice, pooled, and randomly assigned to either DMSO or inhibitor treatment groups; this was repeated for a minimum of five replicates. Bar, 10 µm.

Table 3.1 Quantification of failed chromosome congression to MI spindles after 7 h of treatment				
Treatment	**Total MI oocytes**	**Spindle failure**	**n Spindles**	**Failed Chromosome Congression**
DMSO	154	0	154	0/154
BI2536	133	34	99	98/99
Torin 1	15	0	15	0/15
KU55933	21	0	21	0/21

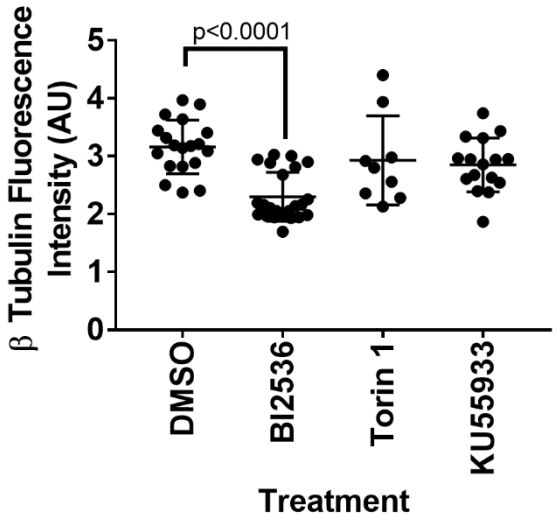

Figure 3.4 Decreased β-tubulin intensity on mouse oocyte MI spindle after 7hr BI2536 treatment. Average β-tubulin intensity was measured on MI spindle after DMSO, BI2536, Torin 1, and KU55933 treatments and the signal was normalized to the background. Inhibitor treatment groups were all compared to the DMSO control. BI2536 treatment significantly decreased average β-tubulin fluorescence on MI spindle. ($p<0.0001$ determined using a Mann-Whitney non-parametric test, Error bars=SD, DMSO n=19, BI2536 n=23, Torin 1 n=9, KU55933 n=16).

The second upstream kinase we tested was mTOR, which regulates EIF4EBP1 in interphase cells in response to insulin stimulation, nutrient restriction and other treatments (Acosta-Jaquez et al., 2009; Heesom et al., 1998). mTOR phosphorylates EIF4EBP1 at T36/45 during insulin stimulation and nutrient restriction (Gingras et al., 1999; Heesom et al., 1998),

and may also impact EIF4EBP1-P-S111 and EIF4EBP1-P-S64 indirectly through interactions with other upstream kinases or by regulating the priming T36/45 phosphorylation. EIF4EBP1-P-S64 (n=17) and EIF4EBP1-P-S111 (n=18) were unaffected at spindle poles by Torin 1 treatment (Figs. 2.1C, 2.1G). PLK1 was also unaffected by Torin 1 treatment (n=14/14) (Figure 3.2.1K). mTOR inhibition did not yield any spindle defects or a decrease in average β-tubulin intensity (Figure 3.4). Chromosomes still congressed (n=15) to the metaphase plate by 7 h of IVM and β-tubulin was still highly expressed and organized similar to the DMSO vehicle controls (Table 3.1). The efficacy of the Torin 1 inhibitor was validated in MEFs (Fig 3.2.2M-N). These results indicate that mTOR inhibition has no significant effect on spindle formation and function during first meiosis, and no effect on phosphorylation at pS111 or pS64 forms of EIF4EBP1 associated with the spindle. The lack of an effect of Torin-1 indicates that mTOR activity is not required for a priming event to allow the CDK1-mediated EIF4EBP1-S64 phosphorylation. These results indicate that mTOR is not a key regulator of EIF4EBP1 phosphorylation on the first meiotic spindle.

The next upstream kinase we tested was ATM. ATM phosphorylates EIF4EBP1 at S111 in other cell types (D. Q. Yang & Kastan, 2000). ATM inhibition by KU55933 treatment did not yield any abnormal spindle phenotypes or defects. Chromosomes still congressed to the metaphase plate by 7 h of IVM (n=21) and β-tubulin was still expressed and organized similar to the DMSO vehicle controls (Figure 3.4, Table 3.1). EIF4EBP1-P-S64 (n=22/22) and EIF4EBP1-P-S111(n=23/23) were both unaffected at spindle poles by KU55933 treatment (Figs. 3.2.1D, 3.2.1H). PLK1 likewise remained present at the spindle poles after KU55933 treatment (n=27/27) (Figure 3.2.1L). However, ATM inhibition caused a partial diminishment of PLK1

staining at the kinetochores (Figure 3.2.1L). The efficacy of the KU55933 inhibitor was validated in MEFs (Figure 3.2.2O-P). These results show that ATM does not directly regulate EIF4EBP1 phosphorylation at the spindle pole, but may have a slight effect by modulating PLK1 association with the kinetochores. The results also highlight key differences in ATM function between oocyte first meiosis and mitotic events in cultured cells.

3.5.3 Upstream kinases affecting EIF4EBP1 phosphorylation and formation of the second (MII) meiotic spindle

The above results revealed a major role for PLK1 in formation and function of the first meiotic spindle, and dramatic effects on spindle-associated phospho-EIF4EBP1. Because the regulation of MI and MII spindle formation and their specific characteristics differ, we evaluated potential effects of PLK1 and other upstream kinases on stability and maintenance of the MII spindle in matured oocytes. Ovulated MII oocytes were treated for 3 h with each inhibitor or with DMSO as a negative control.

Similar to effects on MI spindles during IVM, treatment with the PLK1 inhibitor BI2536 led to a complete loss of EIF4EBP1-P-S111 (n=46) and EIF4EBP1-P-S64 (n=61) on the MII spindle (Figs. 5.1B, 5.1F). There was no effect of DMSO treatment on EIF4EBP1 phosphorylation in nearly all of the treated MII oocytes (n=104/104 for P-S111 study, and n=90/92 for P-S64 study) (Figs. 5.1A & 5.1E). PLK1 staining remained present on spindle poles in all DMSO treated control oocytes (n=95) but was completely abolished in all BI2536 treated MII oocytes (n=51) (Figure 3.5.1I, 3.5.1J).

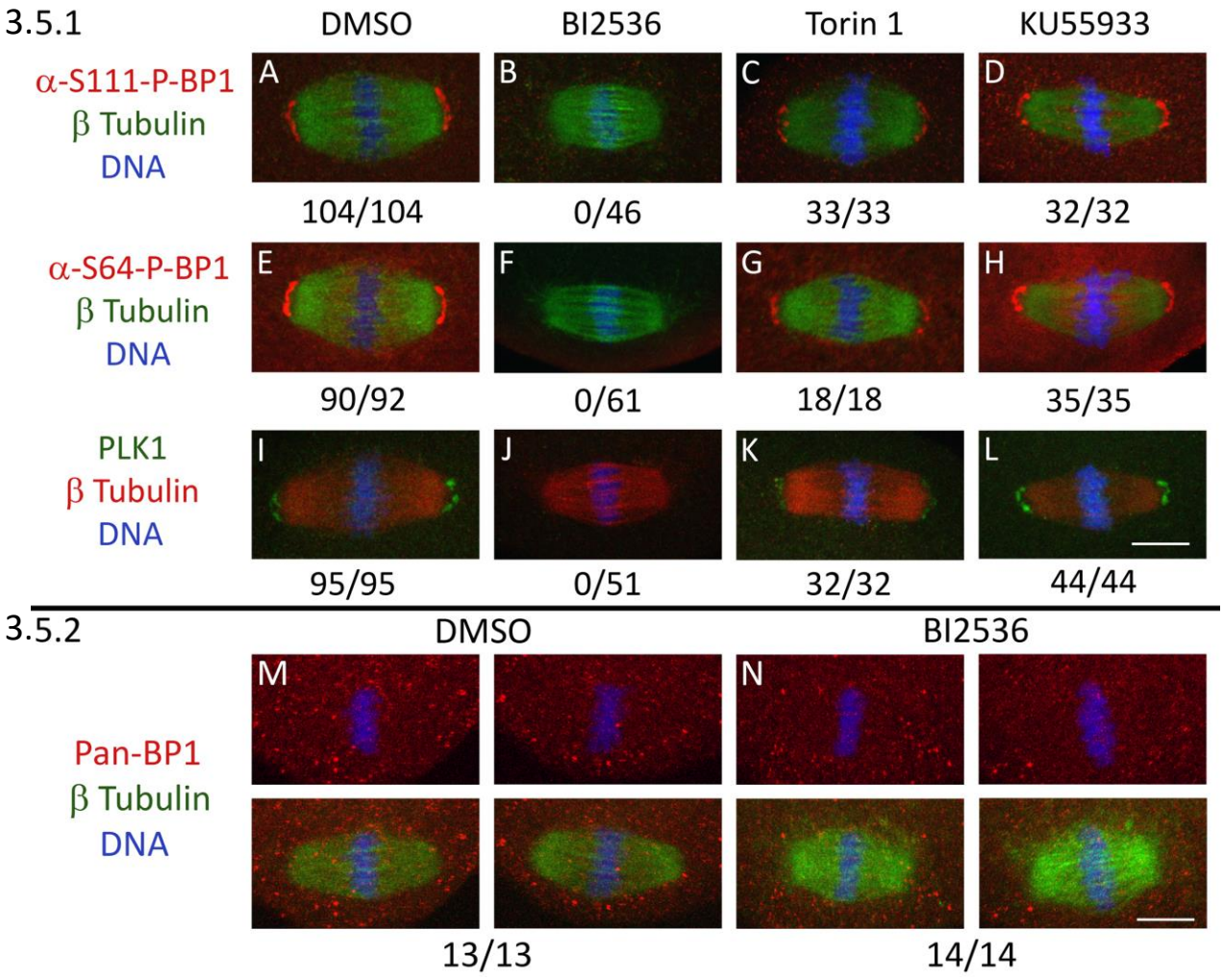

Figure 3.5 Localization of EIF4EBP1-P-S64, -P-S111, and PLK1 signal mouse oocyte MII spindle after DMSO, BI2536, Torin 1, and KU55933 treatment observed by IFCM. **Figure 3.5.1.** MII oocytes were treated with DMSO, BI2536, Torin 1, or KU55933 for 3 hours *in vitro*, fixed, and immunostained. (A-D) EIF4EBP1-P-S111 spindle localization in MII oocytes matured in DMSO, BI2536, Torin 1, or KU55933. (E-H) EIF4EBP1-P-S64 spindle localization in MII oocytes matured in DMSO, BI2536, Torin 1, or KU55933. (I-L) PLK1 spindle localization in MII oocytes matured in DMSO, BI2536, Torin 1, or KU55933. **Figure 3.5.2.** MII oocytes treated with (M) DMSO or (N) BI2536 were stained for total EIF4EBP1.This pan-EIF4EBP1 staining was examined in each confocal section encompassing the spindle to determine if void or difference in signal. Two representative z-stacks are shown for each group. Quantification for number of oocytes with target protein localized to spindle out of total oocytes quantified shown below each images. Oocytes were collected from 5 BDF1 mice, pooled, and randomly assigned to either DMSO or inhibitor treatment groups; this was repeated for a minimum of two replicates. Bar, 10 µm. MII, metaphase II.

As previously shown, IFCM using an antibody to all EIF4EBP1 forms revealed uniform staining across the ooplasm including across the spindle pole region (Figs. 5.2M-N) (Romasko et al., 2013). The uniformity in distribution of total EIF4EBP1 as compared to phosphorylated variants highlights the intense, selective phosphorylation of EIF4EBP1 at the spindle poles. There was no diminishment of total EIF4EBP1 fluorescence at the spindle pole region with BI2536 treatment, indicating there is no large void in staining associated with treated spindle pole regions, which would be indicative of a large loss of total EIF4EBP1 protein from the region, and retention of dephosporylated EIF4EBP1. However, because the pan-EIF4EBP1 antibody yielded high uniform staining across the spindle pole region and surrounding ooplasm, without the same intense foci seen with the phospho-specific antibodies, we cannot rule out that loss of EIF4EBP1-P-S64 and EIF4EBP1-P-S111 with PLK1 inhibition is due to release of previously phosphorylated peptide from the spindle pole region, rather than EIF4EBP1 dephosphorylation and retention, or steady-state turnover without phosphorylation of newly acquired EIF4EBP1 protein.

Because oocytes are arrested in second metaphase when ovulated, we could also compare effects of the inhibitors on spindle area and use this to calculate the effects on total β-tubulin. All inhibitors resulted in a significant decrease in total MII spindle area, but only BI2536 resulted in a decrease in total MII spindle β-tubulin signal (DMSO n=20; BI2536 n=18; Torin 1 n=12; KU55933 n=14)(Figure 3.6A-B). We then quantified that spindle midzone area and found it is significantly decreased after Torin 1 and BI2536 treatments (DMSO n=20; BI2536 n=18; Torin 1 n=12; KU55933 n=14) (Figure 3.6C). We initially noted an increase in the average β-tubulin fluorescence at the spindle midzone but when area is included to calculate total β-

tubulin, the change in total β-tubulin at the midzone is not significant after any of the treatments (DMSO n=20; BI2536 n=18; Torin 1 n=12; KU55933 n=14) (Figure 3.6C-D).

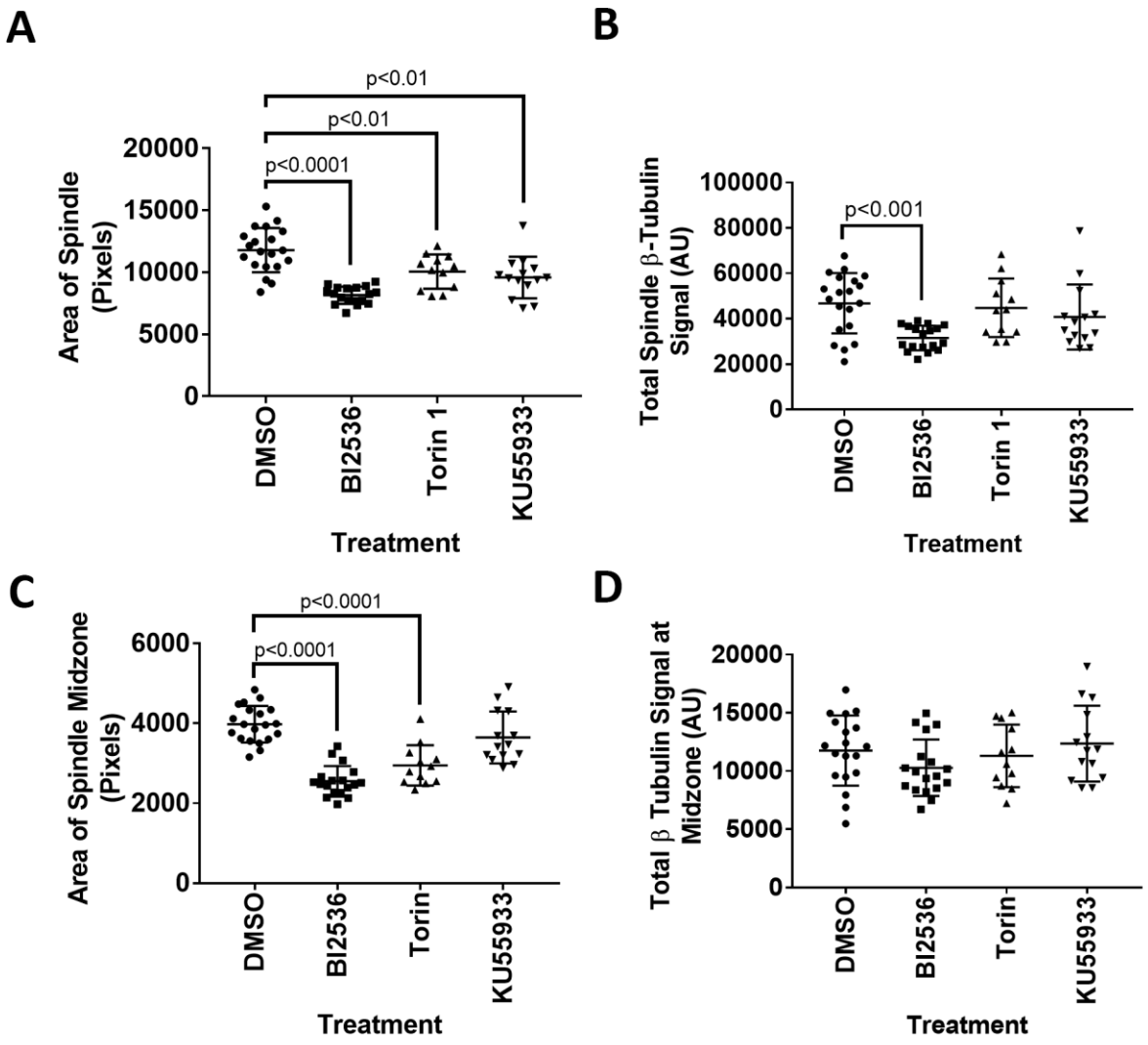

Figure 3.6 Total β-Tubulin decreased on MII spindle after 3hr BI2536 treatment. Quantitative analysis of MII spindle characteristics after DMSO, BI2536, Torin 1, of KU55933 treatment. (A) Quantification of total MII spindle area. (B) Total MII spindle β-tubulin signal. (C) Quantification of MII spindle midzone area. (D) Total MII spindle midzone β-tubulin signal. (p values listed on each graph were determined using a Mann-Whitney non-parametric test, error bars=SD; DMSO n=20, BI2536 n=18, Torin 1 n=12, KU55933 n=14).

To test whether loss of phospho-EIF4EBP1 and PLK1 from the MII spindle poles could be an indirect effect of overall loss of spindle pole structures, we compared NuMA staining between treated and vehicle control MII oocytes (Fig 7A-B). NuMA is a commonly used marker

of spindle poles. NuMA fluorescence intensity remained unchanged in BI2536 treated oocytes (n=11) compared to vehicle controls (n=10) (Figure 3.7C), consistent with a previous study (C. Y. Jang, Coppinger, Seki, Yates, & Fang, 2009). There was also no apparent effect of BI2536 on the maintenance of chromosome congression at the metaphase plates of MII spindles, further indicating stable spindle structures throughout the 3 h of treatment.

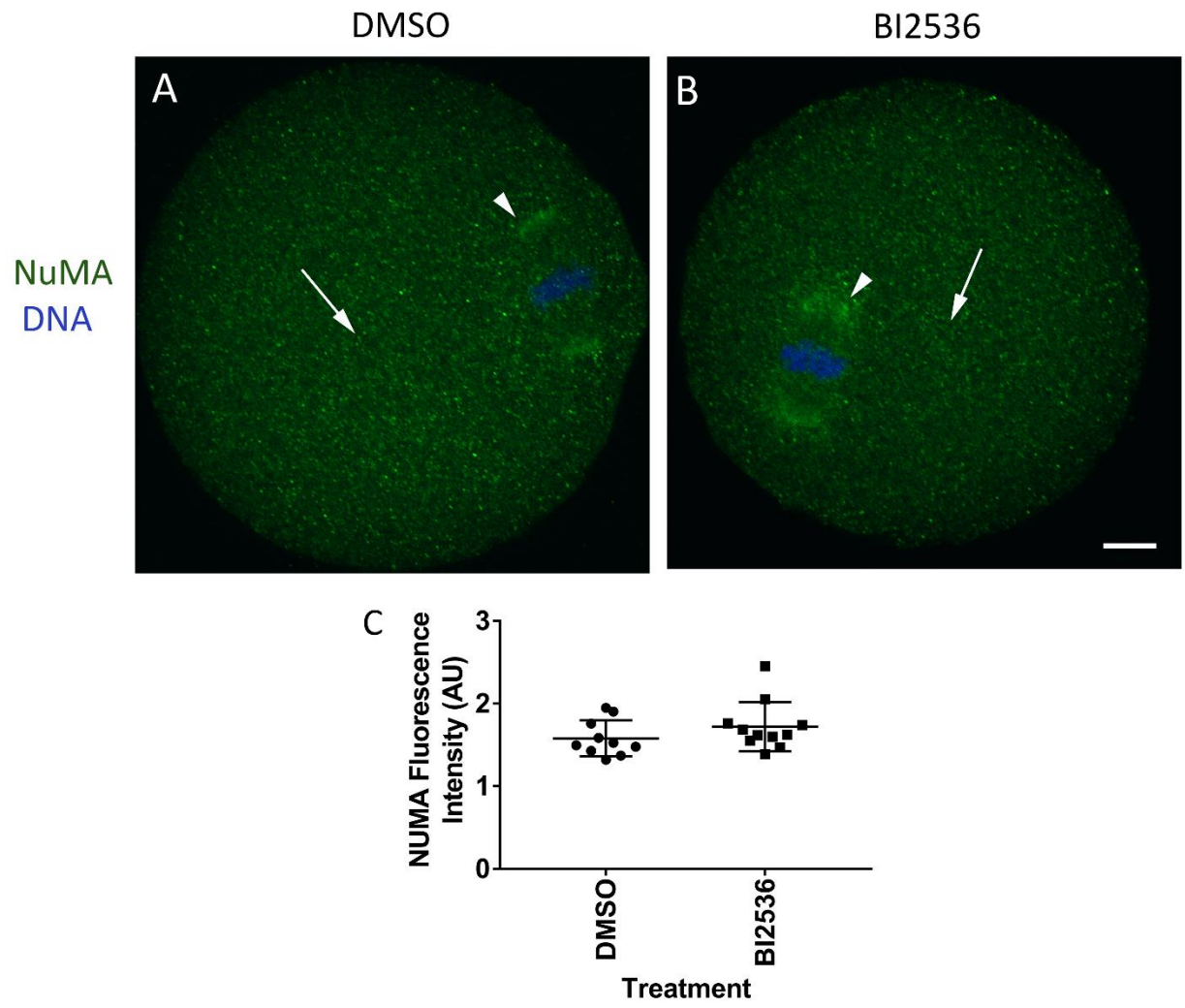

Figure 3.7 NuMA signal unaffected at MII spindle poles after 3hr BI2536 treatment observed by IFCM. MII oocytes were treated with DMSO or BI2536 for 3 hours *in vitro*, fixed, and immunostained. NuMA was quantified at each spindle pole (arrowheads) and normalized to nearby background signal (arrows). (A) NuMA signal in MII spindle treated with DMSO. (B) NuMA signal on MII spindle treated with BI2536. (C) NuMA fluorescence intensity at MII spindle poles not significantly different between DMSO and BI2536 treated oocytes (p=0.7045 determined using a Mann-Whitney non-parametric test , error bars=SD; DMSO n=10, BI2536 n=11). Bar, 10 µm.

We next tested if treatment with mTOR inhibitor Torin 1 would affect EIF4EBP1 phosphorylation at the MII spindle. Torin had no effect on EIF4EBP1-P-S111 presence (n=33, Figs. 5.1C) or intensity on the MII spindle (8A). Although EIF4EBP1-P-S64 remained present on the MII spindle (n=18/18, Figure 3.5.1G), Torin 1 caused a (36%) decrease in the fluorescence intensity EIF4EBP1-P-S64 (Figure 3.8B). Torin 1 had no effect on the presence (n=32, Figure 3.5.1K) or intensity of PLK1 on the MII spindle (Figure 3.8C). As noted above, Torin 1 treatment also significantly decreased the MII spindle area and spindle midzone area (Figure 3.6A, 3.6C), indicating inhibitor efficacy in the oocyte. Torin 1 did not affect total β-tubulin signal on the MII spindle or at the spindle midzone (Figure 3.6B, 3.6D).

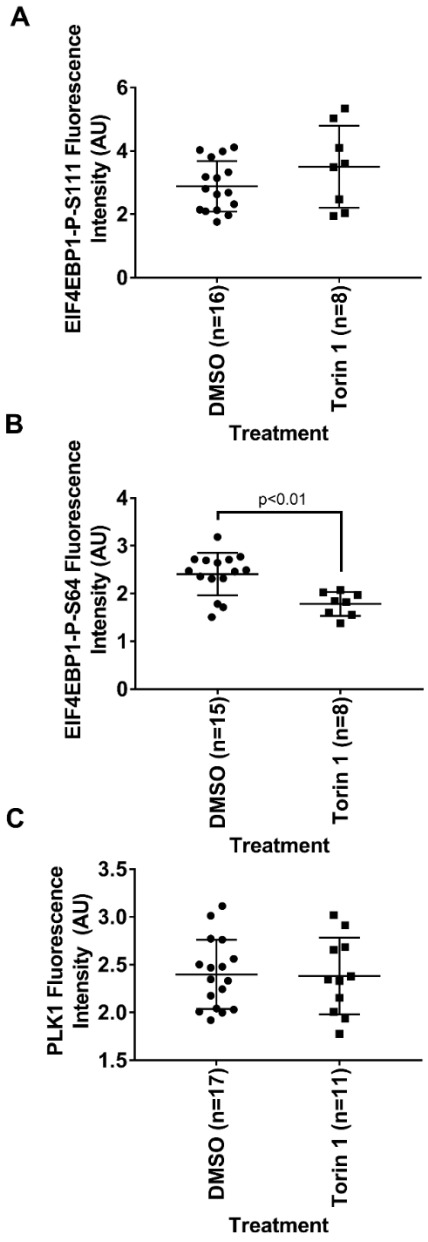

Figure 3.8 Torin 1 treatment has slight effect on EIF4EBP1-P-S64 but not –S111 phosphorylation on MII spindle. (A) Normalized EIF4EBP1-P-S111 average fluorescence intensity on MII spindle poles after DMSO or Torin 1 treatment. (B) Normalized EIF4EBP1-P-S64 average fluorescence intensity on MII spindle poles after DMSO or Torin 1 treatment. ($p<0.01$ figured using unpaired t-test with equal variance) EIF4EBP1-P-S64 is significantly decreased after Torin 1 treatment. (C) Normalized PLK1 fluorescence average intensity on MII spindle poles after DMSO or Torin 1 treatment. The numbers of oocytes analyzed are indicated for each treatment and phosphorylation site. Data are from two replicates of staining containing both DMSO controls and Torin 1 treated oocytes, plus additional identical DMSO controls from other inhibitor studies. Error bars=SD).

Next, we tested if ATM inhibition affects EIF4EBP1 phosphorylation on MII spindles. KU55933 treatment had no significant effect on EIF4EBP1 phosphorylation at the sites tested (n=32 and n=35 for S111 and S64, respectively) (Figs. 3.5.1D, 3.5.1H), no effect on PLK1 (n=44, Figure 3.5.1L). As noted above, KU55933 treatment did significantly decrease the overall area of the MII spindle, indicating inhibitor efficacy in the oocyte (Figure 3.6A) but did not affect spindle midzone area (Figure 3.6C). KU55933 treatment did not affect total β-tubulin at on the MII spindle or at the spindle midzone (Figs. 3.5.1B, 3.5.1D). In addition, MT flaring was not observed with KU55933 treatment (n=15; Table 3.2). An effect on PLK1 presence at kinetochores on MII spindles could not be evaluated because PLK1 does not localize in discrete foci at kinetochores on MII spindles, as it does during MI.

Table 3.2. Quantification of MT flaring on MII spindles after 3 h of treatment

Treatment	n Spindles	MT Flaring
DMSO	126	0/126
BI2536	122	121/122
Torin 1	18	0/18
KU55933	15	0/15

3.5.4 Additional effects of PLK1 inhibitor on oocyte cytoskeleton

In addition to the striking effects of PLK1 inhibition on spindle-associated EIF4EBP1-P-S64 and EIF4EBP1-P-S111 at both MI and MII, effects on spindle structures, effects on chromosome congression at MI, and microtubule flaring at MII spindle poles, we noted striking effects on cytoplasmic microtubules, specifically microtubule hyperpolarization defined as additional microtubules present outside of the spindle structure. After 7 h treatment with BI2536, 47.4% of MI oocytes displayed microtubule (MT) hyperpolarization (n=47/99), a

phenotype only seen in 0.65% of DMSO treated control oocytes (n=1/154) and unseen in Torin1 (n=15) and KU55933 treatment groups (n=21) (Figure 3.9A-D, Table 3.3). These additional microtubules formed in close proximity to the MI spindle and were not seen throughout the rest of the ooplasm. This particular microtubule configuration was not observed in MII stage oocytes. However, hyperpolarization was also seen in 73% MII stage oocytes treated with BI2536 (n=89/122), in a single DMSO control (0.79%, n=1/126), but not in the Torin 1 (n=18) or KU55933 (n=15) group. At the MII stage MT hyperpolarization was observed as microtubules spread throughout the cytoplasm, often appearing in aster-like structures (Figure 3.9E-H, Table 3.4).

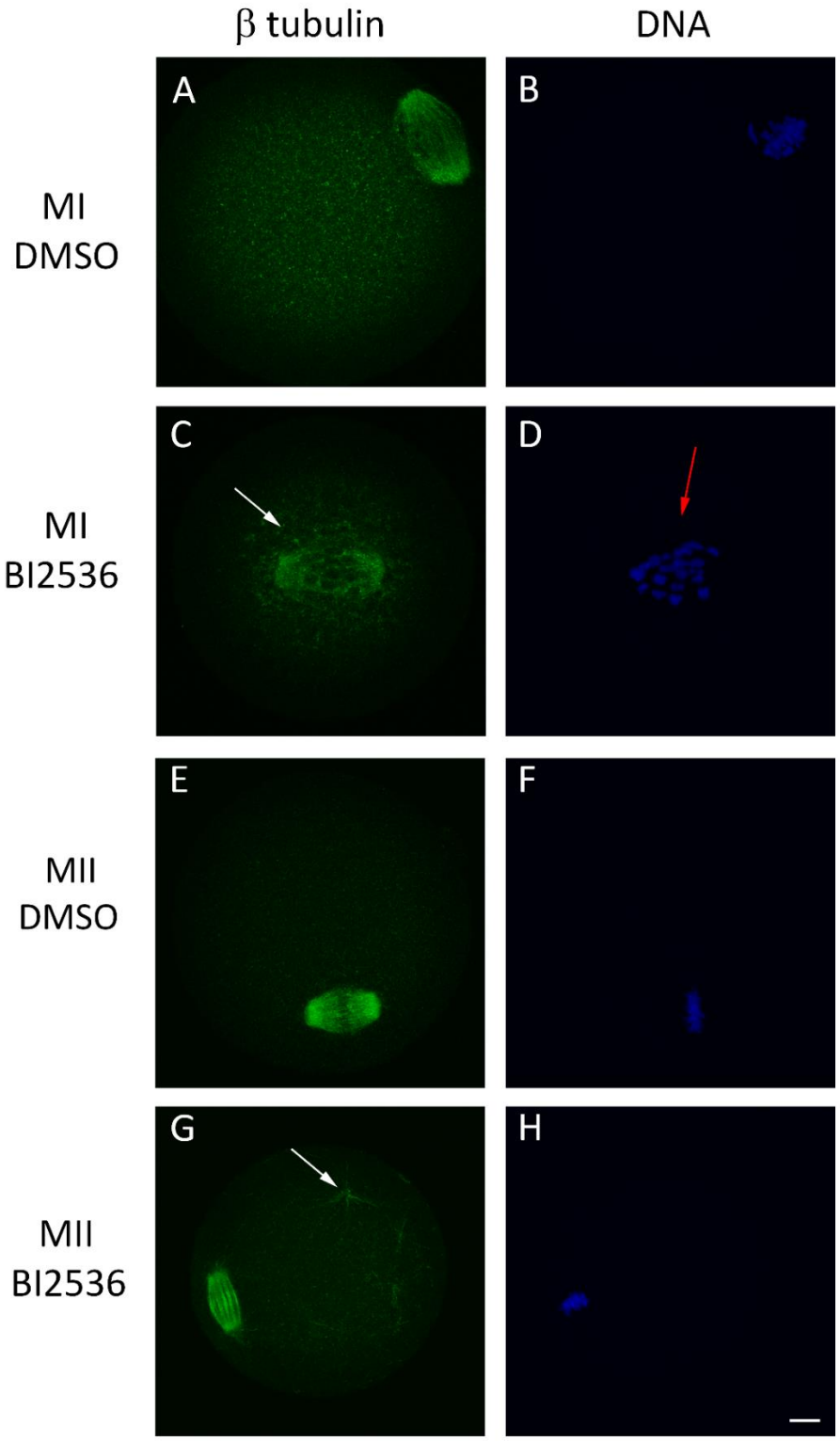

Figure 3.9 Microtubule (MT) hyperpolarization and failed chromosomes congression present in MI and MII oocytes after BI2536 treatment observed by IFCM.

Figure 3.9 (cont'd) Microtubule (MT) hyperpolarization and failed chromosomes congression present in MI and MII oocytes after BI2536 treatment observed by IFCM. β-Tubulin imunoreactive signal shown in green. DNA was stained with DAPI and is shown in blue. (A-D) GV oocytes were matured in DMSO or BI2536 for 7 hours *in vitro*, fixed, and immunostained as described in Materials and Methods (A-B) MI oocytes cultured in DMSO. (C-D) MI oocytes matured in BI2536. (C) White arrow denotes MT hyperpolarization present proximal to MI spindle. (D) Red arrow shows failed chromosome congression. (E-H) MII oocytes were treated for 3h in DMSO or BI2536 fixed, and immunostained. (E-F) MII oocytes treated with DMSO. (G-H) MI oocytes treated with BI2536. (C) White arrow denotes MT hyperpolarization present in ooplasm. Bar, 10 µm. MII, metaphase II.

Table 3.3 Quantification of MT hyperpolarization in MI oocytes after 7 h of treatment

Treatment	n Spindles	MT Hyperpolarization
DMSO	154	1/154
BI2536	99	47/99
Torin 1	15	0/15
KU55933	21	0/21

Table 3.4 Quantification of MT hyperpolarization in MII oocytes after 3 h of treatment

Treatment	n Spindles	MT Hyperpolarization
DMSO	126	1/126
BI2536	122	89/122
Torin 1	18	0/18
KU55933	15	0/15

3.6 Discussion

Meiosis in oocytes is a complex process, involving intricate coordination between endogenous and exogenous signals that allow for alternate phases of meiotic progression and arrest. Many of these signals converge to regulate spindle formation stability, and function, which are essential for successful chromosome congression and segregation. Here provide additional data on the regulated phosphorylation of EIF4EBP1, and its association at the MI and MII spindle poles, extending previous studies of MII oocytes (Romasko et al., 2013). More importantly, we demonstrate an overwhelmingly predominant role for PLK1 in controlling the presence of phsopho-EIF4EBP1 at the spindle pole, spindle formation and chromosome congression. Without disrupting spindle poles themselves, PLK1 inhibition eliminates EIF4EBP1-P-S64 and EIF4EBP1-P-S111 from the spindle and disrupts spindle properties and chromosome congression. Inhibition of mTOR had only a slight effect on EIF4EBP1-S64 on the spindle, and only at the MII stage. ATM inhibition had no significant effect on EIF4EBP1 phosphorylation. The limited impacts of mTOR and ATM inhibition exclude a major role for these kinases in regulating EIF4EBP1 phosphorylation at the spindle. We also find that PLK1 regulates microtubule dynamics throughout the ooplasm, indicating likely coordination between spindle dynamics and broader ooplasm cytoskeletal dynamics.

Earlier studies reported that PLK1 is required for meiosis in oocytes (Solc et al., 2015b) and mitosis in zygotes (Baran et al., 2013). Other studies revealed that PLK1 phosphorylates EIF4EBP1 in cultured cells (Shang et al., 2012). The only known role of EIF4EBP1 is binding to EIF4E and inhibiting cap-dependent translation (Marcotrigiano, Gingras, Sonenberg, & Burley, 1999), a function that is released by EIF4EBP1 phosphorylation (Pause, Belsham, et al., 1994b).

The results here provide the first direct evidence that PLK1 is the principal regulator of EIF4EBP1 phosphorylation and function at the oocyte spindle, identifying a new role for PLK1 during meiosis. Because PLK1 itself is regulated by other major upstream kinases (e.g., AURKs, CDK1) that also affect spindle formation (Pahlavan et al., 2000; Seki, Coppinger, Jang, Yates, & Fang, 2008; K. Shuda, Schindler, Ma, Schultz, & Donovan, 2009), these results further indicate that PLK1 may act as a major regulatory nexus, coupling the control of spindle formation and stability to other endogenous cellular cues, or exogenous signals acting through upstream pathways.

An accumulating body of literature indicates that localized mRNAs associated with spindles in oocytes and mitotic cells contribute to spindle formation by supporting the production of spindle component proteins (Blower et al., 2007; Romasko et al., 2013; Susor et al., 2015b). Additional studies revealed a temporally and spatially dynamic pattern of EIF4EBP1 phosphorylation at MII stage spindles (Romasko et al., 2013). However, the exact role of localized protein synthesis at the spindle has been difficult to resolve, due to the difficulty in dissecting specific effects on spindles from broader effects in the ooplasm. In support of a role for localized protein synthesis, specific mRNAs enriched at the spindle have been identified along with spindle-enriched proteins encoded by some of these mRNAs (Romasko et al., 2013), a localized RNA rich domain coinciding with locally enriched protein synthesis activity has been reported (Blower et al., 2007; Susor et al., 2015b), and spindles contain phosphorylated S6 kinase, a marker of active protein translation (Blower et al., 2007; Romasko et al., 2013). Previous studies with the 4EGI inhibitor supported a role for localized translation in formation and function meiotic spindles (Susor et al., 2015b). Our results extend this result by

demonstrating that release of EIF4EBP1 translation inhibition at the MI spindle facilitates the production of the critical spindle protein, β-tubulin, the mRNA for which is enriched at spindles (Blower et al., 2007), and is required for correct chromosome congression and spindle function. Images from previous study utilizing 4EGI inhibition indicated an effect on β-tubulin was present on MI spindles, but that group did not quantify or note the decreased β-tubulin (Susor et al., 2015b). In addition to decreased β-tubulin, the 4EGI treatment also caused an increase in the number of lagging chromosomes at the MI spindle. Although some phospho-EIF4EBP1 is present in the ooplasm at the GV stage, the intense signals specifically associated with the spindle poles and the impact of 4EGI treatment on the spindle structure indicate local effects of inhibiting EIF4EBP1 phosphorylation at the spindle, as opposed to non-specific effects elsewhere in the cell.

We acknowledge that, while we did not observe a gross diminishment of pan-EIF4EBP1 staining at the spindle pole region, a loss of EIF4EBP1 from the specific foci of staining at the spindle poles might occur, as opposed to dephosphorylation and retention of spindle pole-associated EIF4EBP1, or steady-state turnover and replacement without phosphorylation of newly acquired EIF4EBP1. The first scenario, however, would be expected to result in translational activation, as the only known function for EIF4EBP1 is to inhibit translation and its loss would therefore release this inhibition. The latter two scenarios would result in translational inhibition locally for mRNAs enriched at the spindle and associated with EIF4EBP1. The reduction in tubulin staining observed with PLK1 inhibition was phenocopied by 4EGI treatment and is thus most consistent with translational inhibition leading to deficiency of tubulin production at the spindle forming region. This effect of PLK1 inhibition argues against

the scenario of general EIF4EBP1 loss, and in favor of either of the latter two scenarios involving diminished EIF4EBP1 phosphorylation and a resulting translation inhibition. One caveat to this interpretation would be that PLK1 inhibition might lead to sequestration of EIF4E away from the spindle, which could inhibit translation. Such sequestration has only been reported for nuclei (irrelevant for meiotic cells) and cytoplasmic granules; we did not observe any increase in EIF4EBP1 cytoplasmic granules (Sukarieh, Sonenberg, & Pelletier, 2009). The negative effective of dominant negative hypophosphorylated EIF4EBP1 mimic on oocyte spindles (Jansova reference), demonstrates a negative effect of a hypophosphorylated EIF4EBP1 on local translation at the spindle pole and spindle disruption, which also consistent with the latter interpretation. Previous studies demonstrated that PLK1 directly phosphorylates EIF4EBP1 in vitro, and that PLK1 and phospho-EIF4EBP1 co-localize on mitotic spindles, where they are essential for maintaining spindle integrity (49). The demonstration here that PLK1 and phospho-EIF4EBP1 also co-localize to oocyte meiotic spindles, and that PLK1 inhibition results in a loss of phosphorylated EIF4EBP1 at the oocyte spindle poles and disrupts oocyte spindle function, taken with all of the other available data, are consistent with a role for PLK1 in promoting EIF4EBP1 phosphorylation at the spindle to support spindle formation via translation activation. Our observations thus extend the findings from mitotic cells to the oocyte.

A recent study implied that BI2536 did not affect EIF4EBP1 phosphorylation at the spindle (Jansova et al., 2017). But the data presented in that paper do not address EIF4EBP1 phosphorylation at the spindle. BI2536 was applied for a brief period of just 2 h starting at just 1 h after release from IBMX, a time before MI spindle formation (7 h post-release), so that direct examination of spindle-associated EIF4EBP1 phosphorylation was not possible. Western

blotting data for effects of PLK1 inhibition did not use phospho-specific antibodies, and PLK1 inhibition was not verified. Of note, however, the possible persistence of phospho-EIF4EBP1 at the level of whole oocytes reported there is consistent with our evidence for an effect of PLK1 inhibition on EIF4EBP1 phosphorylation specifically at the spindle poles. While PLK1 inhibition could also reduce S111 phosphorylation on cytoplasmic targets, the intense, spatially specific co-localization of EIF4EBP1-P-S111 at the spindle poles with PLK1 is most easily explained by a localized role for PLK1 regulating EIF4EBP1 phosphorylation and activity at the spindle poles.

PLK1 inhibition with BI2536 produced stronger effects that 4EGI treatment in some regards. For example, chromosome congression was more severely affected with BI2536 than with 4EGI. The enhanced impact of PLK1 inhibition may reflect direct effects of PLK1 on meiotic processes that are independent of EIF4EBP1. PLK1 promotes kinetochore microtubule attachment, which likely accounts for a stronger effect of BI2536 on chromosome congression (Du et al., 2015; Sumara et al., 2004). Despite these broader effects of PLK1, it is clear that PLK1 exerts the predominant effect on EIF4EBP1 phosphorylation.

The effects of PLK1 inhibition observed on spindles were much more pronounced at MI than at MII, although PLK1 inhibition had a clear effect on β-tubulin expression at both stages. After PLK inhibition, the MII spindle displayed increased β-tubulin fluorescence intensity at the spindle midzone. This initially seemed inconsistent with our model of localized β-tubulin translation, but including spindle area as a variable and calculating total β-tubulin we showed that the total amount of β-tubulin is still decreased. This change is consistent with a model of the spindle shrinking in towards the midzone, possibly as a result of the decreased localized β-tubulin translation. The dynamic nature of the MI spindle made spindle area comparison

impossible, but the average β-tubulin intensity was decreased on the MI spindle after PLK1 inhibition. In addition to this, chromosome congression defects not seen at MII spindles were present at MI. This may simply reflect a greater effect of interfering with spindle formation when the inhibitors are applied before metaphase, as opposed to disrupting existing spindles in oocytes already at metaphase. Alternatively, the first and second meiotic divisions may be differentially susceptible to disruption of localized mRNA translation. Lastly, PLK1 is known to regulate multiple event during meiosis and mitosis and the prolonged treatment (7h) may also affect MI spindle formation indirectly via targets in the ooplasm. This may also explain why the chromosome congression defects were more severe with PLK1 inhibition than 4EGI inhibition as PLK1 is likely affecting MI spindle formation in EIF4EBP1-independent ways as well, such as by impairing microtubule organizing center (MTOC) formation dynamics which PLK1 regulates (Clift & Schuh, 2015). The majority of aneuploidies detected in oocytes arise during the first meiotic division (K. T. Jones, 2008). Loss of sister chromatid cohesion also contributes to aneuploidy (Chiang et al., 2010), but defects in spindle assembly may also contribute. Additionally, spindle assembly is driven by a Ran-GTP gradient emanating from the condensed chromosomes, but a Ran-GTP gradient-independent mechanism may also function at MI (J. Dumont et al., 2007b; Kalab et al., 2011). Because MI and MII spindle formation are regulated differently, PLK1 could differentially affect the two processes through a greater disruption of MI-specific events.

We observed no effect of mTOR or ATM inhibition on PLK1 localization at either MI or MII stages, and only a modest effect of mTOR inhibition on EIF4EBP1-P-S64 signal exclusively on the MII stage spindle poles. mTOR regulates insulin signaling, which is dysregulated in diabetes,

and diabetic mice have a variety of oocyte defects including meiotic spindle abnormalities (Takano et al., 2001; Q. Wang et al., 2009). However, the hypothesis that mTOR regulates EIF4EBP1 phosphorylation at the spindle and that this is disrupted in diabetic oocytes to negatively affect spindles is not supported by our results. The limited effects of mTOR inhibition on spindle-associated EIF4EBP1-P-S64, lack of mTOR inhibition effect on EIF4EBP1-P-S111, and the lack of spindle defects instead indicate that the adverse effects of maternal diabetes on meiotic spindle formation occur via an mTOR-independent mechanism or via an indirect effect of mTOR in the ooplasm (Q. Wang et al., 2009). We note that a previous study concluded that mTOR may regulate localized translation in the oocyte (Susor et al., 2015b), based on treatments with the mTOR inhibitor rapamycin. A recent study reported effects of rapamycin on EIF4EBP1 phosphorylation, but the analysis was limited to Western blotting of whole oocytes, and did not provide data for EIF4EBP1 phosphorylation specifically at the spindle (Jansova et al., 2017). It is also important to note that mTOR-mediated EIF4EBP1 phosphorylation is resistant to rapamycin, and Torin 1 is a much more potent and specific inhibitor of this mTOR function (Thoreen et al., 2009), indicating that rapamycin effects on the spindle could occur through a mechanism not involving mTOR. Overall, the available data indicate that the roles of ATM and mTOR in regulating EIF4EBP1 phosphorylation at the spindle are minor. mTOR may regulate EIF4EBP1 phosphorylation within the ooplasm, leading to indirect spindle defects, but PLK1 is the predominant kinase regulating EIF4EBP1 phosphorylation at the spindle poles.

The Aurora kinases (AURKs) are also important regulators of meiotic and mitotic spindle formation and pan AURK inhibitors result in meiotic spindle defects (K. Shuda et al., 2009).

AURKA is present at the spindle poles of meiotic MI and MII spindles (K. Shuda et al., 2009). AURKA phosphorylates PLK1 at the start of mitosis (Seki et al., 2008). AURKB can be phosphorylated by PLK1, and co-localizes with PLK1 at the kinetochores of the meiotic MI spindle (Chu et al., 2011; K. Shuda et al., 2009) Therefore, AURKA may phosphorylate PLK1 at the MI and MII meiotic spindle poles and PLK1 may phosphorylate AURKB at the MI kinetochores. The latter function of AURKB could explain the stronger effect of PLK1 inhibition on chromosome congression at MI that we observe. Additional upstream effects of AURKA on PLK1 would also provide functional connections between other upstream endogenous or exogenous signals and EIF4EBP1 phosphorylation at the spindle.

CDK1 is another kinase that may work additively with PLK1 to regulate EIF4EBP1 phosphorylation. Because global inhibition of CDK1 activity prevents germinal vesicle breakdown and causes oocyte activation at MII (W. I. Jang et al., 2014; Phillips et al., 2002; Saskova et al., 2008), the role of CDK1 in EIF4EBP1 phosphorylation at the spindle cannot be tested directly through chemical inhibition or genetic ablation. Although a role for CDK1 can be inferred from our data as past studies of EIF4EBP1 phosphorylation in cultured cells revealed a complex hierarchy, wherein the T36/45 sites are priming phosphorylation sites and necessary for the subsequent S64 and T69 phosphorylations (Gingras et al., 1999). The presence EIF4EBP1-S64 (which CDK1 phosphorylates) on the MI and MII spindles and the lack of mTOR inhibitor effects on EIF4EBP1 phosphorylation suggests that CDK1 likely works with PLK1 to regulate EIF4EBP1 phosphorylation at the meiotic spindle (Heesom et al., 2001). This interaction is further supported by the known auto-amplification loop between PLK1 and maturation promoting factor (a complex of Cyclin B and CDK1) during meiosis (Pahlavan et al.,

2000). It remains unknown if CDK1 is upstream, downstream, or works in concert with PLK1. If CDK1 activation is downstream of PLK1, then PLK1 is likely regulating CDK1 activity solely at the spindle structure as CDK1 is carefully regulated throughout the rest of the cytoplasm to regulate meiotic progression and PLK1 is only localized at high levels to the spindle structure (Du et al., 2015).

The importance of the EIF4EBP1-S111 phosphorylation site to EIF4E binding has remained unclear, with different results emerging from different experimental systems (Heesom et al., 1998; X. Wang et al., 2003). S111 could be an alternative priming site to promote phosphorylation at other sites, or it could directly affect EIF4EBP1 binding to EIF4E (Heesom et al., 1998; X. Wang et al., 2003). Regardless of which of these functions is fulfilled by S111 phosphorylation, our data indicate that PLK1-mediated phosphorylation at this site may be essential for correct spindle formation and chromosome congression.

Our results highlight the specialized nature and complexity of the meiotic spindle structure in oocytes. First and second meiotic divisions in the oocyte differ in key respects, and both meiotic divisions differ from mitotic divisions. Similar to a mitotic spindle, the first meiotic spindle forms in the center of the oocytes but then the meiotic spindle moves to the cell cortex via an actin-dependent mechanism, an event that does not occur during mitosis. The MII spindle does not form in the oocyte center but instead forms in close proximity to the location of first polar body extrusion (Longo & Chen, 1985). The MI spindle does not arrest at metaphase whereas the MII spindle arrests at metaphase until a sperm penetrates the oocyte (Madgwick & Jones, 2007), a potential explanation for why aneuploidies primarily result for incorrect chromosome segregation at MI as there is not sufficient time to ensure correct homologous

chromosome alignment (Chiang et al., 2010). In addition, the first meiotic spindle requires the alignment and segregation of homologous chromosomes, whereas the second meiotic spindle is more similar to a mitotic spindle in that it is separating sister chromatids. With these key differences in mind, it is perhaps understandable that mammalian oocytes are predisposed to aneuploidy, and sensitive to a range of factors such as maternal age, hormonal stimulation, nutrition, diabetes, obesity, disease, and environmental toxins. Additional future studies to dissect further the roles of PLK1 and EIF4EBP1 in spindle dynamics may offer novel approaches to mitigate these negative effects on oocyte quality and fertility.

CHAPTER 4

Goldilocks and the three eggs: Why F1s are just right

Citation:

Severance, AL, Midic, U, Latham, KE. Goldilocks and the three eggs: Why F1s are just right. BMC-Genome Biology. *Submitted*. July 2018.

4.1 Abstract

This paper addresses the long-standing question of what causes hybrid vigor phenotypes in mammalian oocytes and preimplantation embryos. Answering this question should provide new insight into determinants of oocyte and embryo quality and infertility. Such "hybrid vigor" could arise through a variety of mechanisms, many of which must operate through post-transcriptional mechanisms affecting oocyte mRNAs accumulation, stability, translation and degradation. The differential regulation of such mRNAs must impact as yet unidentified pathways and functions within the cell. We conducted an in-depth transcriptome comparisons of immature and mature oocytes of C57BL/6J and DBA/2J inbred strains and the C57BL/6J x DBA/2J F1 (BDF1) hybrid oocytes using RNA sequencing, combined with novel computational methods of analysis. BDF1 oocyte characteristics arise through a combination of mechanisms visible at the level of the whole transcriptome, chiefly additive dominance, working in conjunction with a lesser degree of transgressive gene expression, as well as intermediate levels of mRNA expression for many genes, collectively affecting specific characteristics, most prominently histone expression, mitochondrial function, and oxidative phosphorylation. The study reveals the major underlying mechanisms that contribute to superior properties of hybrid oocytes. Given the extensive genetic variation in mRNA regulation, including mRNAs encoding proposed markers of oocyte quality, the study also highlights the importance of assessing the value of oocyte quality markers in the context of normal genetic expression variation.

4.2 Introduction

The oocyte has arguably the most colossal task given to any cell type. After a prolonged meiotic arrest that can last up to decades, the oocyte must quickly respond to a hormonal stimulus, grow considerably, finish building the maternal endowment of proteins and mRNAs, resume meiosis, segregate chromosomes, halt meiosis to await fertilization, reprogram the embryonic genome after fertilization, and support early embryogenesis. The oocyte becomes transcriptionally inactive before meiosis resumes and germinal vesicle breakdown (GVBD) occurs (Leatherman & Jongens, 2003). It is of utmost importance that the maternal mRNA endowment is correctly regulated through accumulation, timely poly-adenylation and translation, and degradation. Through these processes, the correct proteins are produced in the correct sequence to ensure high oocyte quality and subsequent high embryonic developmental potential (Gebauer, Xu, Cooper, & Richter, 1994; Paynton, Rempel, & Bachvarova, 1988; Sousa Martins et al., 2016; Stebbins-Boaz, Hake, & Richter, 1996).

Numerous studies have identified essential factors that drive early developmental events, and attempted to identify molecular markers of oocyte quality that support correct oocyte function and early embryogenesis (Bettegowda et al., 2008; Lie Fong et al., 2008; Patrizio, Fragouli, Bianchi, Borini, & Wells, 2007; Q. Wang & Sun, 2007; X. Q. Zhang et al., 2005). The results of studies of oocyte quality markers need to be considered in the context of natural variation among fertile genotypes. Finding that a modest difference in expression of a perceived marker of oocyte quality is well within the range of natural genetic variation in expression among fertile individuals would call into question the value of such a marker, or at least indicate a need for greater understanding of the broader cellular context in which that

factor operates. However, little if any attention has been given to genetic variability in the oocyte transcriptome. The extent of this variation, how fertility is achieved in the face of such variation, and how variations in expression of one gene may be offset by variation in expression of other genes are unsolved questions, because transcriptome studies have typically focused on individual genotypes, or because different analytical platforms have been employed, precluding direct comparisons across genotypes. Moreover, a deeper understanding of how quality oocytes arise and how they dictate embryonic developmental potential will require a deeper understanding of the extent to which gene expression pattern and associated biological functions can vary among fertile genotypes. In essence, it is vital to discover how different genotypes take different pathways to oocyte fertility. Understanding the molecular mechanisms by which maternal mRNA populations may be differentially regulated between genotypes should provide new insight into the underlying processes driving healthy oogenesis. Finally, because germ cells are important determinants of reproductive compatibility, understanding genetic variation in the oocyte is relevant to understanding key aspects of speciation and evolution.

Mouse inbred strains and hybrids between them provide a useful experimental tool for exploring genetic variation in oocyte transcriptomes in order to address the above biological questions using females of defined genotypes and origins, and reproducible and consistent availability to permit long-term experimental replication and enquiry. For example, the C57BL/6J (B6) and DBA/2J (D2) strains are both fertile, as are their F1 hybrid offspring, B6D2F1 (BDF1). However, past studies observed differences in oocyte quality between the three genotypes. BDF1 hybrids display heterosis, or hybrid vigor, for several aspects oocyte quality,

including a superior ability to reprogram somatic nuclei after somatic cell nuclear transfer (SCNT) (Gao, Czirr, Chung, Han, & Latham, 2004; Inoue et al., 2003; Wakayama & Yanagimachi, 2001), lower rates of embryonic fragmentation and 2-cell arrest, ooplasm granularity, size of the embryonic pronuclei, and other morphological attributes (Hadi, Hammer, Algire, Richards, & Baltz, 2005; Z. Han et al., 2010; Latham, Kutyna, & Wang, 1999; Poueymirou, Conover, & Schultz, 1989; Rambhatla & Latham, 1995; Reik et al., 1993). The parental strains also differ in many of these characteristics (Latham, 1994; Latham & Solter, 1991), and several studies have undertaken genetic mapping of these traits (Cheng et al., 2013; Latham & Sapienza, 1998).

Inbred strains may differ from one another at the level of simple genetic polymorphism or genome composition. An F1 genotype can lead to intermediate levels of genetic characteristics, dominance effects or transgressive gene expression. Additive effects of dominance at different genes and transgressive gene expression are of particular interest for understanding hybrid vigor (or hybrid suppression), but even intermediate levels of expression for particular combinations of genes could contribute to unique F1 hybrid phenotypes. Such effects have not been examined in mammalian oocytes. The goal of this study was to determine the effects of parental strain and F1 hybrid genotype on oocyte quality, and particularly to understand the basis for hybrid vigor in mouse oocytes, as a way to understand better the mechanisms that determine oocyte quality. This study is the first to combine oocytes of different stages and different genotypes (two parental inbred strains and F1 hybrid) into a single RNA sequencing (RNAseq) analysis capable of identifying molecular characteristics that distinguish F1 hybrids. Our approach to analysis combined differential gene expression with QIAGEN Ingenuity Pathway Analysis® (IPA), and a powerful new approach to discern the

biological impact of an F1 hybrid genotype by comparison to “predicted” F1 hybrid gene expression data synthesized from parental strain data. Three remarkable findings emerged from the analysis: 1) there are extensive differences in transcriptomes between strains, with roughly one quarter or more of the expressed genes showing differences between the two parental strains at both stages, and the three genotypes modulated their mRNA populations differently during maturation; 2) The superior BDF1 oocyte properties arise through a combination of mechanisms, chiefly additive dominance, working in conjunction with a less degree of transgressive gene expression as well as combined levels of mRNA expression intermediate between the parental levels; and 3) The BDF1 hybrid genotype is associated with differences in expression or activity of certain upstream regulators and canonical pathways, most prominently related to histone expression, mitochondrial function, and oxidative phosphorylation.

4.3 Results

The RNAseq data set presented here is the largest of its kind representing three mouse genotypes and two stages of oocyte. The overall quality of the dataset is high, with an average depth of aligned 28.5M exonic reads per sample (Sup. Table S1). The average number average of detected mRNAs was ~18,600 for germinal vesicle (GV) stage and ~16,400 for second meiotic metaphase (MII) stage.

4.3.1 Comparisons of gene expression between genotypes

Comparisons between the parental strains revealed a striking number of differentially expression genes (DEGs) at both stages (4583, 23% and 5825, 33% DEGs at the GV and MII

stages, respectively, $p < 0.05$) (DEG Table GSE114158). Even at the significance threshold of $p < 0.01$, the fraction of DEGs between parental strains was large (16% and 23% for GV and MII stages, respectively) (DEG Table GSE114158). As expected for a hybrid gene expression pattern, BDF1 oocytes displayed fewer DEGs in comparison to either parental strain, ranging from 32% to 39% ($p < 0.05$) of the number of DEGs identified between the two parental strains at the GV or MII stage, respectively.

There were more differences between genotypes at the MII stage than at the GV stage (Figure 4.1). To understand this change more fully, we determined the proportion of changes at either stage that was shared or stage-specific, and how genotype affected this proportion; sets of genes were designated as groups A-G for the GV stage or A'-G' for the MII stage, according to the Venn diagrams in Figure 4.1. For the three genotype comparisons combined, 3438 of the 4825 DEGs seen at the GV stage were also seen at the MII stage oocytes. Conversely, 3014 (47%) of the total 6452 DEGs seen at the MII stage were also seen at the GV stage. These groups included 465 differences between BDF1 and parental strains specific to the GV stage (Figure 4.1 groups A-F→N', where N'=not DEG at MII stage; DEG Table GSE114158) and 1331 differences between BDF1 and parental strains specific to the MII (Figure 4.1 N→A'-F', where N=not DEG at GV stage; DEG Table GSE114158). Moreover, there were many other differences only seen between parental strains at each stage (922 GV-specific differences, G→N' and 1683 MII-specific differences, N→G'; Figure 4.1; DEG Table GSE114158).

	B6 vs D2	DEGs	B6 vs F1	DEGs	D2 vs F1	DEGs
p<0.05	D2>B6	2269	F1>B6	859	F1>D2	920
	B6>D2	2314	B6>F1	759	D2>F1	618
p<0.01	D2>B6	1571	F1>B6	533	F1>D2	654
	B6>D2	1652	B6>F1	410	D2>F1	329

	B6 vs D2	DEGs	B6 vs F1	DEGs	D2 vs F1	DEGs
p<0.05	D2>B6	2888	F1>B6	1096	F1>D2	1185
	B6>D2	2937	B6>F1	1047	D2>F1	1073
p<0.01	D2>B6	2089	F1>B6	657	F1>D2	778
	B6>D2	2072	B6>F1	502	D2>F1	552

Figure 4.1 Interstrain comparisons at GV and MII. Top-DEGs were first identified for each of the three genotype comparisons (B6 vs BDF1, D2 vs BDF1, and B6 vs D2) at each stage (GV or MII), for significance threshold p<0.05. Then, these DEGs lists were compared with each other to determine the number of DEGs shared between comparisons (within stages). B (GV) and B'(MII) include DEGs where BDF1 mice are different from both parentals at each stage. **Bottom**-Table that shows the directionality of the DEGs between genotypes and the number of DEGs for the p<0.01 significance level at each stage.

4.3.2 Shared and genotype-specific changes in mRNA abundances during maturation

The larger number of DEGs at the MII stage compared to the GV stage indicated that dynamic changes in mRNA abundances occurred during maturation and that many of these were genotype-dependent. In particular, many changes in occurred only in BDF1 oocytes. This genotype effect on maturation was examined in two ways. One way was to compare the DEGs between genotypes for each stage ("within stage" genotype DEGs) and compare those lists across stage. The other was to define DEGs between the GV and MII stages within genotype and then examine the differences in those "maturation sets" between genotypes.

For the first approach, we focused on the differences in the overlap groups D, B, and F at the GV stage and D', B', and F' at the MII stage, (Figure 4.1). The genes were categorized according to mode of regulation (MOR) category for each genotype during maturation (Up, Down or Same, e.g., SSS indicates static expression across maturation for all three genotypes, included in DEG Table GSE114158) and the median and percentile fold changes for members plotted (Figure 4.2). This was done for cases where BDF1 oocytes more closely resembled D2 oocytes (D, D') or B6 oocytes (F, F') at either stage, and where BDF1 oocytes differed from both genotypes (B. B').

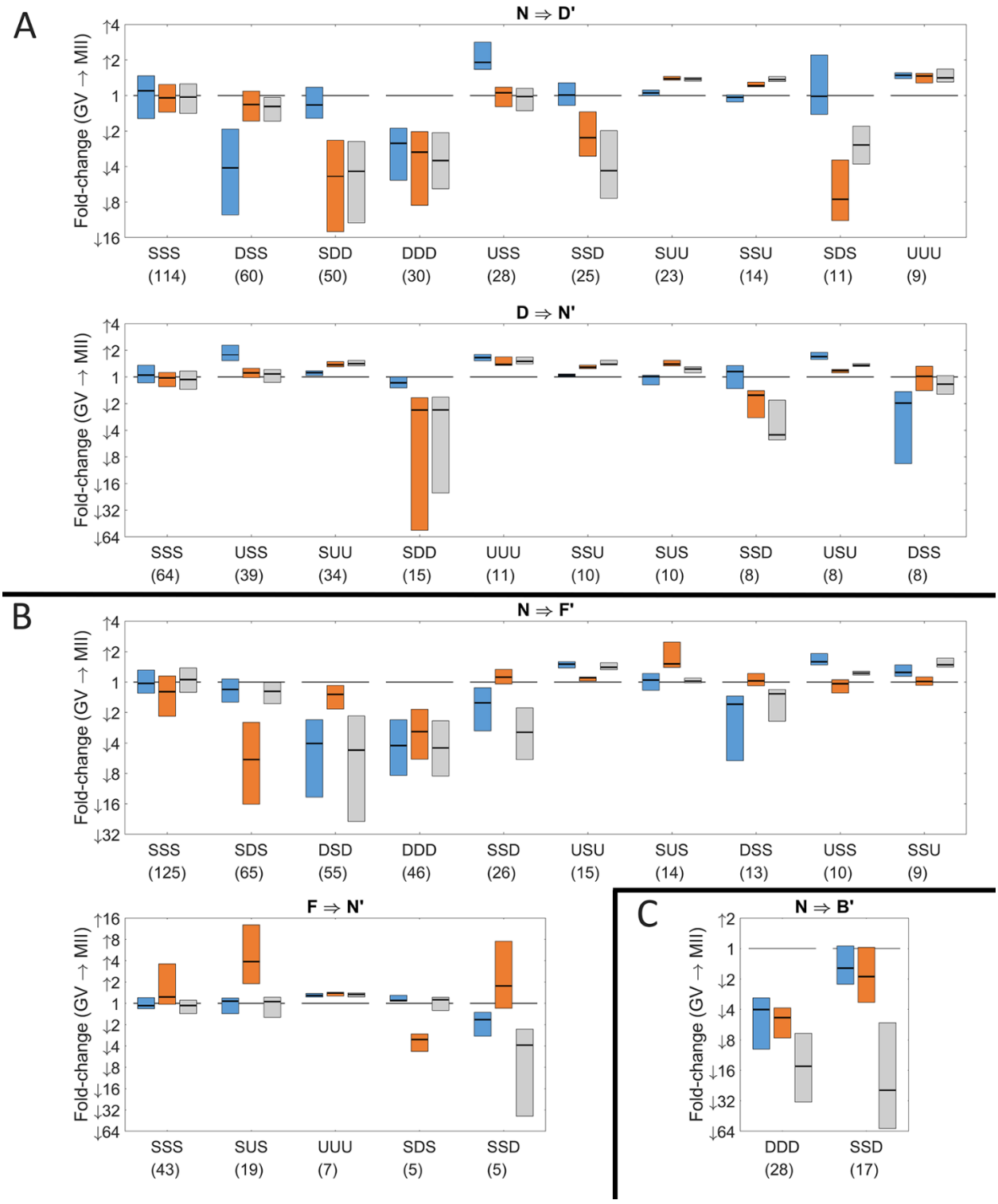

Figure 4.2 GV or MII stage-specific Interstrain DEGs MOR (mode of regulation) groups.

Figure 4.2 GV or MII stage-specific Interstrain DEGs MOR (mode of regulation) groups (cont'd). GV (D,F→N') and MII (N→D', F', B') stage specific DEGs were categorized by changes in mRNA prevalence during maturation. mRNAs can go up (U), down, or remain the same (S) during. The log-fold maturation change were plotted on box plots with the median represented by the horizontal line and 25th and 75th percentile represented by the top and bottom of the box. Number of DEGs in each MOR category are list below in (). Each color represents one of the strains: blue=B6, orange=D2, and grey=BDF1. A) MOR categories where B6 is different from D2 and BDF1 at GV stage (D→N') or MII stage (N→D') but they are not different from each other. B) MOR categories where D2 is different from B6 and BDF1 at GV stage (F→N') or MII stage (N→F') but they are not different from each other. C) MOR categories where BDF1 is different from B6 and D2 at GV stage (D→N') but the parentals are not different from each other. The B→N' transition contained only two mRNAs and is not pictured.

Groups D and D' contain DEGs at the GV and MII stages for which D2 and BDF1 oocytes were more similar to each other than to B6. D→N' denotes genes that only differed from B6 at the GV stage, and N→D' denotes genes that only differed from B6 at the MII stage. The largest MOR category for D→N' genes remained unchanged (SSS) or showed comparatively small changes (USS) during maturation. Two other MOR categories showed increased or decreased prevalence in BDF1 or D2 oocytes but no changes in B6 oocytes during maturation (SUU, SDD), with some mRNAs undergoing particularly large negative fold-changes in D2 and BDF1. The SSD MOR category contained eight mRNAs that underwent large decreases in abundance preferentially in BDF1 oocytes. DEGs found in the same comparisons at MII, group D' (1123), were most likely to be in group N (34%), G (27%), or group D (25%) at GV stage. The reciprocal group (N→ D') became different during maturation and showed a clear trend for genotype differences in mRNA degradation. Although the largest MOR category was again SSS, five MOR categories displayed patterns of preferential mRNA degradation. B6 oocytes preferentially degraded mRNAs in the DSS (n=60) MOR, whereas BDF1 and D2 oocytes preferentially

degraded mRNAs in the SDD, SSD, and SDS MORs. All three genotypes preferentially degraded mRNAs during maturation in the fourth largest MOR for N→ D' (DDD).

F→N' denotes genes that only differed from D2 at the GV stage, and N→F' are genes that only differed from D2 at the MII stage. The largest MOR for F→N' was for genes that remained statistically unchanged (SSS) but displayed a trend to increased abundance for D2 oocytes. The next largest F→N' MOR was SUS with 19 mRNAs significantly increased in D2 oocytes between the GV and MII stages. The SSD MOR also indicated a trend toward increased abundance in D2 oocytes between the GV and MII stages (although not significant). The reciprocal group (N→ F') included mRNAs that became different during maturation and, like N→ D', showed a clear propensity for genotype differences in mRNA degradation. The second largest MOR (SDS) displayed preferential degradation in the defining strain (D2). The N→ F' group differed from N→ D' in that additional MORs (DSD, SUS) were seen indicating greater stabilization in the defining strain (D2 vs. B6).

Groups B and B' contained DEGs at the GV and MII stages where B6 and D2 strains were more similar to each other than to BDF1. These groups were of particular interest as they provide instances where BDF1 oocytes diverge in mRNA expression from both parental strains. Only four DEGs were seen specific to BDF1 oocytes at the GV stage (Group B) and thus were not plotted. The N→B' group had eight MORs (SSS, SSU, SSD, SUD, SDD, UUS, DDS, DDD; two are highlighted in Figure 4.2. The SSD MORs included 17 mRNAs that decreased in abundance only in the BDF1 genotype during maturation. Of particular interest, the DDD MOR category included 28 mRNAs that declined in abundance during maturation in all three genotypes but

decreased more in BDF1 oocytes. In the DDD MOR, BDF1 MII stage oocytes reduced mRNA expression abundances to near background.

For the second approach defining “maturation sets” within genotype and then comparing these between genotypes further revealed extensive genetic differences in mRNA regulation during maturation. The overall fractions of modulated/detected mRNAs were 29% in B6, 30% in D2, and 35% in BDF1 (see DEG Table GSE114158). Substantial fractions of maturation set DEGs were shared across genotypes: 3391 between B6 and D2, 3919 between B6 and BDF1, 4245 between D2 and BDF1, and 3013 genes shared between all three genotypes during (Figure 4.3; see DEG Table GSE114158). Thus, 31% and 28% of the changes that occurred during maturation in B6 and D2 oocytes did not occur in BDF1 oocytes. Additionally, 24% of the changes that occurred in BDF1 oocytes were not observed in either parental strain. These results indicate that there were genetic differences in the regulation of mRNA content during oocyte maturation. Interestingly, even though the BDF1 oocyte gene expression patterns showed less difference to parental genotypes than was observed between the parental genotypes, the BDF1 oocytes displayed the largest number of genotype-specific maturation changes during maturation (Figure 4.3G).

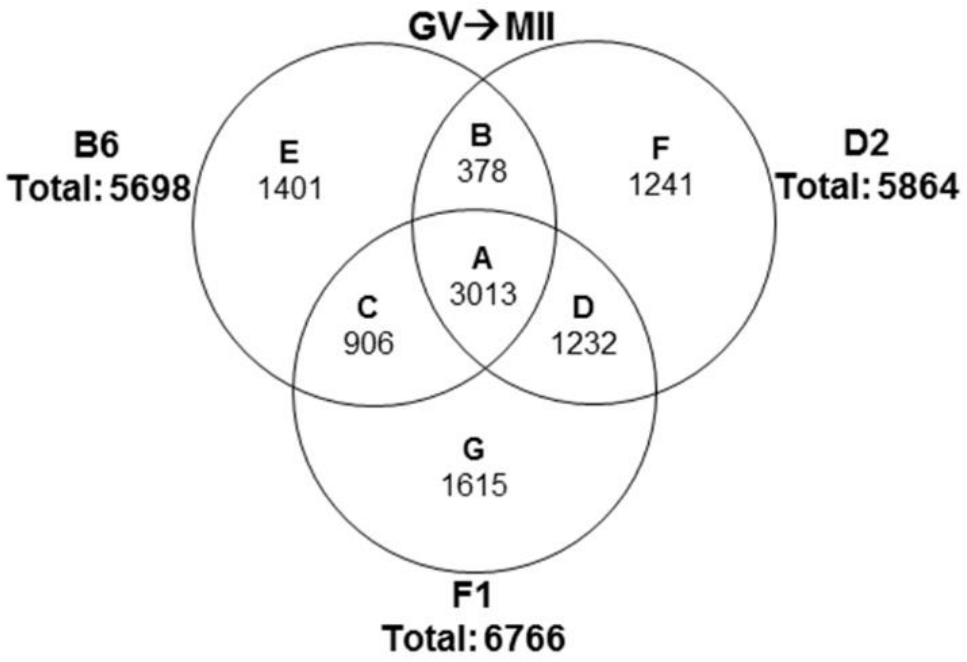

	B6	DEGs	F1	DEGs	D2	DEGs
p<0.05	MII>GV	2104	MII>GV	2603	MII>GV	2197
	GV>MII	3594	GV>MII	4163	GV>MII	3667
p<0.01	MII>GV	1317	MII>GV	1783	MII>GV	1289
	GV>MII	2461	GV>MII	2840	GV>MII	2458

Figure 4.3 Changes associated with oocyte maturation from GV to MII stage. Maturation set DEGs were identified for each of the three genotypes (B6, D2, & BDF1) at each stage (GV or MII), for significant threshold p<0.05. Then, these DEG lists were compared with each other to determine the number of maturation DEGs shared between strains. **Top-**DEGs were organized according to their maturation overlap groups. Group A includes DEGs that changed during oocyte maturation across all three strains. Group G include maturation set DEGs that are specific to BDF1s. **Bottom**-Table that shows the directionality of the maturation set DEGs and also the number of DEGs at the p<0.01 significance level at each strain.

For further insight into these global differences in mRNA regulation, we compared mRNA modulation patterns between genotypes. The modulated mRNAs (3013, p<0.05) underwent significant modulation during oocyte maturation in all three genotypes (Figure 4.3A). Comparing the two parental strains, only 378 mRNAs were modulated in common (Figure

4.3B). This is far smaller than the number of mRNAs that the BDF1 oocytes shared with either B6 (906) or D2 (1232) (Figure 4.3C, D) oocytes.

Collectively, the two approaches combined revealed four clear results: There were more DEGs between genotypes at the MII stage than the GV stage. Many inter-genotype DEGs were observed at only one stage. There were >1000 “maturation set” DEGs unique to each genotype. Lastly, although BDF1 hybrids were more similar to either parental strain than the parental strains were to each other, BDF1s displayed the largest number of genotype-specific maturation changes.

4.3.3 Ingenuity Pathway Analysis of genotype and stage effects on transcriptomes

Because all three genotypes employed are fertile, we were interested to determine whether the three genotypes produced oocytes with differences in specific pathways of biological processes, or whether differences in regulation of different mRNAs between genotypes were compensatory, thereby resulting in little or no overall effect on biological function or cellular phenotype. We first applied IPA to assess the impact of DEGs on upstream regulators (URs) and canonical pathways (CPs) comparing B6 and D2 oocytes, with particular focus on those pathways for which a clear directional difference was apparent by a significant z-score. We then examined differences between BDF1 oocytes and parental oocytes, and finally applied IPA to the “maturation sets” with particular emphasis on BDF1 oocytes and changes unique to them.

IPA revealed hundreds of significant differences in upstream regulators and canonical pathways between B6 and D2 oocytes, indicating that differentially regulated mRNAs are not compensated by each other; i.e., many significant differences likely to impact cellular processes are evident between genotypes. A portion of these was sorted according to the ranking strategy described in Methods (Sup. Tables S4 and S5). Twenty-three upstream regulators were observed with significant z-scores indicating significant activation (n=14) or inhibition (n=9), in D2 compared to B6 at the GV stage oocytes and 22 with significant z-scores (11 inhibited and 11 activated) at the MII stage. Eight of these URs were different between D2 and B6 at both stages, and the direction of the z-scores did not change for any of them between the stages (Table 4.1). A single canonical pathway (sumoylation, z= -2.18 in D2 compared to B6) displayed a significant z-score at the GV stage. Many more canonical pathways were affected at the MII stage, three of which were significantly increased (PPARα/RXRα activation, PTEN signaling, and RhoGDI signaling) and 44 of which were significantly decreased (Including NGF and Thrombin Signaling) in D2 compared to B6 MII stage oocytes (Table 4.2).

Table 4.1 Upstream cellular regulators with significant activation/inhibition states in D2 compared to B6 GV or MII oocytes					
GV			**MII**		
Upstream Regulator	**z-score**	**-log$_{10}$(p)**	**Upstream Regulator**	**z-score**	**-log$_{10}$(p)**
GMNN	2.50	1.79	maslinic acid†	2.67	8.74
SUMO3†	2.36	1.73	CD28	2.61	1.39
↑TAL1*	2.30	1.61	KLF3	2.56	4.60
maslinic acid†	2.24	2.96	SOX1	2.36	1.89
HTT†	2.19	1.40	DMD	2.35	1.59
HOXC6†	2.11	2.36	SUMO3†	2.16	1.83
↓YWHAQ*	2.00	1.35	let-7	2.10	3.74
PARP2	1.99	1.61	HNF4A	2.10	1.66
↓ZBTB10*	1.96	1.95	HOXC6†	2.06	3.92
Vegf†	-3.28	1.73	HTT†	2.02	1.85
↑EGF*†	-3.25	1.81	CD82	1.98	1.74
HGF†	-2.93	1.92	MYC	-3.45	1.33
KLF4†	-2.75	1.43	Vegf†	-3.41	4.10
CREB1	-2.70	3.42	HGF†	-3.40	2.74
ZC3H14	-2.24	1.51	↓STAT6	-2.91	1.51
ADCY	-2.22	1.57	NDRG1	-2.62	1.75
indican	-2.22	2.08	WNT1	-2.52	1.60
RBP1	-2.20	2.03	KLF4†	-2.45	1.66
TRAF2	-2.16	1.52	IL4	-2.42	2.01
EIF4G2	-2.00	1.76	FGF10	-2.36	1.48
CHRNA3	-2	1.61	↑EGF†	-2.24	1.55
CAMK2N2	-1.98	1.76	SOD1	-2.00	1.52
INS	-1.97	1.94			
Significant z score (z>1.96 or z<-1.96) indicates activated or inhibited in D2 oocytes.					
Chemical reagents, drugs, and toxicants were removed					
Cellular upstream regulators restricted to those with FPKM > 0.02 in at least one sample.					
Table restricted to URs with significant -log$_{10}$(p) and z-score.					
*Cellular upstream regulator RNA was DEG in dataset. Arrow indicates direction in D2 GV oocytes.					
†UR was significantly activated/inhibited in D2 compared to B6 at both MII and GV.					

Table 4.2 Canonical pathways significantly increased/decreased in D2 compared to B6 MII oocytes					
Canonical Pathways	**z-score**	**-log$_{10}$(p)**	**Canonical Pathways (Con)**	**z-score**	**-log$_{10}$(p)**
PPARα/RXRα Activation	2.79	2.41	IL-3 Signaling	-2.40	2.31
PTEN Signaling	2.19	3.37	p70S6K Signaling	-2.35	1.77
RhoGDI Signaling	2.06	3.09	IL-8 Signaling	-2.34	3.19
Cholecystokinin/Gastrin-mediated Signaling	-3.84	1.62	Signaling by Rho Family GTPases	-2.34	5.84
NGF Signaling	-3.78	2.29	Rac Signaling	-2.34	4.67
Thrombin Signaling	-3.36	2.61	Remodeling of Epithelial Adherens Junctions	-2.33	7.19
ERK5 Signaling	-3.36	1.40	NF-κB Signaling	-2.33	1.91
Actin Nucleation by ARP-WASP Complex	-3.32	1.34	UVB-Induced MAPK Signaling	-2.32	1.40
mTOR Signaling	-3.18	2.74	Cardiac Hypertrophy Signaling	-2.26	3.45
B Cell Receptor Signaling	-3.16	3.21	NRF2-mediated Oxidative Stress Response	-2.24	3.68
Sphingosine-1-phosphate Signaling	-3.00	1.83	Role of NFAT in Cardiac Hypertrophy	-2.24	2.35
α-Adrenergic Signaling	-2.83	2.74	Macropinocytosis Signaling	-2.18	4.52
CXCR4 Signaling	-2.80	4.43	Integrin Signaling	-2.18	5.98
HGF Signaling	-2.79	3.65	PEDF Signaling	-2.13	2.74
RANK Signaling in Osteoclasts	-2.75	3.13	Glioma Signaling	-2.12	3.36
Production of Nitric Oxide and Reactive Oxygen Species in Macrophages	-2.66	2.55	GNRH Signaling	-2.08	5.65
PKCθ Signaling in T Lymphocytes	-2.65	1.73	Regulation of eIF4 and p70S6K Signaling	-2.07	1.93
PI3K/AKT Signaling	-2.61	5.22	LPS-stimulated MAPK Signaling	-2.07	1.76
14-3-3-mediated Signaling	-2.60	3.96	Regulation of Actin-based Motility by Rho	-2.07	1.34
fMLP Signaling in Neutrophils	-2.60	1.92	Type II Diabetes Mellitus Signaling	-2.04	1.70
NF-κB Activation by Viruses	-2.56	2.39	Thrombopoietin Signaling	-2.00	1.77
Gαq Signaling	-2.54	3.07	CD40 Signaling	-2.00	1.32
SAPK/JNK Signaling	-2.50	3.35	Sumoylation Pathway*	-1.96	2.83
CD27 Signaling in Lymphocytes	-2.50	3.16			
Table restricted to CPs with significant -log$_{10}$(p) and z-score.			*Sumoylation only CP that had significant Z score for B6 vs D2 at GV.		
Significant z score (z>1.96 or z<-1.96) indicates increased or decreased in D2 oocytes.					

Incorporating comparisons of BDF1 oocytes to the two parental strains revealed four classes of effects for URs and CPs: 1) parental strains different and BDF1 displays an intermediate phenotype); 2) BDF1 displays a dominance effect; 3) all three genotypes differ; and 4) BDF1 displays a transgressive quality. The most prevalent classes for affected URs at the GV stage were class 1 and class 2, consistent with many differences between parental strains, along with many dominance effects in the BDF1 oocytes (Table 4.3 & 4.4). Transgressive effects for URs in F1 oocytes were limited to the cellular regulator RICTOR, which had a significant z-score between BDF1 and D2 and a significant p-value between BDF1 and both parental strains in MII stage oocytes. There were no transgressive (class 4) canonical pathways.

Table 4.3 Upstream Regulators with significant activation/inhibition across four classes of interstrain comparisons							
GV				**MII**			
Class 1: B6 different than D2, but neither different from F1							
Upstream Regulator	**z-score**			**Upstream Regulator**	**z-score**		
	GV BvD	**GV BvF**	**GV DvF**		**MII BvD**	**MII BvF**	**MII DvF**
GMNN	2.50			CD28	2.61		
TAL1	2.30			DMD	2.35	2.22	-1.98
maslinic acid	2.24			SUMO3	2.16		
HTT	2.19			let-7	2.10	1.81	
CD24	2.10			HNF4A	2.10		
YWHAQ	2.00			HTT	2.02		
PARP2	1.99			CD82	1.98		
CAMK2N2	-1.98			AKAP12	-1.98		
CHRNA3	-2.00			SOD1	-2.00		
TRAF2	-2.16			beta-1,3-glucan	-2.24		
RBP1	-2.20			EGF	-2.24		
indican	-2.22			FGF10	-2.36		
ADCY	-2.22			IL4	-2.42		
ZC3H14	-2.24			KLF4	-2.45		1.93
CREB1	-2.70	-1.79		NDRG1	-2.62		
KLF4	-2.75			MYC	-3.45		2.57
HGF	-2.93	-2.57					
EGF	-3.25	-2.10					
Vegf	-3.28	-2.59					
Class 2: B6 different than D2, and either B6 or D2 is also different from F1							
SUMO3	2.36	2.00		KLF3	2.56	1.25	
ZBTB10	1.96			SOX1	2.36		-1.67
EIF4G2	-2.00			HOXC6	2.06		-0.82
				WNT1	-2.52		1.32
				STAT6	-2.91		1.84
				HGF	-3.40	-2.28	
				Vegf	-3.41	-2.64	
Class 3: All three strains different							
HOXC6	2.11	1.67	-1.00	None			
INS	-1.97	-1.47	1.25				

Table 4.3 (cont'd) Upstream Regulators with significant activation/inhibition across four classes of interstrain comparisons				
Class 4: F1 different from B6 and D2, but B6 and D2 are not different from each other				
None	RICTOR		-0.65	-2.22
Chemical reagents, drugs and toxicants were removed.				
Significant z score (z>1.96 or z<-1.96) indicates activated or inhibited in second strain listed.				
Cellular upstream regulators restricted to those with FPKM > 0.02 in at least one sample.				
Class 1: Significant z-score between B6 and D2.				
Class 2: Significant z-score between at least one of the parental strain and F1.				
Class 3: Significant z-score between B6 and D2.				
Class 4: Significant z-score for at least 1 comparison.				

Table 4.4 Canonical Pathways significantly increased/decreased MII stage oocytes across four classes of interstrain comparisons							
Class 1: B6 different than D2, but neither different from F1				**Class 2: B6 different than D2, and either B6 or D2 is different from F1**			
Upstream Regulator	**z-score**			**Upstream Regulator**	**z-score**		
	MII BvD	**MII BvF**	**MII DvF**		**MII BvD**	**MII BvF**	**MII DvF**
PPARα/RXRα Activation	2.79	1.41	-2.65	RhoGDI Signaling	2.06	1.00	0.63
Thrombopoietin Signaling	-2.00	-2.00	1.34	Sumoylation Pathway*	-1.96	-1.13	0.82
CD40 Signaling	-2.00	0.00	1.00	Reg. eIF4 and p70S6K	-2.07	n/a	0.82
Type II Diabetes Mellitus Signaling	-2.04	-2.33	0.82	Glioma Signaling	-2.12	-2.00	0.63
LPS-stimulated MAPK Signaling	-2.07	-1.13	0.82	Integrin Signaling	-2.18	-0.28	0.28
Reg. Actin-based Motility by Rho	-2.07	0.00	0.00	NFAT in Cardiac Hypertrophy	-2.24	n/a	n/a
PEDF Signaling	-2.13	-1.34	0.38	Epithelial Adherens Junctions	-2.33	n/a	n/a
NRF2-me. Oxidative Stress Resp.	-2.24	-0.82	0.45	Rac Signaling	-2.34	-0.45	0.33
Cardiac Hypertrophy Signaling	-2.26	-1.29	n/a	IL-3 Signaling	-2.40	-1.34	1.41
UVB-Induced MAPK Signaling	-2.32	n/a	1.00	SAPK/JNK Signaling	-2.50	n/a	0.71
NF-κB Signaling	-2.33	-1.00	0.58	HGF Signaling	-2.79	-1.41	1.67
IL-8 Signaling	-2.34	-3.00	1.27	α-Adrenergic Signaling	-2.83	-1.67	n/a
p70S6K Signaling	-2.35	-1.89	1.00	Thrombin Signaling	-3.36	-2.31	1.73
CD27 Signaling in Lymphocytes	-2.50	n/a	n/a	Cholecystokinin/Gastrin-med.	-3.84	-1.00	2.45
Gαq Signaling	-2.54	-1.27	1.41	**Class 3: All three strains different**			
NF-κB Activation by Viruses	-2.56	-2.45	1.34				
14-3-3-mediated Signaling	-2.60	-2.24	0.82	PTEN Signaling	2.19	1.00	-0.91
fMLP Signaling in Neutrophils	-2.60	-1.41	1.89	GNRH Signaling	-2.08	-0.47	1.27
PI3K/AKT Signaling	-2.61	-2.12	0.33	Macropinocytosis Signaling	-2.18	-1.63	1.13
PKCθ Signaling in T Lymphocytes	-2.65	-1.89	0.63	Signaling by Rho GTPases	-2.34	-1.73	-0.73

Table 4.4 (cont'd) Canonical Pathways significantly increased/decreased MII stage oocytes across four classes of interstrain comparisons							
Production of Nitric Oxide and Reactive Oxygen Species in Macrophages	-2.66	n/a	1.00	CXCR4 Signaling	-2.80	-0.78	0.91
RANK Signaling in Osteoclasts	-2.75	-0.45	0.45	B Cell Receptor Signaling	-3.16	-1.00	0.58
Sphingosine-1-phosphate Signaling	-3.00	-1.63	1.63	mTOR Signaling	-3.18	-2.83	1.41
Actin Nuc. by ARP-WASP Complex	-3.32	n/a	2.00				
ERK5 Signaling	-3.36	-2	1.342	**Class 4: F1 different from B6 and D2, but B6 and D2 are not different from each other**			
NGF Signaling	-3.78	n/a	1.89	None			
Significant z score (z>1.96 or z<-1.96) indicates increased or decreased in second strain listed.							
*Also present in Class 2 in GV stage oocytes.							
Class 1: Significant z-score between B6 and D2.							
Class 2: Significant z-score between at least one of the parental strain and F1.							
Class 3: Significant z-score between B6 and D2.							
Class 4: Significant z-score for at least 1 comparison.							
See supplemental Table 3 for ranking score, p value, and additional information.							

To apply IPA to the “maturation sets”, we analyzed the 1915 DEGs ($p<0.01$) in Figure 4.3A that represent the DEGs that were shared between all three genotypes for comparisons of GV and MII stages. Some of these shared maturation set DEGs likely have important roles in oocyte maturation to have a similar maturation change arcross all three genotypes. The top three non-chemical URs with the greatest activation across all three genotypes were VEGFA, INSR, and IGF1R (Sup. Table S4). The top three non-chemical URs with the largest inhibition across all three genotypes were RICTOR, KDM5A, and Alpha-Catenin (Sup. Table S4). Of the many CPs significantly altered during maturation (Sup. Table S5), three with significant z-scores were seen, including EIF2 signaling (activated), and sirtuin signaling and RhoGDI signaling (inhibited) (Sup. Table S5).

Changes in mRNA abundance shared between parental strains but not in BDF1 oocytes (group B genes, Figure 4.3) revealed many affected URs including two URs that with significant z-scores (PTH, inhibited; NFE2L2, activated) (Sup. Table S4). Very few CPs of this type were identified, none with significant z-scores (Sup. Table S5). We applied UR and CP analysis to all of the mRNAs that changed in abundance during BDF1 oocyte maturation (Figure 4.3A,C,D,G). Of the 941 URs identified by this analysis (see truncated list Sup. Table S4), 24% were only significantly altered during BDF1 maturation, ten of which had significant z-scores (Table 4.5). Of the 183 CPs significantly altered during BDF1 maturation (see truncated list Sup Table S4), 32% were only significantly altered during BDF1 maturation. One of these CPs, cell cycle: G2/M DNA damage checkpoint regulation, displayed a significant activation z-score only for BDF1 maturation. These results highlight specific cellular processes that are uniquely altered during maturation in BDF1 oocytes.

Table 4.5. Upsteam Cellular regulators activation/inhibition states unique to F1 oocyte maturation (GV vs MII)		
Upstream Regulator	**z-score**	**-log$_{10}$(p)**
	F1-all (Fig 3A,C,D,G)	F1-all (Fig 3A,C,D,G)
BNIP3L	3.00	1.55
CD44	2.73	1.54
INHBB	2.21	1.58
S1PR3	2.21	1.32
ETV4	2.08	1.41
EGR1	2.02	1.67
LASP1	2.00	2.99
MTM1	-1.99	1.40
E2f	-2.06	1.33
ACOX1	-2.12	1.49
List restricted to URs with signifncant Z score.		
Significant z score (z>1.96 or z<-1.96) indicates activated or inhibited in F1 MII oocytes.		
Cellular upstream regulators restricted to those with FPKM > 0.02 in at least one sample.		
Chemical reagents, drugs,and toxicants were removed		

4.3.4 Transgressive and dominance effects on BDF1 hybrid oocyte transcriptomes

The preceding results demonstrate that, while many genes in BDF1 oocytes display the expected “blending” of parental expression traits, often BDF1 oocytes appear more similar to one or the other parental strains. This suggested that some genes do not follow the simple blending mode of expression, and thus may confer BDF1 oocytes a combination of B6-like and D2-like characteristics (Figure 4.4). A better understanding of the identities and functions of those specific genes should provide insight into the unique characteristics of BDF1 oocytes.

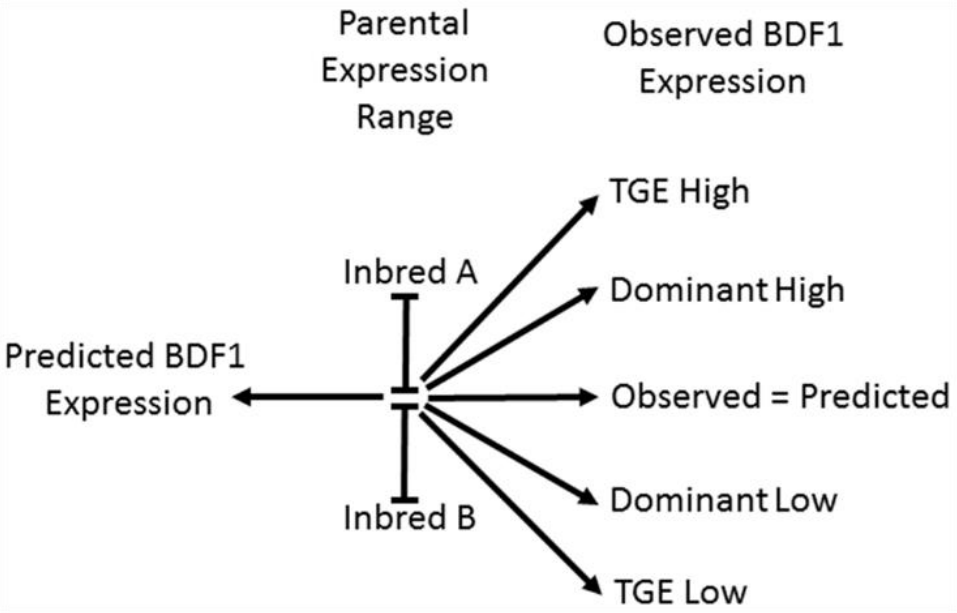

Figure 4.4 Two complementary approaches to discern effects in BDF1 hybrids. Based on Mendelian genetics, F1 gene expression would be predicted as the average between the two parental strains, and sometimes this occurs (Observed = Predicted). When F1 expression closely resembles one parental strain, this is categorized as Dominance (Dom –high or –low). When F1 gene expression exceeds the boundary set by the high or low expression parental strain, it is considered Transgressive Gene Expression (TGE) –High or –Low.

One potential way for genetic hybridization to impact BDF1 oocyte characteristics would be through transgressive gene expression, wherein the BDF1 gene expression level of a gene is significantly higher (TGE-H) or lower (TGE-L) than the level of expression of either parental strain (i.e., outside the range defined by the two parents). However, we observed only a single gene displaying TGE at the GV stage (4933406M09Rik), and a total of just 25 genes displaying TGE in MII stage oocytes (22 TGE-L and 3 TGE-H; Sup. Table S6). Among the most highly repressed TGE-L genes in BDF1 oocytes were *Fads2, Qrsl1, Ebf1* and *Sim1*. The tiny number of TGE genes relative to the vast number observed BDF1 DEGs suggested the need for a different

hypothesis to explain how BDF1 oocytes are so different from expected based solely on blending of parental expression.

A second way BDF1 hybrids could diverge from intermediate levels of expression is to display a dominant pattern of gene expression, wherein the BDF1 resembles one parental type closely, but is significantly different from the other parental type. We initially observed dominance effects using IPA above. For a more comprehensive focused evaluation of dominance at the level of individual genes, we identified subsets inter-strain DEGs (B6 vs. D2) that displayed dominance in BDF1 oocytes. We assigned dominance to a DEG when BDF1 and parental strain A expression were both significantly different from parental strain B, and BDF1 and parental strain A expression levels were within 20% (of the parental range) of each other. We used a dominance ratio (DR) to determine these relationships. For gene *g*, we defined dominance ratio $DR(g) = (expr_{F1}(g) – expr_B(g))/(expr_A(g) – expr_B(g))$, where A and B were parental strains. We call the strain A dominant for gene *g* if: $DR(g) \geq .8$ and g was differentially expressed in comparisons A vs B and BDF1 vs B. We used the specific terms “dominance-high” for $expr_A(g) > expr_B(g)$, and “dominance-low” for $expr_A(g) < expr_B(g)$.

This analysis revealed 368 genes displaying dominance at the GV stage and 528 genes displaying dominance at the MI stage, for a total of 896 genes displayed dominance in mRNA expression in BDF1 oocytes (Sup. Table S7 & S8; Figure 4.5). Only 47 of these genes displayed similar dominance patterns at both stages (Figure 4.5), with most (849) displaying dominance only at one stage, further indicating vast changes in the mRNA population during maturation unique to BDF1 oocytes.

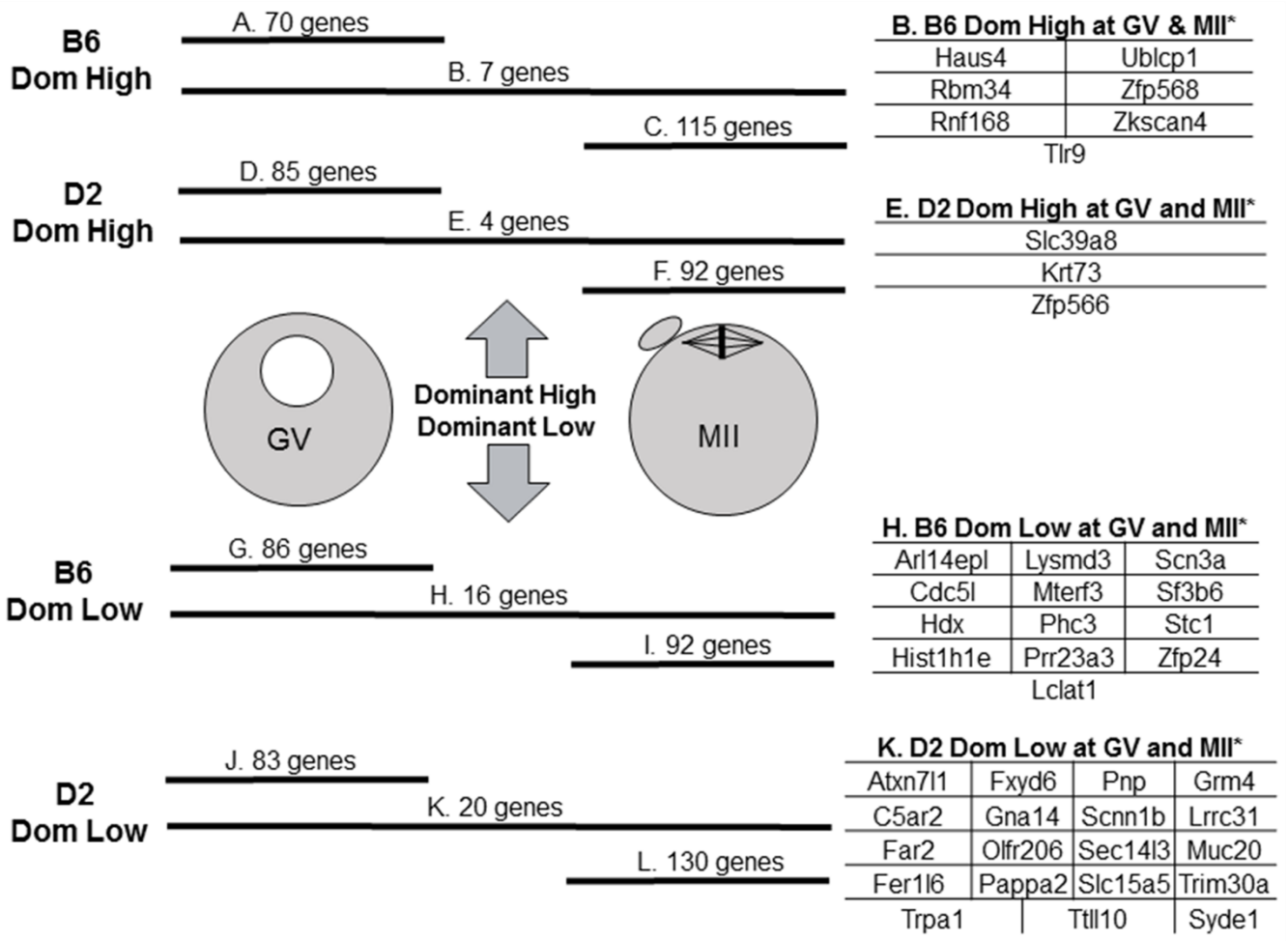

Figure 4.5 RNAs that display parental dominance in BDF1 at MII, GV, or both stages. Dominance DEG lists from each stage were compared to each other to identify what dominance genes are stage-specific (A, C, D, F, G, I, J, L) and which ones display the same dominance pattern of expression at both stages (B, E, H, K). *Some unnannoted RNAs were removed from tables: (E) 1700024I08Rik, (H) 1810013L24Rik, Gm5039, LOC101056073, (K) Gm36876.

Recognizing that BDF1 oocytes manifest both high and low B6-like and D2-like expression dominance effects concurrently at each stage, and that the effects on phenotype would therefore be additive, we created “additive dominance” (AddDom) gene lists for each stage. We then applied IPA to simple dominance DEG sets and the AddDom DEG set to determine the extent to which URs and CPs associated with dominance effects in BDF1 oocytes were driven by simple effects of either parental genetic contribution acting alone, or by additive dominance effects of both genetic contributions acting together.

At the GV stage, there were many URs significantly associated with individual dominance DEGs sets (Sup. Table S9), but more URs that emerged when assessing additive dominance. Thirty-seven URs only rise to significance using the AddDom DEG set at the GV stage, indicating a strong additive effect of the two parental genetic contributions together on BDF1 oocyte features. Fifteen of these 37 URs encompassed at least five associated DEGs (Table 4.6). The top three of these Huntington (HTT) URs significantly associated with observed DEGs in the MII dataset. Thirty-six URs only rose to significance at the MII stage in the AddDom category (see truncated list Sup. Table S9), of which 14 had five or more associated DEGs (Table 4.6). The top three of these URs with the most associate DEGs were an immune regulation factor (IL4), and two transcriptional regulators (CREB1 & EP300) (Table 4.6). Thirty-eight CPs only rose to significance in the AddDom analysis at the GV stage (Table 4.7, see truncated list Sup. Table S10). Among these were NRF2-mediated oxidative stress response and role of NFAT in cardiac hypertrophy (Table 4.7). In MII stage oocytes, five CPs only rose to significance with the AddDom gene set (Sup. Table S10), four with at least five associated DEGs, including Gαq signaling, mTOR signaling, and CXCR4 signaling (Table 4.7). The major IPA results for URs and

CPs affected specifically in the AddDom analysis indicating combined effects of dominance for the two parental genetic contributions are summarized in Figure 4.6.

Table 4.6. Cellular upstream regulators at GV and MII that are only significant in the additive dominance category

GV			MII		
Upstream Regulator	**-log_{10}(p)**	**Associated DEGs**	**Upstream Regulator**	**-log_{10}(p)**	**Associated DEGs**
UCHL1	2.05	4	CD28	1.79	13
EGR2	1.82	6	FOXO3	1.73	12
HIST1H1T	1.57	4	IL5	1.68	11
Hist1h1a	1.57	4	CREB1	1.57	18
ADORA2A	1.53	5	MYOC	1.56	5
E2F4	1.52	7	FOXO4	1.47	5
STAT5a/b	1.50	4	CXCL12	1.46	8
CAV1	1.49	5	APC	1.42	6
CNR1	1.45	5	EP300	1.39	14
SOD2	1.44	4	INSR	1.37	13
IL6ST	1.43	3	IL4	1.33	24
HES1	1.41	3	MYCN	1.32	10
IL32	1.41	3			
HIF1A	1.41	10			
HTT	1.33	15			
Chemical reagents, drugs, and toxicants were removed					
Cellular upstream regulators restricted to those with FPKM > 0.02 in at least one sample.					
No UR listed had significant -log_{10}(p) values in either the B6 or D2 dominance lists alone.					
*Activated in additive dominance category					

Table 4.7. Canonical Pathways at GV and MII that are only significant in the additive dominance category			
GV			
Ingenuity Canonical Pathway	**-log$_{10}$(p)**	**Molecules**	**Associated DEGs**
Insulin Receptor Signaling	2.01	↓PRKCI, ↑NRAS, ↓SOS2, ↓FGFR2, ↑TLR9, ↓SCNN1B	5
Glioblastoma Multiforme Signaling	1.74	↓TP53, ↑IGF2, ↑NRAS, ↓SOS2, ↓FGFR2, ↑TLR9	6
14-3-3-mediated Signaling	1.57	↑TUBB3, ↓PRKCI, ↑NRAS, ↓FGFR2, ↑TLR9	5
PKCÎ¸ Signaling in T Lymphocytes	1.54	↑NRAS, ↓HLA-DMA, ↓SOS2, ↓FGFR2, ↑TLR9	5
Th1 Pathway	1.52	↓ITGB2, ↓HLA-DMA, ↓FGFR2, ↑TLR9, ↓NOTCH1	5
Gα12/13 Signaling	1.52	↑NRAS, ↑CDH17, ↓FGFR2, ↑TLR9, ↑MEF2B	5
NRF2-mediated Oxidative Stress Response	1.41	↓PRKCI, ↑NRAS, ↑DNAJA3, ↓FGFR2, ↓GCLM, ↑TLR9	6
Role of NFAT in Cardiac Hypertrophy	1.41	↓PRKCI, ↑NRAS, ↓SOS2, ↓FGFR2, ↑TLR9, ↑MEF2B	6
Th2 Pathway	1.35	↓ITGB2, ↓HLA-DMA, ↓FGFR2, ↑TLR9, ↓NOTCH1	5
MII			
Gαq Signaling	1.93	↑RHOB, ↓ITPR2, ↓RGS7, ↓RHOU, ↓GNA14, ↓GSK3B, ↑TLR9, ↑GYS2	8
mTOR Signaling	1.42	↓RPS4Y1, ↑RHOB, ↓RHOU, ↓RPS27A, ↓PPP2R5E, ↓RPS5, ↑TLR9, ↓PRKAG1	8
CXCR4 Signaling	1.42	↓PXN, ↑RHOB, ↓ITPR2, ↓RHOU, ↓ARHGEF11, ↓GNA14, ↑TLR9	7
Cholecystokinin/Gastrin-mediated Signaling	1.37	↓PXN, ↑RHOB, ↓ITPR2, ↓RHOU, ↓MAPK7	5
Canonical Pathways shown only if had 5 target DEGs identified.			

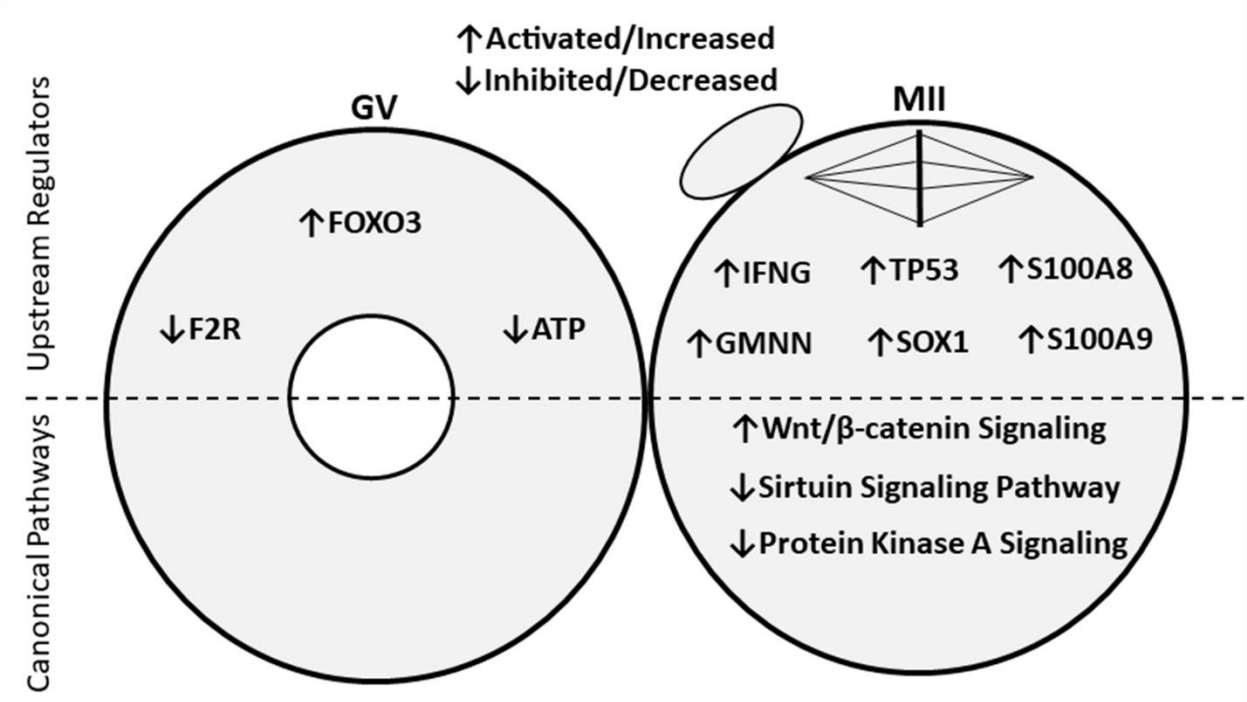

Figure 4.6 Upstream regulators and canonical pathways significantly activated/increased or inhibited/decreased in additive dominance category. URs and CPs with significant z-scores at GV or MII in additive dominance category.

4.3.5 Divergence of actual BDF1 hybrid oocyte gene expression from predicted BDF1 oocyte gene expression pattern

The above analyses, particularly the AddDom analysis, required the application of specific thresholds to generate mRNA lists for IPA analysis (e.g., the degree of parental and BDF1 similarity to conclude dominance). The use of such thresholds creates a degree of imprecision because including/excluding genes near the threshold can affect outcomes. To overcome the need for such thresholding, we applied an alternate approach to identify genes that are most highly affected by BDF1 hybridization and used that list of genes for IPA analysis. This process began by generating groups of five "predicted BDF1" RNAseq expression libraries

for each stage by averaging the gene expression levels between randomly selected B6 and D2 parent libraries. This was repeated multiple times using different random pairings of parental libraries to produce the five predicted BDF1 transcriptomes. Comparing the predicted and actual transcriptomes yielded a list of DEGs, for which BDF1 oocytes display greater or lesser than expected mRNA levels, without the need for thresholding.

At the GV stage (q=0.05), we observed 32 DEGs comparing actual and synthetic BDF1 transcriptomes (Table 4.8, Sup. Table S11). Most of these were lower in the actual F1 than the predicted BDF1 transcriptome. IPA suggested significant effects on the activation states of 14 upstream cellular regulators. Two of these (estrogen receptor, ESR, and V-Ha-Ras Harvey rat sarcoma viral oncogene homolog, HRAS) had at least three-affected target DEGs, but neither remained significant at the MII stage (Sup. Table S13). Two canonical pathways (protein kinase A signaling and synaptic long-term depression) had at least three affected DEGs, but neither of these remained significant at the MII stage (Sup. Table S13). At the MII stage (q=0.05), the analysis revealed 207 DEGs differing between actual and synthetic BDF1 transcriptomes (Table 4.8, Sup. Table S12). As with the GV stage oocytes, most of these DEGs were lower in actual BDF1 than the predicted BDF1 transcriptome. IPA revealed 38 significantly affected upstream cellular regulators that met our threshold criteria and had least three associated DEGs, six of which displayed significant z-scores (Table 4.9 & Sup. Table S12). This included three inhibited URs (RICTOR, FFAR3, and ACOX1), and three activated URs (IGF1R, INSR, and MAP3K1) in the actual BDF1 compared to the predicted BDF1 transcriptome. We observed seven altered canonical pathways (with three associated DEGs) including the Sirtuin Signaling Pathway that was decreased in actual BDF1 MII oocytes compared to the predicted BDF1 MII transcriptome

(Sup. Table S14; Figure 4.7). The signaling pathways for INSR and sirtuin were also affected in the AddDom analysis above.

Table 4.8 Number of DEGs between B6D1F1/J and predicted B6D2F1/J mice (q=0.05)

	GV	MII
Actual F1 > Predicted F1	9	49
Actual F1 < Predicted F1	23	158

Table 4.9 Cellular upstream regulators with different activation/inhibition state in actual B6D2F1/J compared to predicted B6D2F1/J MII oocytes					
Upstream Regulator	**Molecule Type**	**Predicted Activation State**	**z-score**	**-log$_{10}$(p)**	**Target DEGs**
RICTOR	other	Inhibited	-3.000	3.77	↓ATP5O, ↓COX4I1**, ↓Cox5b*, ↓RPL41*, ↓Rplp1 (includes others), ↓RPS19, ↓RPSA, ↓Uba52**, ↓UQCRQ**
IGF1R	transmembrane receptor	Activated	2.236	1.30	↓ATP5O, ↑BCL2, ↓COX4I1**, ↓Cox5b*, ↓SFMBT2*
INSR	kinase	Activated	2.213	1.54	↓ACADVL, ↓ATP5O, ↓CDC5L*, ↓COX4I1**, ↓Cox5b*, ↓MBD1*, ↓SFMBT2*
FFAR3	g-protein coupled receptor	Inhibited	-2.000	2.54	↓FADS2**, ↓Foxp2*, ↓PITPNM3, ↓TRPC4
ACOX1	enzyme	Inhibited	-1.982	1.64	↓ACADVL, ↓CD63, ↓MFGE8, ↓PIGP
MAP2K1	kinase	Activated	1.980	1.98	↑BCL2, ↓GLI2**, ↓ITGB4*, ↓MMP14, ↓UBC*
Chemical reagents, drugs,and toxicants were removed					
*Displays dominant expression in F1 oocytes.					
**Displays TGE expression in F1 oocytes.					
Significant z score (z>1.96 or z<-1.96) indicates activated or inhibited in actual F1 MII oocytes.					

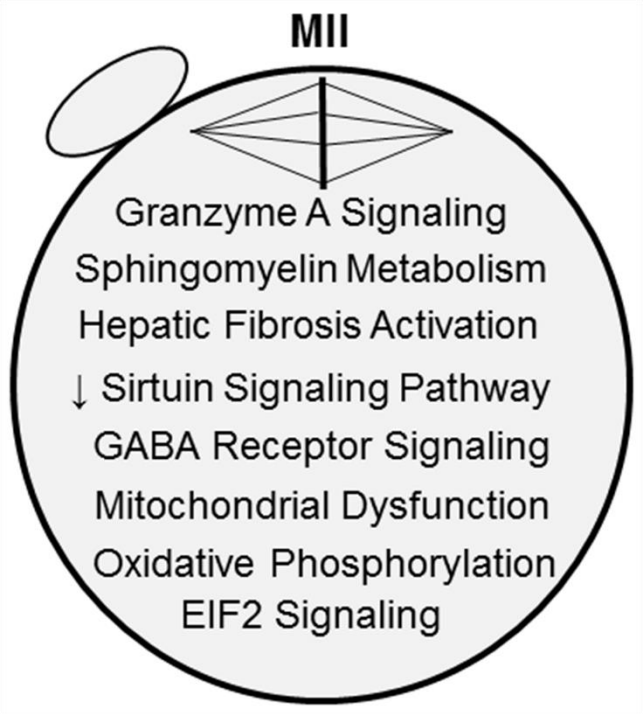

Figure 4.7 Canonical pathways significantly different between actual and predicted BDF1 MII stage oocytes. Canonical pathways with at least three associated DEGs. Sirtuin Signaling also had a significant z-score and was decreased in actual BDF1 MII stage oocytes compared to the predicted BDF1 expression.

Although IPA indicated an effect on sirtuin signaling, we noted that none of the associated sirtuin mRNAs implicated by IPA for this CP (*sirt1-7)* s were identified as DEGs, suggesting that the underlying reason for the IPA result for sirtuin signaling rested at the level of differentially expressed downstream genes associated with the pathway. Several of these downstream genes were in the histone 1H gene cluster (*Hist1h1c, Histh1e, Hist1h1d*). Upon further examination of the expression of all members of this cluster, we found that 21 of the 55 were significantly downregulated during maturation only in BDF1 oocytes (Table 4.10). One member, *Histh1t*, increases during meiotic maturation.

Table 4.10 *Hist1h* mRNAs only significantly altered in BDF1 oocytes during meiotic maturation			
ID	**GV vs MII (fold-chage)**		
	B6	**D2**	**F1**
Hist1h1d	-1.83	-1.17	-2.53
Hist1h1t	1.16	1.40	25.40
Hist1h2aa	1.30	-1.32	-1.61
Hist1h2ac	-1.10	-1.58	-2.08
Hist1h2ae	-1.25	-1.59	-2.35
Hist1h2ag	-1.18	-1.61	-2.22
Hist1h2ah	-1.20	-1.58	-2.36
Hist1h2an	-1.17	-1.61	-2.45
Hist1h2bb	1.24	-1.21	-1.37
Hist1h2bc	-1.15	-1.10	-1.27
Hist1h2be	1.11	-1.22	-1.50
Hist1h2bf	1.19	-1.21	-1.41
Hist1h2bg	1.18	-1.07	-1.35
Hist1h2bh	1.22	-1.03	-1.31
Hist1h2bl	1.10	-1.21	-1.49
Hist1h2bm	-1.02	-1.35	-1.41
Hist1h2bn	1.25	-1.08	-1.46
Hist1h2bp	1.10	-1.17	-1.37
Hist1h2bq	1.16	-1.21	-1.41
Hist1h2br	1.18	-1.16	-1.36
Hist1h4d	-1.16	-1.22	-1.74

4.4 Discussion

The goal of this study was to use RNAseq analysis combined with IPA and novel computational approaches to discover the effects genotype on mouse oocyte transcriptomes comparing two fertile inbred strains, and more importantly to understand how F1 hybrid oocytes acquire their superior characteristics (i.e., 'hybrid vigor'). The main discoveries of these studies are three-fold. First, there is a large amount of difference in oocyte transcriptomes between inbred parental strains. Second, a key aspect of superior BDF1 hybrid phenotype is attributable to additive dominance effects, with additional input by genes displaying

intermediate levels of gene expression. A much lesser effect of transgressive gene expression (affecting <30 mRNAs) is seen. Third, the IPA analysis reveals effects of the BDF1 hybrid genotype on a discrete set of CPs and URs, with contributions mediated by intermediate expression, dominance expression, and transgressive gene expression gene categories, many of which only became apparent using a novel comparison of predicted versus actual mRNA expression values for BDF1 oocytes.

4.4.1 Extensive differences between parental strains and between parental strains and BDF1 hybrids

The vast differences between the transcriptomes of the three genotypes is surprising, given that all three genotypes are fertile. The transcriptomes differed more between the two parental strains than between either parental strain and BDF1 hybrids. BDF1 oocytes displayed an intermediate level of expression for many genes. Despite this, BDF1 oocytes displayed many unique affected processes that distinguish them from the parental strain oocytes. Although the oocytes of the three genotypes display many differences in phenotypic characteristics, this vast difference in mRNA expression in oocytes might not have been predicted a priori. We observed differences in the expression of prominently expressed mRNAs and mRNAs for genes known to be important in oogenesis and meiosis, such as genes encoding proteins with roles in chromosome alignment [AURKB, (K. Shuda et al., 2009)], sister-chromatid separation [CDC20, (Jin et al., 2010)], microtubule-organizing center stretching [KIF11, (Clift & Schuh, 2015)], zygotic genome activation [YAP1, (Yu et al., 2016)], and microtubule-organizing center formation [CEP192, (I. W. Lee et al., 2018)].

These differences are accompanied by differences in level of activation/increase or inhibition/decrease in URs and CPs between parental strains. This includes SUMO3, a contributor to GVBD and spindle formation in the oocyte (Ding, Kaido, Llano, Pendas, & Kitajima, 2018; Feitosa & Morris, 2018), and VEGF, which supports pre-ovulatory angiogenesis (Levitas et al., 2000), and the pathways for sumoylation, signaling by RHO family GTPases, and mTOR signaling.

We also observed extensive differences in mRNA regulation during maturation. While the number of mRNAs undergoing changes in abundance were somewhat similar, BDF1 hybrid oocytes displayed more changes during maturation (35%) than B6 (29%) or D2 (30%) oocytes. Additionally, the distribution of changes between relative increases and decreases in mRNA abundance during maturation varied with strain, with > 60% of the DEGs declining in abundance in maturing B6 and BDF1 oocytes, but < 40% declining in D2 oocytes. This indicates profound genotype effects on maternal mRNA translation and degradation, further emphasizing the large variation possible between fertile oocytes.

Such large genetic differences in mRNA regulation raise new concerns about the use of single or small numbers of molecular markers of oocyte quality, by indicating that putative markers may vary in expression but have little effect on phenotype due to variations in expression of other genes. We compared our DEG lists to lists of putative oocyte quality markers reported in other studies, and find that a substantial fraction of these [36% bovine; (E. Orozco-Lucero, 2014), 46% rhesus monkey (Y. S. Lee, Latham, & Vandevoort, 2008), and 50% human (Grondahl et al., 2010)] are differentially expression between the mouse genotypes in this study. Additionally, for 25% of the primate and 36% of the human oocyte-quality markers

the fold-change differences between mouse genotypes exceeded the fold-change differences between the different quality oocytes. This indicates that the natural variability of these genes between healthy oocytes could limit their utility as markers of oocyte quality. Consequently, knowledge of genetic modifiers and compensatory mechanisms that confer fertility even in the face of dramatically variation in particular transcript levels is needed, and the value of putative markers needs to be assessed across genotypes. Moreover, studies that address impacts of environmental factors, maternal health and nutrition, and other oocyte-extrinsic parameters must address genetic variability before being widely generalized.

Yet, >3000 mRNAs show similar modes of regulation across all three genotypes during maturation. This indicates that a large number of mRNAs likely possess shared regulatory motifs and are acted upon by translation/degradation regulators similarly across genotypes, thereby comprising a core set of RNAs that must be regulated in a specific manner to maintain fertility. The extensive set of core mRNAs thus identified lends new relevance to applying and extending on earlier studies of translation regulatory motifs and mRNA binding protein described previously (Franciosi, Manandhar, & Conti, 2016; Paynton & Bachvarova, 1994; Reyes & Ross, 2016; Schwab et al., 1999; Tomek et al., 2002).

4.4.2 Extensive differences between parental strains and between parental strains and BDF1 hybrids

Additive dominance appears to be a major means by which the BDF1 oocytes may acquire unique phenotypic characteristics. The potential mechanism (i.e., affected cellular processes) responsible for additive dominance effects have not been evaluated previously in

oocytes. Doing so here required combining individual B6 vs BDF1 and D2 vs BDF1 dominance DEG lists into a single DEG list and subjecting that list to IPA analysis. This approach revealed a number of significant effects on canonical pathways and revealed changes in activation/inhibition states of several upstream regulators. There were many URs and CPs that are only reached significance in the AddDom category (Table 4.6 & 4.7). These included URs with roles in regulating the oocyte cortex [UCHL1, (Mtango, Sutovsky, Vandevoort, Latham, & Sutovsky, 2012)], oocyte maturation, [CNR1, (Lopez-Cardona et al., 2017)], oxidative stress protection [SOD2, (L. Zhang et al., 2015)], and initiation of oocyte growth [FOXO3, (John, Gallardo, Shirley, & Castrillon, 2008)]. These also included CPs with roles in maintenance of quality in aged oocytes [insulin receptor signaling, (Templeman et al., 2018), maintenance of meiotic arrest [14-3-3-mediated signaling, (Meng et al., 2013)], and first meiotic spindle migration [mTOR signaling, (S. E. Lee, Sun, Choi, Uhm, & Kim, 2012)].

Further evidence of additive dominance effects was provided by the comparison of actual BDF1 transcriptome to 'predicted' BDF1 transcriptome expression values. While there was some overlap between the additive dominance IPA results (UR and CP results with significant z-scores) comparing genotypes directly and the IPA dominance results obtained using the actual BDF1 versus predicted BDF1 comparison, the latter analysis yielded additional significantly affected CPs and URs, some of which that possessed a significant z-score and others that did not. We attribute the detection of these effects to the elimination of a need to apply thresholding to define dominance effects.

We note that a relatively small number of DEGs was returned for both the dominance (n=896 genes) and the actual vs. predicted (n=239 genes) analyses. However, this small number

of DEGs collectively appears to make a significant contribution to the phenotypic characteristics of BDF1 oocytes as we identified several URs and CPs that were significantly altered in BDF1 oocytes. One CP, sirtuin signaling, was identified in both analyses. Because expression of the relevant S*irt* mRNAs was not substantially altered in BDF1 oocytes, effects on this CP is likely be mediated by differences in the expression of downstream target DEGs. Among these were several genes located in the histone 1H gene cluster on mouse chromosome 13. Further analysis showed that BDF1 oocytes selectively degrade nearly half the histone 1H cluster genes during meiotic maturation. Histone variants have important roles in embryonic development, stem cell formation, cell plasticity, and reprogramming (Santoro & Dulac, 2015; Shinagawa et al., 2014; Wen et al., 2014). The differential regulation of the histone 1H cluster mRNAs in BDF1 oocytes during maturation may support a unique chromatin architecture in BDF1 oocytes, and/or reflect differential chromatin regulation after fertilization, either of which could be a key contributor to the hybrid phenotype.

Several mechanisms may contribute to apparent dominance effects in BDF1 hybrids, including inter-strain differences in genomic imprinting, genetic variation in promoter or enhancer strength impacting transcription rate, and genetic polymorphisms affecting mRNA stability. Two imprinted genes displayed dominance at the GV stage (*Igf2* and *Plagl1*) and two at the MII stage (*Smfbt2* and *Zrsr1*) but all four are regulated in a manner that suggests differential control of mRNA stability rather than a genome effect on imprinting. Of the 528 genes displaying dominance at the MII stage, only 47 did so at the GV stage as well. This suggests that the vast majority of dominance displayed at the MII stage is related to mRNA stability, and thus may be driven by differences in mRNA sequence. Dominance effects at the

GV stage may be attributable to differential mRNA synthesis or degradation or a combination of the two.

Only a few genes at the GV stage and < 30 genes at the MII stage displayed transgressive expression using a thresholding method for defining such expression. Interestingly, the vast majority of TGE genes were expressed lowest in BDF1 oocytes. But the small number identified, initially indicated that transgressive gene expression is not a major contributor to the special BDF1 oocyte characteristics. However, four TGE genes (*Coc4l1, Uba52, Fads2*, and *Gli1*) were DEGs that contributed to the activated/inhibited URs in the comparison between actual and predicted BDF1 transcriptomes (Table 4.9). In the same comparison, five of the DEGs that contributed to the activated/inhibited URs were also dominant DEGs (*Cox5b, Rpl41, Roxp2, Itgb4*, and *Ubc*). Taken together, this indicates that these few TGE genes may cooperate with the dominance genes to contribute further to the BDF1 phenotype.

Unique BDF1 phenotypes might also arise through “blending”, i.e., intermediate levels of expression of combinations of genes. This was evident in the overall number of DEGs between strains, and more readily apparent in the comparison of actual versus predicted (blended values) BDF1 oocyte transcriptomes, in which just 0.17 % (32 genes) and 1.26% (207 genes) differed at the GV and MII stages, respectively. This extensive blending of gene expression values may contribute to hybrid vigor, raising the possibility that the expression values observed in the inbred parental strains for many genes may not be advantageous to overall fertility. Conversely, the small number of differences between observed and predicted BDF1 expression values indicates that undiscovered mechanisms operate to drive unexpected

mRNA abundances for some genes; these differences may also contribute to unique BDF1 hybrid oocyte properties, marking these genes as worthy of more in-depth study.

4.4.3 Upstream regulators and c*anonical pathways and associated with BDF1 characteristic phenotype*

Using multiple approaches, we observed URs and CPs that were uniquely affected in BDF1 oocytes compared to parental strain oocytes, which may contribute to BDF1 heterosis. Several of the URs uniquely affected in BDF1 oocytes have well-known roles in oocyte maturation [UCHL1, (Mtango et al., 2012), CNR1, (Lopez-Cardona et al., 2017), HES1, (Manosalva, Gonzalez, & Kageyama, 2013)]. Other URs uniquely affected in BDF1 oocytes have roles in ovulation [IL6ST, (Molyneaux, Schaible, & Wylie, 2003)], are oocyte secreted factors [INHBB, (Dragovic et al., 2007)], or may arise from a combination of somatic cell and oocyte expression [CD44, (Yokoo et al., 2007)]. Additionally, BDF1 oocytes may differentially regulate transcription factors with roles in early embryos [E2F, (Palena et al., 2000), EGR1 (B. Guo et al., 2014), and STAT5A/B (Nakasato et al., 2006). Other affected URs (ETV4, LASP1, EGR2, ADORA2A, IL32, FFAR3, MTM1) have not been previously associated with oocyte function, but emerge here as new candidates for controlling oocyte characteristics. Other URs uniquely affected in BDF1 oocytes are related to diverse cellular functions important to oocyte quality such as oxidative phosphorylation, redox state, oxidative stress, mitochondrial turnover, and apoptosis [BNIP3L, (Ashrafi & Schwarz, 2013), S1PR3, (Guo, Ou, Li, & Han, 2014), SOD2, (Perkins, Das, Panzera, & Bickel, 2016), HIF1A, (Yalu, Oyesiji, Eisenberg, Imbar, & Meidan, 2015)]. Interestingly, BDF1 MII stage oocytes showed gene expression patterns consistent with

activation of IGF1R and INSR, two proteins that are not necessary for oocyte maturation in mice (Pitetti et al., 2009) but that may contribute to survival under conditions of stress (Maiorca, Cancarini, Brunori, Camerini, & Manili, 1993). Greater activation states of pathways involving INSR and IGF1R may contribute to resiliency in hybrid oocytes. One other interesting UR, ACOX1, is an enzyme that regulates β-oxidation and causes sterility when lost (Fan et al., 1996), but remains poorly studied in the oocyte. Maturation changes specific to BDF1 oocytes suggest that ACOX1 becomes inhibited during oocyte maturation. ACOX1 is also observed in the actual vs predicted dataset where it appears to be more inhibited in the actual BDF1 oocytes at MII than would be predicated by the parental expressions. An interesting future direction would be to better characterize the role of ACOX1 in during oocyte maturation to determine if it contributes to BDF1 heterosis.

Along with these affected URs, there are a number of important CPs uniquely affected in the BDF1 oocytes. These include INSR signaling, 14-3-3 signaling, and mTOR. All of these pathways are connected to INSR1 and IGF1R, identified above as affected URs (Morrison, 2009; Yoon, 2017). The analysis also indicated altered responses of BDF1 oocytes to cumulus cells via CXCR4 (R. N. Zhang et al., 2018). Another CP (sirtuin signaling) likely to be key in oocyte health emerged in the comparison between actual and predicted BDF1 transcriptomes as being decreased in activity.

4.4.4 Overall Conclusions

To our knowledge, this is the first RNAseq study comparing oocytes from different maturational stages from three fertile genotypes of mice. The major new discoveries of this

study are three-fold. First, there are numerous DEGs between each mouse genotype at both oocyte stages and the three genotypes differ in mRNA handling during maturation. Interestingly, BDF1 oocytes have more changes in mRNA abundances during maturation than either parental strain. Oocytes from the three genotypes become more different from each other during maturation. Secondly, additive dominance is a major source of unique BDF1 oocyte characteristics, working in conjunction with a limited number of genes showing transgressive RNA expression and many other genes showing intermediate levels of expression. Lastly, these differences in mRNA expression are associated with changes in the predicted activation states of an important URs and CPs related to oocyte health and function, impacting prominent functions such as histone expression, mitochondrial function, and oxidative phosphorylation. These results highlight the complexity of the oocyte, the distinct paths that the genetically different oocytes may take during oocyte maturation, and how BDF1 oocytes optimize this system to develop superior phenotypic characteristics and make their oocyte maturation “just right”.

4.5 Materials and Methods

4.5.1 Oocyte isolation

This dataset consists of GV and MII stage oocytes from B6, D2, and BDF1 mice. Oocytes from individual mothers were pooled for each biological replicate to become one sample. A total of 32 samples were analyzed, comprising at least five for each of the stages/genotypes analyzed. Females were obtained from Jackson Laboratories at 7 weeks age and used from 8 to

12 weeks age. Oocytes were collected as described (Severance & Latham, 2017). Briefly, both GV and MII stage oocytes were collected into room temperature HEPES-buffered M2 medium. During GV stage oocyte collection, M2 medium was supplemented with 0.225M 3-Isobutyl-1-methylxanthine (IBMX) (Sigma: I7018) to prevent GVBD. Immediately after collection the zonae pellucidae were removed using acidified Tyrode's buffer (Tyrode, 1910) for approximately 30 sec followed by immediate washing through M2 medium for 1 min. This treatment eliminated cumulus cell processes as a possible source of RNA contamination. Some MII stage oocytes had polar bodies remaining attached. All studies were approved by the Michigan State University Institutional Animal Care and Use Committee, consistent with National Institutes of Health (NIH) Guide for the Care of Use of Laboratory Animal, and with the Association for Assessment and Accreditation of Laboratory Animal Care (AAALAC) accreditation.

4.5.2 Oocyte RNA sequencing

RNA was extracted from pools of GV or MII stage oocytes (n=9 to 20) using the ARCTURUS PicoPure RNA Isolation kit (ThermoFisher #12204-01), following the manufacturer protocol, consisting of lysis in 20 µL PicoPure extraction buffer and heat treatment at 40^{o}C for 30 minutes. Lysates were processed immediately or stored at -80^{o}C. During the RNA isolation, DNase treatment was applied for 15 minutes at RT (Qiagen #79254). Isolated RNA was eluted into 11 µl of the PicoPure elution buffer and was immediately used or stored at -80^{o}C. Five microliters of each eluate was processed and amplified with SPIA technology using the Ovation RNAseq System V2 (NUGEN #7102-32). The cDNA libraries were purified using a Qiagen MinElute Cleanup Kit (Qiagen #28204), quantified on a Nanodrop (ThermoFisher NanoDrop

Lite) or Biodrop (uLite), and stored at -80^{o}C. For each library, approximately 1µg of DNA was diluted into 1X Tris-EDTA buffer (TE) for a total volume of 130 µL and fragmented to an average length of 300 bp on a Covaris shearer. Twenty µl of each fragmented library were mixed with 14 µl water, 4 µl 10X S1 nuclease buffer, and 2 µl S1 nuclease for a 40 µL total reaction volume that was incubated for 30 minutes at RT (Promega # M5761)(Head et al., 2011). Starting with an additional bead purification, SPIA libraries were processed through the Ovation Ultralow System V2 1-16 (Nugen #0344-32) with amplification for 12 cycles. After the last bead purification, amplified-barcoded libraries were eluted in 30 µL of 1X TE.

Libraries were sequenced on an Illumina HiSeq 2500 system or an Illumina HiSeq 4000 system. Libraries were loaded at 65% of standard concentration with PhiX DNA added up to 10% of the input (HiSeq 2500) or with PhiX loaded to 1% with no decrease in total loading (HiSeq 4000). Sample for all genotypes and stages were represented on both platforms. Sequencing was performed with 50 nt unpaired end reads. The number of PF (passed-filter) reads ranged from 25.5 M to 53.6 M, the fraction of Q30 bases from 90.7% to 95.4% and average Q from 36.9 to 38.9 (Sup. Table S1). Sequencing data are available in Gene Expression Omnibus (GSE114158: https://www.ncbi.nlm.nih.gov/geo/query/acc.cgi?acc=GSE114158). Results of the two sequencers were comparable, and any batch effect was accounted for in later processing as described below. Small increase of quality parameters for HiSeq 4000 was expected due to change in technology.

Reads were aligned to the mouse genome (build GRCm38.p4) using HISAT2 (D. Kim, Langmead, & Salzberg, 2015), and the option to avoid alignment of reads to pseudogenes. Reads aligned to ribosomal RNA (rRNA) or rRNA-like genes were removed, as were the

duplicates caused by the sequencing technology, which were defined as one read in a pair of identical reads found within the distance of 100 units (optical duplicates in libraries sequenced on HiSeq 2500) or 2500 units ("ExAmp" duplicates in libraries sequenced on HiSeq 4000) on the same tile of a sequencing lane. A total of 18.7 M to 39.7 M reads per library were successfully aligned to unique non-rRNA gene transcript sequences (Sup Table 14). Reads aligned to genes were quantified with featureCounts (part of Subread 1.5.1 package) (Liao, Smyth, & Shi, 2013). DeSeq2 (Love, Huber, & Anders, 2014) was used for differential expression analyses between the genotypes (within the GV or MII stage), or between two stages (within a genotype). Because samples were processed and sequenced in two batches on two different sequencing systems, the batch identifier was provided to DESeq2 as a factor, and there were at least two samples in each batch for all six genotype/stage combinations. Initially, differentially expressed genes (DEGs) were defined as those with q-value (false discovery rate) ≤ 0.05. Due to the large number of DEGs identified at this threshold, a q-value of ≤ 0.01 was used in subsequent IPA. A comprehensive table of DEGs is provided (Gene Expression Omnibus GSE114158: https://www.ncbi.nlm.nih.gov/geo/query/acc.cgi?acc=GSE114158).

4.5.3 Predicted BDF1 versus actual BDF1

For analysis of dominance effects, direct comparisons between the three genotypes employed a thresholding approach. As an alternative method to avoid thresholding, we devised a novel strategy of comparing the actual BDF1 transcriptomes to values calculated to be the intermediate values between the two parental genotypes ("predicted" BDF1). For each of the two stages, the expected expression profiles for BDF1 oocytes were predicted as the average of

the expression profiles for B6 and D2 oocytes and compared to the actual BDF1 oocyte expression profiles. Since samples from B6 and D2 can be paired in different ways, a randomization procedure was used: 1) Samples from B6 and D2 were randomly paired (only within batch, keeping samples from two batches apart) and their expression profiles were averaged. 2) The combined B6/D2 samples were then compared to BDF1 samples using DESeq2. 3) Steps 1 and 2 were repeated 10 times and a gene was considered differentially expressed between the actual and predicted BDF1 transcriptomes if such outcome was obtained in at least 9 out of 10 repetitions.

4.5.4 Ingenuity Pathway Analysis

IPA was used to analyze the biological relevance of DEGs. Analysis tools applied from IPA included CP and UR analyses. For CP analysis, IPA calculates overlap p-values, taking into account the number of DEGs and the number of molecules in the knowledge database associated with that pathway, and the number of DEGs and the number of molecules in the knowledge database. For UR analysis, results are based on the number of DEGs regulated by a given UR. In addition to overlap p-values, z-scores are calculated for CPs and URs. The z-score reflects activation ($z > 0$) or inhibition ($z < 0$) of CPs and URs; it is based on the number of associated DEGs for which the direction of regulation (up- or down-) is consistent with activation or with inhibition. Because $P(|z| > 1.96) = 0.05$ for normal N(0,1) distribution, we consider CPs and URs with $z > 1.96$ to be significantly activated, and those with $z < -1.96$ to be significantly decreased. We note that characterization of URs as “affected”, “activated”, or

"inhibited" does not necessarily imply a change in the expression of that UR itself, but rather may reflect a change in the expression profiles of its downstream effectors.

As the initial IPA analyses provided a large number of URs or CPs, we truncated the output by retaining two categories of results: category 1 URs and CPs having both $|z|>1.96$ and $p<.05$ ($-\log_{10}p>1.3$) for at least one comparison, category 2 URs and CPs with $p<0.05$ for at least one comparison, but no significant z-score for the same comparison. Within these two categories, chemical URs had at least one comparison with both $|z|>1.96$ and $p<0.05$, and URs expressed within the cell had FPKM >0.02 (corresponds to approximately one mRNA transcript in our MII stage dataset) in at least one genotype/stage. Secreted factors as URs ($p < 0.05$) were initially included. We removed all biologic drugs. The two categories were further truncated using a ranking score calculated according to the equation: $\text{sum}_{\text{all comparisons}}(|z|+2)*(-\log_{10}(p))$ and retaining the top 200 ranked URs and CPs. All IPA analyses were truncated based on this equation.

We note that some UR-effector relationships and intra-CP relationships are assigned in IPA on the basis of protein-protein interactions or other post-transcriptional events. Because the DEG data that were entered into IPA were derived by mRNA expression analysis, the interpretation of the IPA results incorporated inspection of UR and CP member gene expression patterns, and their functional classes (transcription factor, kinase, enzyme, transporter, etc.). Where necessary, mRNA expression data for these genes and related gene family members were assessed in order to clarify the biological significance of IPA results.

CHAPTER 5

Overall Discussion and Future Directions

This dissertation elucidates two key aspect of oocyte biology during meiotic maturation, spindle formation and mRNA regulation. I showed that EIF4EBP1 phosphorylation is important for both first and second meiotic spindle formation and that this phosphorylation is regulated by PLK1. Moreover, I revealed the dynamic nature of mRNA regulation during meiotic maturation across three genotypes of fertile mice, and how that regulation varies with genotype. My dissertation highlights the key role of mRNA regulation during oocyte maturation.

5.1 mRNA regulation at the spindle

The essential function of any oocyte is to segregate a maternal haploid genome to the embryo. This requires correct formation and function of spindles during two successive divisions, using modes of regulation to meet specific oocyte meiotic requirements, such as spindle migration (MI), spindle tethering (MI), asymmetric spindle localization, specialized chromatin-mediated microtubule nucleation, and a prolonged meiotic arrest at second metaphase with the spindle remaining intact, among other features (reviewed in Chapter 2). An additional challenge of oocyte meiosis is three-dimensional space; the oocyte is large, and there is a need to ensure that the spindle proteins are available in the region where the spindle forms. Previous studies showed an enrichment of phosphorylated EIF4EBP1 on the meiotic spindles (Romasko et al., 2013). When hyperphosphorylated, EIF4EBP1 is not able to bind to

EIF4E and conditions are permissive of translation (T. Lin et al., 1994; Pause, Methot, Svitkin, Merrick, & Sonenberg, 1994). I tested the hypothesis that EIF4EBP1 phosphorylation locally at the spindle is necessary for spindle formation and function by activating localized mRNA translation. I showed that inhibition of EIF4EBP1 phosphorylation showed a variety of spindle defects on the first meiotic spindle. I investigated several potential upstream regulatory kinases (mTOR, ATM, PLK1). Using a collection of highly specific kinase inhibitors, I observed little effect of inhibiting mTOR or ATM, but observed that PLK1 inhibition results in a loss of two phosphorylation sites on EIF4EBP1 on both the first and second meiotic spindles. Spindles of the two meiotic stages showed different susceptibility to perturbations in translation and PLK1 inhibition, with a more severe phenotype seen at the first meiotic spindle. This result is particularly provocative because the first meiotic spindle is thought to be the primary source of embryonic aneuploidy (Hassold, Hall, & Hunt, 2007; Hassold & Hunt, 2001). The exciting results of my research raise a number of important future questions to ask about localized translation on the meiotic spindles.

One question is what is the exact relationship of PLK1 and CDK1 in relation to EIF4EBP1 phosphorylation at the oocyte spindle? I showed that PLK1 inhibition resulted in a loss of both EIF4EBP1-S111 and EIF4EBP1-S64 on both meiotic spindles. Based on biochemical data from other cells and models, S64 is not (Shang et al., 2012). Instead, CDK1 likely regulates S64 phosphorylation (Heesom et al., 2001; M. Shuda et al., 2015). PLK1 and CDK1 interact in the oocyte (Renner et al., 2010), indicating that CKD1 is responsible for EIF4EBP1-S64 phosphorylation on the oocyte spindle, but that this is controlled by PLK1 action. Whether PLK1 does this in the oocyte by actions on EIF4EBP1 or CDK1 is not known. Given the important roles

of both CDK1 and PLK1 during meiosis, understanding the complete relationship between the two in relation to EIF4EBP1 phosphorylation could yield important insights into how meiotic progression and exogenous insults connect to spindle function and formation.

A second future direction is to determine if there is a hierarchy of EIF4EBP1 phosphorylation in the oocyte. In other cells and under other conditions, there is a specific order in which sites of EIF4EBP1 undergo phosphorylation (Acosta-Jaquez et al., 2009; Fletcher et al., 1998; Gingras et al., 1999; Heesom et al., 2001). In EIF4EBP1, the T36/45 sites are considered priming sites that must undergo phosphorylation first to facilitate subsequent phosphorylation events in human embryonic kidney (HEK) 293 cells (Gingras et al., 1999). However, this hierarchy may vary according to cell type and physiological state (Acosta-Jaquez et al., 2009; Fletcher et al., 1998; Gingras et al., 1999; Heesom et al., 2001; Shang et al., 2012). The S111 (S112 in humans) site is the most poorly understood of all the EIF4EBP1 phosphorylation sites, and can serve as a priming site or exert direct effects on EIF4EBP1 function (Heesom et al., 1998; D. Q. Yang & Kastan, 2000). The PLK1 effect on S64-EIF4EBP1 could therefore also be explained as a hierarchical effect of S111 phosphorylation. Distinguishing between the possible explanation of S64-EIF4EBP1 phosphorylation could reveal an additional level by which cap-dependent translation is regulated at the oocyte meiotic spindles.

A third future direction would be to understand further the role of translation at the meiotic spindle. Although several mRNAs are enriched at the second meiotic spindle (Romasko et al., 2013), it remains unknown which of these are actively translated, and which of those require EIF4EBP1 phosphorylation. Additionally, the considerable differences between the first

and second meiotic spindles suggest that the pool of actively translation mRNAs may differ between the two. Other questions remaining to be answered are: What happens to translation during first spindle migration? How are the mRNAs tethered to the spindle? What proportion of spindle proteins are synthesized in the spindle forming region versus elsewhere in the cytoplasm? Is there translocation of newly synthesized proteins along the spindle? These exciting questions that need to be answered in order to understand the specific functions of localized translation at the meiotic spindles.

5.2 mRNA regulation in whole oocytes

The second focus of my dissertation was on the dynamic regulation of the whole mRNA population during oocyte maturation. I addressed what mRNAs were present and at what abundances in immature and mature oocytes from three fertile mice genotypes. The reason for doing this was to understand the effect of maternal genotype on meiosis, which has not been addressed. In particular, the mechanisms contributing to F1 hybrid vigor in oocytes have not been examined. Accordingly, I identified differentially expression genes (DEGs), upstream regulators, and canonical pathways that are significantly affected in BDF1 oocytes, including alterations in mitochondrial physiology and oxidative phosphorylation. Because mitochondria modulate the cellular redox state and cellular metabolism, produce ATP, and regulate apoptosis (Babayev & Seli, 2015), their implication in BDF1 hybrid vigor suggests they may be a central regulator driving oocyte quality. Future functional studies could focus on each mitochondrial function separately to determine contribution to the BDF1 heterosis phenotype.

A second finding is that BDF1 oocytes have higher rates of degradation of cluster 1 histone mRNAs during meiotic maturation than the two parental strains (D2 and B6). This cluster group of histone genes includes RNAs that code for the H1, H2A, H2B, and H4 histones. Generally, histones regulate packaging and accessibility of the genome for transcriptional machinery, but there is no active transcription during this time in the oocyte (Leatherman & Jongens, 2003). Alternative histone use is critical to nuclear reprogramming and zygotic genome activation (Shinagawa et al., 2014; Skene & Henikoff, 2013; Wen et al., 2014; P. Yang, Wu, & Macfarlan, 2015). Therefore, it is probable that this cluster 1 histone mRNA degradation better prepares the BDF1 oocyte to reprogram the paternal genomes and may help package the genome differently to assist zygotic genome activation or other transcriptional processes in the embryo. It is also possible that this cluster of histones has a conserved regulatory element that targets them for degradation specifically in BDF1 oocytes. Therefore, it would be critical to know what protein is binding to these RNAs and facilitating their degradation. Do other mRNAs possess the same regulatory element? More interestingly, how specifically does this degradation contribute to hybrid vigor? What is different in B6 and D2 oocytes so that they do not degrade the target mRNAs? Is the regulatory protein not expressed, not activated, or localized in a different part of the oocyte? Is it possible to improve fertility in lower quality oocytes by targeting specific proteins and phenocopying BDF1? These exciting questions and ideas give exciting insights into a potential means by which we could target specific pathways in a poor quality oocyte to improve fertility.

A broader idea revealed in this dataset is that fertile oocytes can have very different transcriptomes. Thousands of DEGs and hundreds of upstream regulators and canonical

pathways were different between the three mouse genotypes. Could these differences make B6 oocytes more susceptible than D2 for some insults and more resistant to others? How do we account for these differences in an *in vitro* culture system? How does variation in human oocyte transcriptome compare to the variation between mouse genotypes? Does the human oocyte transcriptome more closely resemble one of the three genotypes? Utilizing different mouse genotypes to address these specific questions may give much better insights into the human oocyte and give us the ability to improve human fertility.

5.3 Overall Conclusions

The ultimate goal of any species is to survive long enough to procreate. To have any chance at this requires the oocyte to maintain both fertilization competency and a sufficient supply of maternal determinants to support the early embryo. This dissertation elucidates the key role that maternal mRNA regulation has in the oocyte, both at the spindle and throughout the ooplasm. A greater understanding of these processes and the overall complexities of the oocyte could greatly improve our understanding of fertility in humans and other species.

APPENDIX

APPENDIX

Oogenesis & Ovulation: Oocyte Maturation and Ovulation, comparative

Citation:

Severance, A., Sen, A. Oogenesis & Ovulation: Oocyte Maturation and Ovulation, comparative. Encyclopedia of Reproduction 2nd Edition. Academic Press. *Accepted. To be published August 2018.*

A.1 Abstract

This chapter highlights the conserved and distinct mechanisms of oogenesis and ovulation across various species and animals, namely *C. elegans* (hermaphroditic), *Drosophila* (fruit fly), *Xenopus* (amphibian), mouse, bovine, porcine, chicken, and humans. With respect the mammals discussed in this chapter, both mono ovulatory, human and bovine, and poly ovulatory, mouse and porcine, are discussed. Although key events, such as the primary meiotic arrest, are highly conserved, the underlying molecular mechanism by which each animal achieves this state have distinct differences.

A.2 Introduction

Across species, the release of a mature healthy egg for fertilization is the center of the entire reproductive process. From the time of embryonic development until fertilization, the oocyte undergoes several stop-and-go periods that are tightly regulated throughout the reproductive cycle. Oocytes undergo first meiotic progression during embryonic development, and at the time of birth, they become arrested in the prophase stage. This meiotic arrest of oocytes is maintained until shortly before ovulation, when resumption of meiosis occurs and there is progression to metaphase II (MII), a process commonly termed *oocyte maturation*. Following resumption of meiosis I, there is organized disassembly of the nuclear envelope (germinal vesicle, GV) referred to as germinal vesicle breakdown (GVBD), followed by chromosome condensation, spindle formation and extrusion of the first polar body. Thereafter, the oocyte enters meiosis II and again gets arrested at metaphase II stage until fertilization. Upon fertilization, the oocyte resumes meiosis II extrudes the second polar body, thereby completing

maturation (Dekel, 1995; J. J. Eppig, Viveiros, Bivens, & De La Fuente, 2004). Oocyte maturation is one of the major steps for the oocyte to attain competence for successful fertilization and subsequent embryonic development. Acquisition of this developmental competence of the oocyte involves multiple factors regulated by different signaling pathways at various stages prior to fertilization (Keith T. Jones, 2004; Lisa M. Mehlmann, 2005). While some crucial components of the signaling pathways involved in oocyte maturation are conserved from amphibians to mammals, there exists significant species-specific differences. This chapter highlights the differences in oocyte maturation among species and compares the various signaling pathways and underlying intracellular mechanisms involved in maintaining the meiotic arrest, regulation of oocyte maturation and ovulation across species.

A.3 Primary Meiotic Arrest

The segregation of the germ cell from the somatic lineage occurs very early during development in both invertebrates and vertebrates. Once the primordial germ cells (PGC) get committed to the germ cell lineage and enter meiosis, they progress to prophase I, where the first meiotic cycle is then arrested. This primary meiotic arrest occurs in all organisms considered in this chapter. The potential evolutionary rational behind this highly conserved arrest (Mira, 1998) is based on three non-exclusive hypothesis. First, the “mutational hypothesis” suggests that the occurrence of prophase I arrest, early during meiosis to ensure that oocytes are made before division or prior to environmental perturbations causing DNA damage. This ensures that oocytes are as close to the “master-copy” as possible. The second “repair hypothesis” elucidates that by arresting at this stage when sister chromatids are present and held tightly together, the

sister chromatid can be used as an ideal template to repair any DNA damage that arises. Lastly, an interesting "minimize conflict" hypothesis proposes that some type of inter-gamete competition may exist and arresting at prophase I ensures that all oocytes have four copies of each gene, discouraging the selection of oocytes based on genetic components solely useful to outcompete siblings instead of long-term offspring survival. Whether any or all of the above hypotheses are true or not is debatable, but the prophase I meiotic arrest is highly conserved from *C. elegans* and *Drosophila* to humans, and this arrest is critical to the oocyte growth and future embryonic development. However, the molecular means by which this arrest is maintained does differ somewhat (Sagata, 1998).

In 1935, Pincus and Enzmann were the first to show that the removal of prophase I arrested rabbit oocytes from their follicular environment resulted in the spontaneous resumption of meiosis (Pincus & Enzmann, 1935). This finding supported a model where the surrounding somatic cells regulated maintenance of the prophase I meiotic arrest. The prophase I meiotic arrest is maintained by several similar mechanisms across different species with some distinct differences. In general, in mouse, *Xenopus*, human, porcine, bovine, chicken, and *C. elegans* the primary meiotic arrest is maintained by synthesis of inhibitory factors in the somatic cells surrounding the oocyte and within the oocyte itself that result in CDK1/CDC2 inactivation in the oocyte (Bilodeau, Fortier, & Sirard, 1993; Cook, 2017; Govindan, Cheng, Harris, & Greenstein, 2006; Parker & Piwnica-Worms, 1992; Shimada, 2012). One of the primary factors involved in maintaining the oocyte in the prophase I meiotic arrest is cAMP. In mammals and *Xenopus*, cAMP is synthesized both in the oocyte and the surrounding cumulus cells where it is continuously transported into the oocyte by gap junctions (Shimada, 2012). In contrast, in the *C. elegans*

oocyte, instead of direct transport of cAMP in the oocyte, the somatic gonadal sheath cells synthesize $G_{g/i}\alpha$ and transport it into the developing oocytes, which activates adenylate cyclase and elevates cAMP levels (Govindan et al., 2006; Govindan, Nadarajan, Kim, Starich, & Greenstein, 2009). This differs slightly in mammalian oocytes where the constitutively active GS-linked receptors, GPR3 and GPR12, stimulate adenylate cyclase to make cAMP (Arur, 2017). The resulting high levels of cAMP in the oocytes activates the cAMP-dependent kinase, PKA, which then phosphorylates and activates Wee kinase family members, including the oocyte-specific Wee1B kinase (S. J. Han, Chen, Paronetto, & Conti, 2005). Wee kinase family members include Wee1 and Myt kinases which can phosphorylate and inactivate CDK1/CDC20 at two highly-conserved residues, Thr14 andThr15 (Fattaey & Booher, 1997; Parker & Piwnica-Worms, 1992). This CDK1/CDC20 inactivation prevents activation of the maturation promoting factor (MFP; a complex consisting of cyclin B and CDK1/CDC20) and continually holds the oocytes in prophase I arrest (S. J. Han et al., 2005). In bovine, it appears that cAMP is degraded to AMP which activates adenosine monophosphate-activated protein kinase (AMPK), and although this is necessary for meiotic arrest, it is currently unknown how AMPK activity relates to low MPF which is also necessary to maintain the prophase I arrest (Bilodeau-Goeseels, 2011). There is evidence in mouse, *Xenopus*, human, and porcine that activation of Wee kinases and inhibition of CDK1/CDC20 is a conserved mechanism, although whether the target kinase is Wee1 or Myt differs between organisms (S. J. Han et al., 2005; Shimada, 2012; Shimaoka, Nishimura, Kano, & Naito, 2009). Despite being a powerful model organism, surprisingly little is known regarding mechanisms for maintenance of the prophase I arrest in *Drosophila*. It is clear that the *Drosophila* oocyte accumulates the CDK1-inhibitor, Dap, which keeps it in S-phase whereas the nurse cells

have low levels of Dap and being multiple rounds of endoduplication and as a result, become highly polyploid (Hong, Lee-Kong, Iida, Sugimura, & Lilly, 2003). An unique feature of the *Drosophila* arrest is that the surrounding somatic cells (nurse cells) are dispensable for maintenance of the prophase I arrest, which is quite interesting considering the important role nurse cells have in oocyte determination and growth and that they are also directly connected to the oocyte by cytoplasmic bridges (Bohrmann & Zimmermann, 2008). In summation, although the prophase I arrest is highly conserved across all organisms discussed, the mechanisms employed to maintain it are quite different across species including the importance of the surrounding somatic cells and specific downstream targets that modulate CDK and MPF activity.

A.4 Meiotic Resumption/Maturation

While the prophase I arrest is highly conserved, the resumption of meiosis in response to an extracellular stimulus varies across species. For example, in *C. elegans*, major sperm protein (MSP) has been identified as the hormonal stimulus that stimulates both meiotic resumption as well as somatic gonadal sheath cell contraction to move oocytes towards the proximal gonad (McCarter, Bartlett, Dang, & Schedl, 1999; Miller et al., 2001). *Xenopus* meiotic resumption occurs in response to progesterone which causes a rapid drop in intracellular cAMP levels in the oocyte (Maller, Butcher, & Krebs, 1979). In mammals and chickens, an endogenous luteinizing hormone (LH) surge stimulates meiotic resumption (Cook, 2017; Jaffe, 2010; Seibel, Smith, Levesque, Borten, & Taymor, 1982). In mouse oocytes, inactive MPF is present throughout ooplasm and the LH surge causes a rapid decrease in cellular cAMP levels which subsequently decreases PKA and Wee1b activity, and activates CDK1 (J. J. Eppig, Viverios, M. M., Marin Bivens, C. L. & De La Fuente,

R, 2004). Androgens (Hammes, 2004) have also been shown to induce meiotic resumption in *Xenopus* (Lutz et al., 2001) and mouse oocytes (Gill, Jamnongjit, & Hammes, 2004). Unlike rodents, bovine and porcine oocyte have very low levels of cyclin B throughout the ooplasm and require active translation of the MPF regulatory subunit to resume meiosis (Levesque & Sirard, 1996; Naito et al., 1995). The signal that initiates meiotic resumption in *Drosophila* remains unknown, but MPF activation is also necessary (Von Stetina & Orr-Weaver, 2011).

After MPF activation and subsequent meiotic resumption, oocytes proceed through several physiological processes in preparation for fertilization. MPF is the master regulator during M phase, and active MPF phosphorylates multiple target proteins which mediate nuclear envelope breakdown (NEBD) also referred as germinal vesicle breakdown (GVBD), chromatin remodeling, and spindle formation (Sagata, 1998). In all species discussed in this chapter, oocytes do not resume transcription during meiotic maturation, highlighting the importance of maternal mRNA polyadenylation, stability, and degradation (De La Fuente et al., 2004). MPF activates ERK1/2, which then phosphorylates and activates CPEB (Sha et al., 2017), which is a sequence-specific RNA-binding protein that regulates polyadenylation-induced translation. Active CPEB polyadenylates specific mRNAs throughout the ooplasm for targeted translation even as global translation rates are decreasing during meiotic maturation (Schultz, Lamarca, & Wassarman, 1978a; Sha et al., 2017). Unlike mitosis, during meiosis, chromosomes remain tightly condensed as oocytes progress from meiosis I to meiosis II. As mammalian, *Xenopus*, and chicken oocytes progress through meiosis I, they give off a small polar body (PBI), and then continue to metaphase of meiosis II (Cook, 2017; J. N. Dumont, 1972; L. M. Mehlmann, 2005). Interestingly, in *C. elegans,* meiotic maturation first involves downregulation of MPK-1 (ERK) and later cellular levels rebound

to ensure correct maturation of the oocyte, indicating MPK-1 has a dual purpose specific to *C. elegans* oocytes (Arur, 2017). In *Drosophila*, a protein called ENDOS , which is a member of a group of small proteins called α-Endosulfines with wide expression but largely of unknown functions is believed to be involved in meiotic maturation (Von Stetina & Orr-Weaver, 2011). ENDOS encodes a phosphoprotein that regulates all aspect of meiotic maturation, most likely through regulating MPF activity, although what controls activation of ENDOS remains unknown (Von Stetina et al., 2008). Also unique to *Drosophila* is that there is no extrusion of first or second polar body during meiosis (Page & Orr-Weaver, 1997). Taken together, while the organisms discussed here have some distinct features, the critical role of MFP in regulating meiotic maturation is highly conserved.

A.5 Secondary Meiotic Arrest

With respect to the secondary meiotic arrest, *C. elegans* and *Drosophila* stand out as very different from the other animals discussed in this chapter. Unlike the other gonochoristic species in this chapter, the hermaphroditic *C. elegans* utilizes the major sperm protein (MSP) hormone as a signal for meiotic maturation, thereby ensuring the presence of sperm for fertilization and bypassing the need for a second meiotic arrest (I. Yamamoto, Kosinski, & Greenstein, 2006). *C. elegans* MSPs are the most abundant proteins in sperm, where they function as intracellular cytoskeletal proteins and secreted hormones. Secreted MSPs bind to multiple receptors on oocyte and ovarian sheath cell surfaces to activate MPK-1 and induce oocyte maturation and sheath contraction (Y. F. Yang, Han, & Miller, 2010). The coupling of meiotic resumption and meiotic maturation directly to sperm-sensing confers a selective advantage in *C. elegans* as they

continually produce oocytes when sperm is present, and therefore are able to save energy by not producing the metabolically-costly oocytes when sperm is not available (I. Yamamoto et al., 2006). In *Drosophila*, oocytes arrest at metaphase I and MPF is critically important in maintenance of the second meiotic arrest. For meiotic completion, Cyclin B must be degraded. The completion of meiosis in *Drosophila* is sperm-independent and results from the mechanical pressure on the oocyte as it passes through the oviduct. It has been proposed that lack of coupling of fertilization to meiotic completion is a remnant from a time when *Drosophila* was able to asexually reproduce. Although most species of *Drosophila* do not support parthenogenic development, some species such as *Drosophila mercatorum* have viable progeny from parthenogenically-activated oocytes (Eisman & Kaufman, 2007; Von Stetina & Orr-Weaver, 2011).

In mammals, chickens, and *Xenopus*, the second meiotic arrest occurs at metaphase of meiosis II (MII) due to the cytostatic factor (CSF) (Nakamura, Kagami, & Tagami, 2013; Nishiyama, 2010). CSF was first discovered in *Rana pipiens* where it was shown that injecting the cytoplasm from a MII oocyte halts cell division in a 2-cell blastomere, indicating some transferable cytoplasmic factor in MII oocytes that is responsible for the MII arrest (Masui, 1974). Ultimately, the Mos/MEK/MAPK/Rsk signaling cascade (MOS is a germ cell-specific Raf) has been identified as the CSF in *Xenopus* (Nishiyama, 2010). The downstream effect of this cascade is activation of Emi-related protein 1 (ERP1), which is an inhibitor of the anaphase-promoting complex/cyclosome (APC/C), the result of which is maintaining the MII arrest until fertilization occurs (Schmidt et al., 2005). In mice, the CSF also involves MOS and MAPK but not Rsk, although activation of ERP1 is still the end result (Nishiyama, 2010). In bovine, porcine and human oocytes,

MAPK is also required for the MII arrest, and although the downstream targets are likely similar to mouse or *Xenopus*, these have not been directly assayed (Gordo, He, Smith, & Fissore, 2001; Q. Y. Sun et al., 1999; Tatemoto & Muto, 2001). This MII arrest is carefully coupled to fertilization as sperm entry causes a Ca^{2+} wave throughout the oocyte, resulting in the destruction of ERP1, followed by destruction of cyclin B, activation of the APC/C, and finally initiation of zygotic development. Coupling the completion of meiosis with fertilization ensures that the maternal and paternal pronuclei form at the same time and will be in sync upon entry into S phase.

A.6 Ovulation

Ovulation is the release of the growing oocyte from the ovary into the reproductive tract for fertilization. Achievement of successful ovulation is carefully orchestrated by the mural granulosa cells responding to the LH surge by activation of their LH-receptor (Russell & Robker, 2007). In all animals discussed in this chapter the structure receiving the ovulated oocyte is called the oviduct, except in *C. elegans* where oocytes move into the spermatheca. The rate and efficiency of ovulation is a major factor in successful reproduction as it ensures that the oocyte is at the right time and place for successful fertilization. In *Xenopus*, mouse, bovine, and porcine normal ovulation is controlled by the release of luteinizing hormone and follicle-stimulating hormone from the pituitary gland. An important consideration when studying ovulation is whether the species of interest is a mono or poly-ovulator. The majority of the time, bovine and humans are both mono-ovulators whereas porcine and mice are poly-ovulators (Hunter, Robinson, Mann, & Webb, 2004). Distinct from all other animals is *Xenopus* ovulation involving

the expulsion of hundreds of mature oocytes into an aquatic environment for external fertilization.

In addition to the unique external fertilization in *Xenopus d*iscussed above, *C. elegans* and *Drosophila,* and chickens have some distinct ovulation features. In *C. elegans*, the oocyte ovulates into a specialized structure, the spermatheca, is rapidly fertilized and then moves into the uterus within 4 minutes of ovulation (S. Kim, Spike, & Greenstein, 2013). In *Drosophila*, surrounding somatic secretory cells in the reproductive tract secrete HR39 (a nuclear hormone receptor steroidogenic factor 1, SF1; NR5A1-related Drosophila nuclear hormone receptor), which stimulates ovulation, in addition to other proteins necessary for sperm storage in the reproductive tract after mating (J. Sun & Spradling, 2013). During *Drosophila* ovulation, only one of the many mature oocytes in the ovaries is released into the oviduct. Furthermore, in *Drosophila*, ovulation serves the dual-purpose of moving the oocyte forward and stimulating meiotic resumption (Von Stetina & Orr-Weaver, 2011). A common feature between *Drosophila*, *C. elegans*, and the chicken is that the female (or hermaphrodite in *C. elegans*) has the ability to store sperm for an extended period of time for fertilization of individually ovulated oocytes in an assembly-line fashion. After a single mating event in flies, females store the sperm and can remain fertile for up to two weeks (Schnakenberg, Siegal, & Bloch Qazi, 2012). Female *Drosophila* directly regulate fertilization as she controls the release of sperm from her storage seminal receptacle. *C. elegans* are hermaphroditic and therefore make their own sperm, but they only make a finite amount during a short period of development which is then stored in the spermathecal. Chickens possess specialized sperm storage tubules in their oviduct where they can store sperm until needed for fertilization (Sasanami, Matsuzaki, Mizushima, & Hiyama, 2013).

The mechanisms by which viable sperm can be stored for an extended period of time is of great interest in other species where sperm storage would be financially beneficial, such as pigs.

A.7 Conclusion

This chapter summarizes the conserved and distinct features and the underlying mechanisms of four important stages of oogenesis and ovulation. In oogenesis, a critical feature of meiosis is the presence of primary and secondary meiotic arrests. While the primary meiotic arrest is conserved across species and organisms, *C. elegans* lack the secondary meiotic arrest. Intriguingly, in Drosophila the secondary meiotic arrest occurs in metaphase of meiosis I while in other organisms it takes place at metaphase of meiosis II (Figure A.1). Another important point of consideration while comparing oogenesis and ovulation across species and organisms are the various intra-cellular regulators involved at different stages of oogenesis and the conserved and distinct signaling pathways/underlying mechanisms, as shown in Table A1. Careful consideration of these patterns of conservation are critical when selecting the ideal animal model with the most similarity to humans for that particular process.

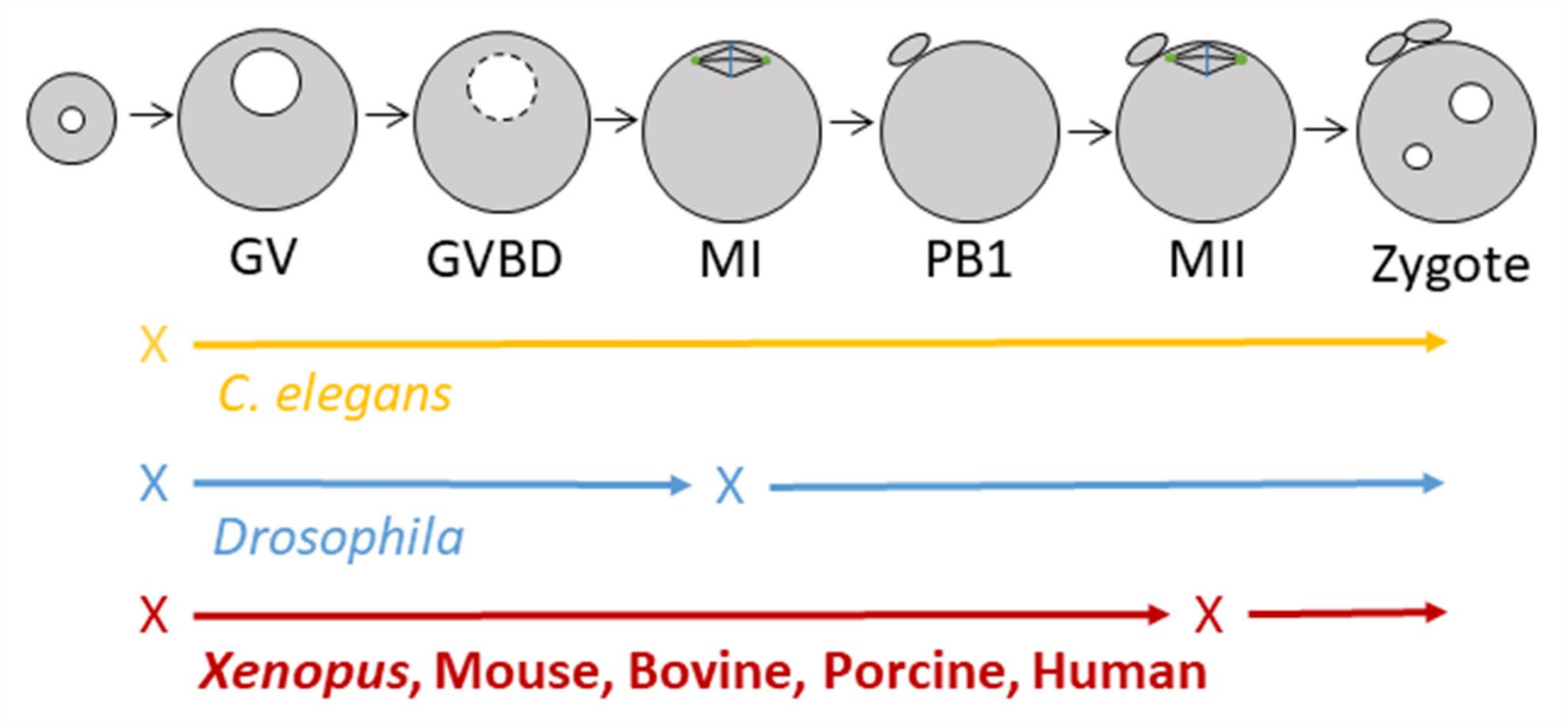

Figure A.1 Conserved primary and secondary meiotic arrests during meiosis. "X" represents points of meiotic arrest. The primary meiotic arrest is conserved across all organisms in this review. C. elegans does not have a secondary meiotic arrest. Drosophila has a unique secondary meiotic arrest that occurs at metaphase of meiosis I (MI). All other animals considered have a secondary meiotic arrest at metaphase of meiosis II (MII).

Table A.1 Summary of conserved processes and regulators of meiosis across species

<table>
<tr><th rowspan="2"></th><th rowspan="2">Primary Meiotic Arrest</th><th colspan="2">Meiotic</th><th rowspan="2">Secondary Meiotic Arrest</th><th colspan="2">Ovulation</th></tr>
<tr><th>Resumption</th><th>Maturation</th><th>Mono or Poly</th><th>Store Sperm</th></tr>
<tr><td>Human</td><td rowspan="8">Prophase I</td><td rowspan="6">LH</td><td rowspan="8">MPF</td><td rowspan="5">MII</td><td rowspan="2">Mono</td><td rowspan="2">No</td></tr>
<tr><td>Bovine</td></tr>
<tr><td>Chicken</td><td>Mono</td><td>Yes</td></tr>
<tr><td>Mouse</td><td rowspan="3">Poly</td><td rowspan="3">No</td></tr>
<tr><td>Porcine</td></tr>
<tr><td>Xenopus</td><td>Progesterone</td></tr>
<tr><td>Drosophila</td><td>Unknown</td><td>MI</td><td rowspan="2">Mono</td><td rowspan="2">Yes</td></tr>
<tr><td>C. elegans</td><td>MSP</td><td>None</td></tr>
</table>

REFERENCES

REFERENCES

Acosta-Jaquez, H. A., Keller, J. A., Foster, K. G., Ekim, B., Soliman, G. A., Feener, E. P., . . . Fingar, D. C. (2009). Site-specific mTOR phosphorylation promotes mTORC1-mediated signaling and cell growth. *Molecular and Cellular Biology, 29*(15), 4308-4324. doi:10.1128/MCB.01665-08

Adhikari, D., Zheng, W., Shen, Y., Gorre, N., Ning, Y., Halet, G., . . . Liu, K. (2012). Cdk1, but not Cdk2, is the sole Cdk that is essential and sufficient to drive resumption of meiosis in mouse oocytes. *Hum Mol Genet, 21*(11), 2476-2484. doi:10.1093/hmg/dds061

Ai, J. S., Wang, Q., Yin, S., Shi, L. H., Xiong, B., OuYang, Y. C., . . . Sun, Q. Y. (2008). Regulation of peripheral spindle movement and spindle rotation during mouse oocyte meiosis: new perspectives. *Microsc Microanal, 14*(4), 349-356. doi:10.1017/S1431927608080343

Almonacid, M., Terret, M. E., & Verlhac, M. H. (2014). Actin-based spindle positioning: new insights from female gametes. *J Cell Sci, 127*(Pt 3), 477-483. doi:10.1242/jcs.142711

Arur, S. (2017). Signaling-Mediated Regulation of Meiotic Prophase I and Transition During Oogenesis. *Results Probl Cell Differ, 59*, 101-123. doi:10.1007/978-3-319-44820-6_4

Ashrafi, G., & Schwarz, T. L. (2013). The pathways of mitophagy for quality control and clearance of mitochondria. *Cell Death Differ, 20*(1), 31-42. doi:10.1038/cdd.2012.81

Athale, C. A., Dinarina, A., Mora-Coral, M., Pugieux, C., Nedelec, F., & Karsenti, E. (2008). Regulation of microtubule dynamics by reaction cascades around chromosomes. *Science, 322*(5905), 1243-1247. doi:10.1126/science.1161820

Babayev, E., & Seli, E. (2015). Oocyte mitochondrial function and reproduction. *Curr Opin Obstet Gynecol, 27*(3), 175-181. doi:10.1097/GCO.0000000000000164

Balboula, A. Z., Stein, P., Schultz, R. M., & Schindler, K. (2014). Knockdown of RBBP7 unveils a requirement of histone deacetylation for CPC function in mouse oocytes. *Cell Cycle, 13*(4), 600-611. doi:10.4161/cc.27410

Baran, V., Solc, P., Kovarikova, V., Rehak, P., & Sutovsky, P. (2013). Polo-Like Kinase 1 Is Essential for the First Mitotic Division in the Mouse Embryo. *Molecular Reproduction and Development, 80*(7), 522-534. doi:10.1002/mrd.22188

Battaglia, D. E., Goodwin, P., Klein, N. A., & Soules, M. R. (1996). Influence of maternal age on meiotic spindle assembly in oocytes from naturally cycling women. *Human Reproduction, 11*(10), 2217-2222.

Battaglia, D. E., Klein, N. A., & Soules, M. R. (1996). Changes in centrosomal domains during meiotic maturation in the human oocyte. *Molecular Human Reproduction, 2*(11), 845-851.

Becalska, A. N., & Gavis, E. R. (2009). Lighting up mRNA localization in Drosophila oogenesis. *Development, 136*(15), 2493-2503. doi:10.1242/dev.032391

Bennabi, I., Terret, M. E., & Verlhac, M. H. (2016). Meiotic spindle assembly and chromosome segregation in oocytes. *Journal of Cell Biology, 215*(5), 611-619. doi:10.1083/jcb.201607062

Bettegowda, A., Patel, O. V., Lee, K. B., Park, K. E., Salem, M., Yao, J., . . . Smith, G. W. (2008). Identification of novel bovine cumulus cell molecular markers predictive of oocyte competence: functional and diagnostic implications. *Biol Reprod, 79*(2), 301-309. doi:10.1095/biolreprod.107.067223

Bilodeau-Goeseels, S. (2011). Cows are not mice: the role of cyclic AMP, phosphodiesterases, and adenosine monophosphate-activated protein kinase in the maintenance of meiotic arrest in bovine oocytes. *Molecular Reproduction and Development, 78*(10-11), 734-743. doi:10.1002/mrd.21337

Bilodeau, S., Fortier, M. A., & Sirard, M. A. (1993). Effect of adenylate cyclase stimulation on meiotic resumption and cyclic AMP content of zona-free and cumulus-enclosed bovine oocytes in vitro. *J Reprod Fertil, 97*(1), 5-11.

Bischoff, F. R., Klebe, C., Kretschmer, J., Wittinghofer, A., & Ponstingl, H. (1994). RanGAP1 induces GTPase activity of nuclear Ras-related Ran. *Proc Natl Acad Sci U S A, 91*(7), 2587-2591.

Bischoff, F. R., & Ponstingl, H. (1991). Catalysis of guanine nucleotide exchange on Ran by the mitotic regulator RCC1. *Nature, 354*(6348), 80-82. doi:10.1038/354080a0

Blower, M. D., Feric, E., Weis, K., & Heald, R. (2007). Genome-wide analysis demonstrates conserved localization of messenger RNAs to mitotic microtubules. *Journal of Cell Biology, 179*(7), 1365-1373. doi:10.1083/jcb.200705163

Bohrmann, J., & Zimmermann, J. (2008). Gap junctions in the ovary of Drosophila melanogaster: localization of innexins 1, 2, 3 and 4 and evidence for intercellular communication via innexin-2 containing channels. *BMC Dev Biol, 8*, 111. doi:10.1186/1471-213X-8-111

Bonner, M. K., Poole, D. S., Xu, T., Sarkeshik, A., Yates, J. R., 3rd, & Skop, A. R. (2011). Mitotic spindle proteomics in Chinese hamster ovary cells. *PLoS One, 6*(5), e20489. doi:10.1371/journal.pone.0020489

Bouniol-Baly, C., Hamraoui, L., Guibert, J., Beaujean, N., Szollosi, M. S., & Debey, P. (1999). Differential transcriptional activity associated with chromatin configuration in fully grown mouse germinal vesicle oocytes. *Biol Reprod, 60*(3), 580-587.

Cavazza, T., & Vernos, I. (2015). The RanGTP Pathway: From Nucleo-Cytoplasmic Transport to Spindle Assembly and Beyond. *Front Cell Dev Biol, 3*, 82. doi:10.3389/fcell.2015.00082

Chaigne, A., Campillo, C., Gov, N. S., Voituriez, R., Azoury, J., Umana-Diaz, C., . . . Terret, M. E. (2013). A soft cortex is essential for asymmetric spindle positioning in mouse oocytes. *Nat Cell Biol, 15*(8), 958-966. doi:10.1038/ncb2799

Chaigne, A., Campillo, C., Gov, N. S., Voituriez, R., Sykes, C., Verlhac, M. H., & Terret, M. E. (2015). A narrow window of cortical tension guides asymmetric spindle positioning in the mouse oocyte. *Nature Communications, 6*, 6027. doi:10.1038/ncomms7027

Cheng, Y., Gaughan, J., Midic, U., Han, Z., Liang, C. G., Patel, B. G., & Latham, K. E. (2013). Systems genetics implicates cytoskeletal genes in oocyte control of cloned embryo quality. *Genetics, 193*(3), 877-896. doi:10.1534/genetics.112.148866

Chiang, T., Duncan, F. E., Schindler, K., Schultz, R. M., & Lampson, M. A. (2010). Evidence that weakened centromere cohesion is a leading cause of age-related aneuploidy in oocytes. *Curr Biol, 20*(17), 1522-1528. doi:10.1016/j.cub.2010.06.069

Chu, Y., Yao, P. Y., Wang, W., Wang, D., Wang, Z., Zhang, L., . . . Yao, X. (2011). Aurora B kinase activation requires survivin priming phosphorylation by PLK1. *J Mol Cell Biol, 3*(4), 260-267. doi:10.1093/jmcb/mjq037

Ciemerych, M. A., Mesnard, D., & Zernicka-Goetz, M. (2000). Animal and vegetal poles of the mouse egg predict the polarity of the embryonic axis, yet are nonessential for development. *Development, 127*(16), 3467-3474.

Clark, B. F. C., GrunbergManago, M., Gupta, N. K., Hershey, J. W. B., Hinnebusch, A. G., Jackson, R. J., . . . Voorma, H. O. (1996). Prokaryotic and eukaryotic translation factors. *Biochimie, 78*(11-12), 1119-1122. doi:Doi 10.1016/S0300-9084(97)86738-7

Clift, D., & Schuh, M. (2015). A three-step MTOC fragmentation mechanism facilitates bipolar spindle assembly in mouse oocytes. *Nature Communications, 6*, 7217. doi:10.1038/ncomms8217

Cook, M. E. (2017). Sturkie's Avian PhysiologySturkie's Avian Physiology. 6th Ed. By Colin Scanes (editor). Elsevier Inc., Waltham, Massachusetts. 2015. 1056 pp. ISBN 978-0-12-0407160-5. US $120 hardback. *Journal of Wildlife Diseases, 53*(3), 703-705. doi:10.7589/0090-3558-53.3.703

Davis, D. B., Lavine, J. A., Suhonen, J. I., Krautkramer, K. A., Rabaglia, M. E., Sperger, J. M., . . . Attie, A. D. (2010). FoxM1 is up-regulated by obesity and stimulates beta-cell proliferation. *Mol Endocrinol, 24*(9), 1822-1834. doi:10.1210/me.2010-0082

Davydenko, O., Schultz, R. M., & Lampson, M. A. (2013). Increased CDK1 activity determines the timing of kinetochore-microtubule attachments in meiosis I. *Journal of Cell Biology, 202*(2), 221-229. doi:10.1083/jcb.201303019

De La Fuente, R., & Eppig, J. J. (2001). Transcriptional activity of the mouse oocyte genome: companion granulosa cells modulate transcription and chromatin remodeling. *Dev Biol, 229*(1), 224-236. doi:10.1006/dbio.2000.9947

De La Fuente, R., Viveiros, M. M., Burns, K. H., Adashi, E. Y., Matzuk, M. M., & Eppig, J. J. (2004). Major chromatin remodeling in the germinal vesicle (GV) of mammalian oocytes is dispensable for global transcriptional silencing but required for centromeric heterochromatin function. *Dev Biol, 275*(2), 447-458. doi:10.1016/j.ydbio.2004.08.028

Debey, P., Szollosi, M. S., Szollosi, D., Vautier, D., Girousse, A., & Besombes, D. (1993). Competent mouse oocytes isolated from antral follicles exhibit different chromatin organization and follow different maturation dynamics. *Molecular Reproduction and Development, 36*(1), 59-74. doi:10.1002/mrd.1080360110

Dekel, N. (1995). Molecular control of meiosis. *Trends Endocrinol Metab, 6*, 165-169.

Ding, Y., Kaido, M., Llano, E., Pendas, A. M., & Kitajima, T. S. (2018). The Post-anaphase SUMO Pathway Ensures the Maintenance of Centromeric Cohesion through Meiosis I-II Transition in Mammalian Oocytes. *Curr Biol, 28*(10), 1661-1669 e1664. doi:10.1016/j.cub.2018.04.019

Dragovic, R. A., Ritter, L. J., Schulz, S. J., Amato, F., Thompson, J. G., Armstrong, D. T., & Gilchrist, R. B. (2007). Oocyte-secreted factor activation of SMAD 2/3 signaling enables initiation of mouse cumulus cell expansion. *Biol Reprod, 76*(5), 848-857. doi:10.1095/biolreprod.106.057471

Du, J., Cao, Y., Wang, Q., Zhang, N., Liu, X., Chen, D., . . . Ma, W. (2015). Unique subcellular distribution of phosphorylated Plk1 (Ser137 and Thr210) in mouse oocytes during meiotic division and pPlk1(Ser137) involvement in spindle formation and REC8 cleavage. *Cell Cycle, 14*(22), 3566-3579. doi:10.1080/15384101.2015.1100770

Dumont, J., & Desai, A. (2012). Acentrosomal spindle assembly and chromosome segregation during oocyte meiosis. *Trends Cell Biol, 22*(5), 241-249. doi:10.1016/j.tcb.2012.02.007

Dumont, J., Petri, S., Pellegrin, F., Terret, M. E., Bohnsack, M. T., Rassinier, P., . . . Verlhac, M. H. (2007a). A centriole- and RanGTP-independent spindle assembly pathway in meiosis I of vertebrate oocytes. *Journal of Cell Biology, 176*(3), 295-305. doi:10.1083/jcb.200605199

Dumont, J., Petri, S., Pellegrin, F., Terret, M. E., Bohnsack, M. T., Rassinier, P., . . . Verlhac, M. H. (2007b). A centriole- and RanGTP-independent spindle assembly pathway in meiosis I of vertebrate oocytes. *Journal of Cell Biology, 176*(3), 295-305. doi:10.1083/jcb.200605199

Dumont, J. N. (1972). Oogenesis in Xenopus laevis (Daudin). I. Stages of oocyte development in laboratory maintained animals. *J Morphol, 136*(2), 153-179. doi:10.1002/jmor.1051360203

E. Orozco-Lucero, M.-A. S., M. A. (2014). Molecular markers of fertility in cattle oocytes and embryos: progress and challenges. *Animal Reproduction, 11*(3), 186-194.

Eisman, R., & Kaufman, T. C. (2007). Cytological investigation of the mechanism of parthenogenesis in Drosophila mercatorum. *Fly (Austin), 1*(6), 317-329.

Ellederova, Z., Kovarova, H., Melo-Sterza, F., Livingstone, M., Tomek, W., & Kubelka, M. (2006). Suppression of translation during in vitro maturation of pig oocytes despite enhanced formation of cap-binding protein complex eIF4F and 4E-BP1 hyperphosphorylation. *Molecular Reproduction and Development, 73*(1), 68-76. doi:10.1002/mrd.20368

Eppig, J. J., Viveiros, M., Bivens, C., & De La Fuente, R. (2004). Regulation of Mammalian Oocyte Maturation. . *Chapter 7. The Ovary. Second Edition. Editors: Peter C.K. Leung & Eli Y. Adashi.*, 113-129.

Eppig, J. J., Viverios, M. M., Marin Bivens, C. L. & De La Fuente, R. (2004). Regulation of mammalian oocyte maturation. *The Ovary*.

Fan, C. Y., Pan, J., Chu, R., Lee, D., Kluckman, K. D., Usuda, N., . . . Reddy, J. K. (1996). Hepatocellular and hepatic peroxisomal alterations in mice with a disrupted peroxisomal fatty acyl-coenzyme A oxidase gene. *J Biol Chem, 271*(40), 24698-24710.

Farrell, T., Neale, L., & Cundy, T. (2002). Congenital anomalies in the offspring of women with type 1, type 2 and gestational diabetes. *Diabet Med, 19*(4), 322-326.

Fattaey, A., & Booher, R. N. (1997). Myt1: a Wee1-type kinase that phosphorylates Cdc2 on residue Thr14. *Prog Cell Cycle Res, 3*, 233-240.

Feitosa, W. B., & Morris, P. L. (2018). Sumoylation Regulates Germinal Vesicle Break-down and the Akt/Pkb Pathway during Mouse Oocyte Maturation. *Am J Physiol Cell Physiol*. doi:10.1152/ajpcell.00038.2018

Fletcher, C. M., McGuire, A. M., Gingras, A. C., Li, H., Matsuo, H., Sonenberg, N., & Wagner, G. (1998). 4E binding proteins inhibit the translation factor eIF4E without folded structure. *Biochemistry, 37*(1), 9-15. doi:10.1021/bi972494r

Fonseca, B. D., Alain, T., Finestone, L. K., Huang, B. P., Rolfe, M., Jiang, T., . . . Proud, C. G. (2011). Pharmacological and genetic evaluation of proposed roles of mitogen-activated protein kinase/extracellular signal-regulated kinase kinase (MEK), extracellular signal-regulated kinase (ERK), and p90(RSK) in the control of mTORC1 protein signaling by phorbol esters. *J Biol Chem, 286*(31), 27111-27122. doi:10.1074/jbc.M111.260794

Franciosi, F., Manandhar, S., & Conti, M. (2016). FSH Regulates mRNA Translation in Mouse Oocytes and Promotes Developmental Competence. *Endocrinology, 157*(2), 872-882. doi:10.1210/en.2015-1727

Gao, S., Czirr, E., Chung, Y. G., Han, Z., & Latham, K. E. (2004). Genetic variation in oocyte phenotype revealed through parthenogenesis and cloning: correlation with differences in pronuclear epigenetic modification. *Biol Reprod, 70*(4), 1162-1170. doi:10.1095/biolreprod.103.024216

Gebauer, F., Xu, W., Cooper, G. M., & Richter, J. D. (1994). Translational control by cytoplasmic polyadenylation of c-mos mRNA is necessary for oocyte maturation in the mouse. *Embo Journal, 13*(23), 5712-5720.

Gill, A., Jamnongjit, M., & Hammes, S. R. (2004). Androgens promote maturation and signaling in mouse oocytes independent of transcription: a release of inhibition model for mammalian oocyte meiosis. *Mol Endocrinol, 18*(1), 97-104. doi:10.1210/me.2003-0326

Gingras, A. C., Gygi, S. P., Raught, B., Polakiewicz, R. D., Abraham, R. T., Hoekstra, M. F., . . . Sonenberg, N. (1999). Regulation of 4E-BP1 phosphorylation: a novel two-step mechanism. *Genes Dev, 13*(11), 1422-1437.

Gingras, A. C., Raught, B., Gygi, S. P., Niedzwiecka, A., Miron, M., Burley, S. K., . . . Sonenberg, N. (2001). Hierarchical phosphorylation of the translation inhibitor 4E-BP1. *Genes & Development, 15*(21), 2852-2864.

Gladding, C. M., Fan, J., Zhang, L. Y., Wang, L., Xu, J., Li, E. H., . . . Raymond, L. A. (2014). Alterations in STriatal-Enriched protein tyrosine Phosphatase expression, activation, and downstream signaling in early and late stages of the YAC128 Huntington's disease mouse model. *J Neurochem, 130*(1), 145-159. doi:10.1111/jnc.12700

Gordo, A. C., He, C. L., Smith, S., & Fissore, R. A. (2001). Mitogen activated protein kinase plays a significant role in metaphase II arrest, spindle morphology, and maintenance of maturation promoting factor activity in bovine oocytes. *Molecular Reproduction and Development, 59*(1), 106-114. doi:10.1002/mrd.1012

Govindan, J. A., Cheng, H., Harris, J. E., & Greenstein, D. (2006). Galphao/i and Galphas signaling function in parallel with the MSP/Eph receptor to control meiotic diapause in C. elegans. *Curr Biol, 16*(13), 1257-1268. doi:10.1016/j.cub.2006.05.020

Govindan, J. A., Nadarajan, S., Kim, S., Starich, T. A., & Greenstein, D. (2009). Somatic cAMP signaling regulates MSP-dependent oocyte growth and meiotic maturation in C. elegans. *Development, 136*(13), 2211-2221. doi:10.1242/dev.034595

Greene, M. F. (1999). Spontaneous abortions and major malformations in women with diabetes mellitus. *Semin Reprod Endocrinol, 17*(2), 127-136. doi:10.1055/s-2007-1016220

Groisman, I., Huang, Y. S., Mendez, R., Cao, Q. P., Theurkauf, W., & Richter, J. D. (2000). CPEB, maskin, and cyclin B1 mRNA at the mitotic apparatus: Implications for local translational control of cell division. *Cell, 103*(3), 435-447. doi:Doi 10.1016/S0092-8674(00)00135-5

Grondahl, M. L., Yding Andersen, C., Bogstad, J., Nielsen, F. C., Meinertz, H., & Borup, R. (2010). Gene expression profiles of single human mature oocytes in relation to age. *Human Reproduction, 25*(4), 957-968. doi:10.1093/humrep/deq014

Gruss, O. J., Carazo-Salas, R. E., Schatz, C. A., Guarguaglini, G., Kast, J., Wilm, M., . . . Mattaj, I. W. (2001). Ran induces spindle assembly by reversing the inhibitory effect of importin alpha on TPX2 activity. *Cell, 104*(1), 83-93.

Gu, L., Wang, Q., & Sun, Q. Y. (2010). Histone modifications during mammalian oocyte maturation: dynamics, regulation and functions. *Cell Cycle, 9*(10), 1942-1950. doi:10.4161/cc.9.10.11599

Guo, B., Tian, X. C., Li, D. D., Yang, Z. Q., Cao, H., Zhang, Q. L., . . . Yue, Z. P. (2014). Expression, regulation and function of Egr1 during implantation and decidualization in mice. *Cell Cycle, 13*(16), 2626-2640. doi:10.4161/15384101.2014.943581

Guo, L., Ou, X., Li, H., & Han, Z. (2014). Roles of sphingosine-1-phosphate in reproduction. *Reprod Sci, 21*(5), 550-554. doi:10.1177/1933719113512534

Hadi, T., Hammer, M. A., Algire, C., Richards, T., & Baltz, J. M. (2005). Similar effects of osmolarity, glucose, and phosphate on cleavage past the 2-cell stage in mouse embryos from outbred and F1 hybrid females. *Biol Reprod, 72*(1), 179-187. doi:10.1095/biolreprod.104.033324

Halet, G., & Carroll, J. (2007). Rac activity is polarized and regulates meiotic spindle stability and anchoring in mammalian oocytes. *Dev Cell, 12*(2), 309-317. doi:10.1016/j.devcel.2006.12.010

Hammes, S. R. (2004). Steroids and oocyte maturation--a new look at an old story. *Mol Endocrinol, 18*(4), 769-775. doi:10.1210/me.2003-0317

Han, S. J., Chen, R., Paronetto, M. P., & Conti, M. (2005). Wee1B is an oocyte-specific kinase involved in the control of meiotic arrest in the mouse. *Curr Biol, 15*(18), 1670-1676. doi:10.1016/j.cub.2005.07.056

Han, Z., Liang, C. G., Cheng, Y., Duan, X., Zhong, Z., Potireddy, S., . . . Latham, K. E. (2010). Oocyte spindle proteomics analysis leading to rescue of chromosome congression defects in cloned embryos. *J Proteome Res, 9*(11), 6025-6032. doi:10.1021/pr100827j

Hassold, T., Hall, H., & Hunt, P. (2007). The origin of human aneuploidy: where we have been, where we are going. *Hum Mol Genet, 16 Spec No. 2*, R203-208. doi:10.1093/hmg/ddm243

Hassold, T., & Hunt, P. (2001). To err (meiotically) is human: the genesis of human aneuploidy. *Nat Rev Genet, 2*(4), 280-291. doi:10.1038/35066065

Head, S. R., Komori, H. K., Hart, G. T., Shimashita, J., Schaffer, L., Salomon, D. R., & Ordoukhanian, P. T. (2011). Method for improved Illumina sequencing library preparation using NuGEN Ovation RNA-Seq System. *Biotechniques, 50*(3), 177-180. doi:10.2144/000113613

Heesom, K. J., Avison, M. B., Diggle, T. A., & Denton, R. M. (1998). Insulin-stimulated kinase from rat fat cells that phosphorylates initiation factor 4E-binding protein 1 on the rapamycin-insensitive site (serine-111). *Biochem J, 336 (Pt 1)*, 39-48.

Heesom, K. J., Gampel, A., Mellor, H., & Denton, R. M. (2001). Cell cycle-dependent phosphorylation of the translational repressor eIF-4E binding protein-1 (4E-BP1). *Curr Biol, 11*(17), 1374-1379.

Hellen, C. U., & Sarnow, P. (2001). Internal ribosome entry sites in eukaryotic mRNA molecules. *Genes Dev, 15*(13), 1593-1612. doi:10.1101/gad.891101

Ho, Y., Wigglesworth, K., Eppig, J. J., & Schultz, R. M. (1995). Preimplantation development of mouse embryos in KSOM: augmentation by amino acids and analysis of gene expression. *Molecular Reproduction and Development, 41*(2), 232-238. doi:10.1002/mrd.1080410214

Holubcova, Z., Blayney, M., Elder, K., & Schuh, M. (2015). Human oocytes. Error-prone chromosome-mediated spindle assembly favors chromosome segregation defects in human oocytes. *Science, 348*(6239), 1143-1147. doi:10.1126/science.aaa9529

Holzenspies, J. J., Roelen, B. A., Colenbrander, B., Romijn, R. A., Hemrika, W., Stoorvogel, W., & van Haeften, T. (2010). Clathrin is essential for meiotic spindle function in oocytes. *Reproduction, 140*(2), 223-233. doi:10.1530/REP-10-0045

Hong, A., Lee-Kong, S., Iida, T., Sugimura, I., & Lilly, M. A. (2003). The p27cip/kip ortholog dacapo maintains the Drosophila oocyte in prophase of meiosis I. *Development, 130*(7), 1235-1242.

Hughes, J. M. X., Ptushkina, M., Karim, M. M., Koloteva, N., von der Haar, T., & McCarthy, J. E. G. (1999). Translational Repression by Human 4E-BP1 in Yeast Specifically Requires Human eIF4E as Target. *Journal of Biological Chemistry, 274*(6), 3261-3264. doi:10.1074/jbc.274.6.3261

Hunt, P. A., & Hassold, T. J. (2008). Human female meiosis: what makes a good egg go bad? *Trends Genet, 24*(2), 86-93. doi:10.1016/j.tig.2007.11.010

Hunter, M. G., Robinson, R. S., Mann, G. E., & Webb, R. (2004). Endocrine and paracrine control of follicular development and ovulation rate in farm species. *Anim Reprod Sci, 82-83*, 461-477. doi:10.1016/j.anireprosci.2004.05.013

Inoue, K., Ogonuki, N., Mochida, K., Yamamoto, Y., Takano, K., Kohda, T., . . . Ogura, A. (2003). Effects of donor cell type and genotype on the efficiency of mouse somatic cell cloning. *Biol Reprod, 69*(4), 1394-1400. doi:10.1095/biolreprod.103.017731

Jaffe, L., Norris, R. (2010). Initiation of the meiotic prophase-to-metaphase transition in mammalian oocytes. *Oogenesis: The Universal Process*.

Jang, C. Y., Coppinger, J. A., Seki, A., Yates, J. R., 3rd, & Fang, G. (2009). Plk1 and Aurora A regulate the depolymerase activity and the cellular localization of Kif2a. *J Cell Sci, 122*(Pt 9), 1334-1341. doi:10.1242/jcs.044321

Jang, W. I., Lin, Z. L., Lee, S. H., Namgoong, S., & Kim, N. H. (2014). A specific inhibitor of CDK1, RO-3306, reversibly arrests meiosis during in vitro maturation of porcine oocytes. *Anim Reprod Sci, 144*(3-4), 102-108. doi:10.1016/j.anireprosci.2013.12.001

Jansova, D., Koncicka, M., Tetkova, A., Cerna, R., Malik, R., Del Llano, E., . . . Susor, A. (2017). Regulation of 4E-BP1 activity in the mammalian oocyte. *Cell Cycle, 16*(10), 927-939. doi:10.1080/15384101.2017.1295178

Jin, F., Hamada, M., Malureanu, L., Jeganathan, K. B., Zhou, W., Morbeck, D. E., & van Deursen, J. M. (2010). Cdc20 is critical for meiosis I and fertility of female mice. *PLoS Genet, 6*(9), e1001147. doi:10.1371/journal.pgen.1001147

John, G. B., Gallardo, T. D., Shirley, L. J., & Castrillon, D. H. (2008). Foxo3 is a PI3K-dependent molecular switch controlling the initiation of oocyte growth. *Dev Biol, 321*(1), 197-204. doi:10.1016/j.ydbio.2008.06.017

Jones, K. T. (2004). Turning it on and off: M-phase promoting factor during meiotic maturation and fertilization. *Mol. Hum. Reprod., 10*(1), 1-5. doi:10.1093/molehr/gah009

Jones, K. T. (2008). Meiosis in oocytes: predisposition to aneuploidy and its increased incidence with age. *Hum Reprod Update, 14*(2), 143-158. doi:10.1093/humupd/dmm043

Kalab, P., Solc, P., & Motlik, J. (2011). The role of RanGTP gradient in vertebrate oocyte maturation. *Results Probl Cell Differ, 53*, 235-267. doi:10.1007/978-3-642-19065-0_12

Kelly, A. E., Sampath, S. C., Maniar, T. A., Woo, E. M., Chait, B. T., & Funabiki, H. (2007). Chromosomal enrichment and activation of the aurora B pathway are coupled to spatially regulate spindle assembly. *Dev Cell, 12*(1), 31-43. doi:10.1016/j.devcel.2006.11.001

Kim, D., Langmead, B., & Salzberg, S. L. (2015). HISAT: a fast spliced aligner with low memory requirements. *Nat Methods, 12*(4), 357-360. doi:10.1038/nmeth.3317

Kim, H. J., Cho, J. H., & Kim, J. R. (2013). Downregulation of Polo-like kinase 1 induces cellular senescence in human primary cells through a p53-dependent pathway. *J Gerontol A Biol Sci Med Sci, 68*(10), 1145-1156. doi:10.1093/gerona/glt017

Kim, S., Spike, C., & Greenstein, D. (2013). Control of oocyte growth and meiotic maturation in Caenorhabditis elegans. *Adv Exp Med Biol, 757*, 277-320. doi:10.1007/978-1-4614-4015-4_10

Kogasaka, Y., Hoshino, Y., Hiradate, Y., Tanemura, K., & Sato, E. (2013). Distribution and association of mTOR with its cofactors, raptor and rictor, in cumulus cells and oocytes during meiotic maturation in mice. *Molecular Reproduction and Development, 80*(4), 334-348. doi:10.1002/mrd.22166

Larson, S. M., Lee, H. J., Hung, P. H., Matthews, L. M., Robinson, D. N., & Evans, J. P. (2010). Cortical mechanics and meiosis II completion in mammalian oocytes are mediated by myosin-II and Ezrin-Radixin-Moesin (ERM) proteins. *Mol Biol Cell, 21*(18), 3182-3192. doi:10.1091/mbc.E10-01-0066

Latham, K. E. (1994). Strain-specific differences in mouse oocytes and their contributions to epigenetic inheritance. *Development, 120*(12), 3419-3426.

Latham, K. E., Garrels, J. I., Chang, C., & Solter, D. (1991). Quantitative-Analysis of Protein-Synthesis in Mouse Embryos .1. Extensive Reprogramming at the One-Cell and 2-Cell Stages. *Development, 112*(4), 921-932.

Latham, K. E., Kutyna, K., & Wang, Q. (1999). Genetic variation in trophectoderm function in parthenogenetic mouse embryos. *Dev Genet, 24*(3-4), 329-335. doi:10.1002/(SICI)1520-6408(1999)24:3/4<329::AID-DVG16>3.0.CO;2-U

Latham, K. E., & Sapienza, C. (1998). Localization of genes encoding egg modifiers of paternal genome function to mouse chromosomes one and two. *Development, 125*(5), 929-935.

Latham, K. E., & Solter, D. (1991). Effect of egg composition on the developmental capacity of androgenetic mouse embryos. *Development, 113*(2), 561-568.

Lawitts, J. A., & Biggers, J. D. (1993). Culture of preimplantation embryos. *Methods Enzymol, 225*, 153-164.

Leader, B., Lim, H., Carabatsos, M. J., Harrington, A., Ecsedy, J., Pellman, D., . . . Leder, P. (2002). Formin-2, polyploidy, hypofertility and positioning of the meiotic spindle in mouse oocytes. *Nat Cell Biol, 4*(12), 921-928. doi:10.1038/ncb880

Leatherman, J. L., & Jongens, T. A. (2003). Transcriptional silencing and translational control: key features of early germline development. *Bioessays, 25*(4), 326-335. doi:10.1002/bies.10247

Lee, I. W., Jo, Y. J., Jung, S. M., Wang, H. Y., Kim, N. H., & Namgoong, S. (2018). Distinct roles of Cep192 and Cep152 in acentriolar MTOCs and spindle formation during mouse oocyte maturation. *Faseb Journal, 32*(2), 625-638. doi:10.1096/fj.201700559RR

Lee, K. S., Grenfell, T. Z., Yarm, F. R., & Erikson, R. L. (1998). Mutation of the polo-box disrupts localization and mitotic functions of the mammalian polo kinase Plk. *Proc Natl Acad Sci U S A, 95*(16), 9301-9306.

Lee, S. E., Sun, S. C., Choi, H. Y., Uhm, S. J., & Kim, N. H. (2012). mTOR is required for asymmetric division through small GTPases in mouse oocytes. *Molecular Reproduction and Development, 79*(5), 356-366. doi:10.1002/mrd.22035

Lee, Y. S., Latham, K. E., & Vandevoort, C. A. (2008). Effects of in vitro maturation on gene expression in rhesus monkey oocytes. *Physiol Genomics, 35*(2), 145-158. doi:10.1152/physiolgenomics.90281.2008

Lenart, P., Petronczki, M., Steegmaier, M., Di Fiore, B., Lipp, J. J., Hoffmann, M., . . . Peters, J. M. (2007). The small-molecule inhibitor BI 2536 reveals novel insights into mitotic roles of polo-like kinase 1. *Curr Biol, 17*(4), 304-315. doi:10.1016/j.cub.2006.12.046

Levesque, J. T., & Sirard, M. A. (1996). Resumption of meiosis is initiated by the accumulation of cyclin B in bovine oocytes. *Biol Reprod, 55*(6), 1427-1436.

Levitas, E., Chamoun, D., Udoff, L. C., Ando, M., Resnick, C. E., & Adashi, E. Y. (2000). Periovulatory and interleukin-1 beta-dependent up-regulation of intraovarian vascular endothelial growth factor (VEGF) in the rat: potential role for VEGF in the promotion of periovulatory angiogenesis and vascular permeability. *J Soc Gynecol Investig, 7*(1), 51-60.

Liao, Y., Smyth, G. K., & Shi, W. (2013). The Subread aligner: fast, accurate and scalable read mapping by seed-and-vote. *Nucleic Acids Res, 41*(10), e108. doi:10.1093/nar/gkt214

Lie Fong, S., Baart, E. B., Martini, E., Schipper, I., Visser, J. A., Themmen, A. P., . . . Laven, J. S. (2008). Anti-Mullerian hormone: a marker for oocyte quantity, oocyte quality and embryo quality? *Reprod Biomed Online, 16*(5), 664-670.

Lin, T., Kong, X., Haystead, T., Pause, A., Belsham, G., Sonenberg, N., & Lawrence, J. (1994). PHAS-I as a link between mitogen-activated protein kinase and translation initiation. *Science, 266*(5185), 653-656. doi:10.1126/science.7939721

Lin, T. A., Kong, X., Haystead, T. A., Pause, A., Belsham, G., Sonenberg, N., & Lawrence, J. C., Jr. (1994). PHAS-I as a link between mitogen-activated protein kinase and translation initiation. *Science, 266*(5185), 653-656.

Lin, Z. K., N. . (2015). Role of ataxia-telangiectasia mutated (ATM) in porcine oocyte in vitro maturation. *Cell Biology International, 39*, 710-720. doi:10.1002/cbin.10439

Longo, F. J., & Chen, D. Y. (1985). Development of cortical polarity in mouse eggs: involvement of the meiotic apparatus. *Dev Biol, 107*(2), 382-394.

Lopez-Cardona, A. P., Perez-Cerezales, S., Fernandez-Gonzalez, R., Laguna-Barraza, R., Pericuesta, E., Agirregoitia, N., . . . Agirregoitia, E. (2017). CB1 cannabinoid receptor drives oocyte maturation and embryo development via PI3K/Akt and MAPK pathways. *Faseb Journal, 31*(8), 3372-3382. doi:10.1096/fj.201601382RR

Lopez-Mateo, I., Villaronga, M. A., Llanos, S., & Belandia, B. (2012). The transcription factor CREBZF is a novel positive regulator of p53. *Cell Cycle, 11*(20), 3887-3895. doi:10.4161/cc.22133

Love, M. I., Huber, W., & Anders, S. (2014). Moderated estimation of fold change and dispersion for RNA-seq data with DESeq2. *Genome Biol, 15*(12), 550. doi:10.1186/s13059-014-0550-8

Lutz, L. B., Cole, L. M., Gupta, M. K., Kwist, K. W., Auchus, R. J., & Hammes, S. R. (2001). Evidence that androgens are the primary steroids produced by Xenopus laevis ovaries and may signal through the classical androgen receptor to promote oocyte maturation. *Proc Natl Acad Sci U S A, 98*(24), 13728-13733. doi:10.1073/pnas.241471598

Ma, D., Yu, H., Lin, D., Sun, Y., Liu, L., Liu, Y., . . . Cao, J. (2009). S6K1 is involved in polyploidization through its phosphorylation at Thr421/Ser424. *J Cell Physiol, 219*(1), 31-44. doi:10.1002/jcp.21647

Madgwick, S., & Jones, K. T. (2007). How eggs arrest at metaphase II: MPF stabilisation plus APC/C inhibition equals Cytostatic Factor. *Cell Div, 2*, 4. doi:10.1186/1747-1028-2-4

Maiorca, R., Cancarini, G. C., Brunori, G., Camerini, C., & Manili, L. (1993). Morbidity and mortality of CAPD and hemodialysis. *Kidney Int Suppl, 40*, S4-15.

Maller, J. L., Butcher, F. R., & Krebs, E. G. (1979). Early effect of progesterone on levels of cyclic adenosine 3':5'-monophosphate in Xenopus oocytes. *J Biol Chem, 254*(3), 579-582.

Manosalva, I., Gonzalez, A., & Kageyama, R. (2013). Hes1 in the somatic cells of the murine ovary is necessary for oocyte survival and maturation. *Dev Biol, 375*(2), 140-151. doi:10.1016/j.ydbio.2012.12.015

Marcotrigiano, J., Gingras, A. C., Sonenberg, N., & Burley, S. K. (1999). Cap-dependent translation initiation in eukaryotes is regulated by a molecular mimic of eIF4G. *Molecular Cell, 3*(6), 707-716.

Maro, B., & Verlhac, M. H. (2002). Polar body formation: new rules for asymmetric divisions. *Nat Cell Biol, 4*(12), E281-283. doi:10.1038/ncb1202-e281

Masui, Y. (1974). A cytostatic factor in amphibian oocytes: its extraction and partial characterization. *J Exp Zool, 187*(1), 141-147. doi:10.1002/jez.1401870116

Masui, Y., & Markert, C. L. (1971). Cytoplasmic control of nuclear behavior during meiotic maturation of frog oocytes. *J Exp Zool, 177*(2), 129-145. doi:10.1002/jez.1401770202

McCarter, J., Bartlett, B., Dang, T., & Schedl, T. (1999). On the control of oocyte meiotic maturation and ovulation in Caenorhabditis elegans. *Dev Biol, 205*(1), 111-128. doi:10.1006/dbio.1998.9109

Mehlmann, L. M. (2005). Stops and starts in mammalian oocytes: recent advances in understanding the regulation of meiotic arrest and oocyte maturation. *Reproduction, 130*(6), 791-799. doi:10.1530/rep.1.00793

Mehlmann, L. M. (2005). Stops and starts in mammalian oocytes: recent advances in understanding the regulation of meiotic arrest and oocyte maturation. *Reproduction, 130*(6), 791-799. doi:10.1530/rep.1.00793

Meng, J., Cui, C., Liu, Y., Jin, M., Wu, D., Liu, C., . . . Yu, B. (2013). The role of 14-3-3epsilon interaction with phosphorylated Cdc25B at its Ser321 in the release of the mouse oocyte from prophase I arrest. *PLoS One, 8*(1), e53633. doi:10.1371/journal.pone.0053633

Miller, M. A., Nguyen, V. Q., Lee, M. H., Kosinski, M., Schedl, T., Caprioli, R. M., & Greenstein, D. (2001). A sperm cytoskeletal protein that signals oocyte meiotic maturation and ovulation. *Science, 291*(5511), 2144-2147. doi:10.1126/science.1057586

Mira, A. (1998). Why is meiosis arrested? *J Theor Biol, 194*(2), 275-287. doi:10.1006/jtbi.1998.0761

Moerke, N. J., Aktas, H., Chen, H., Cantel, S., Reibarkh, M. Y., Fahmy, A., . . . Wagner, G. (2007). Small-molecule inhibition of the interaction between the translation initiation factors eIF4E and eIF4G. *Cell, 128*(2), 257-267. doi:10.1016/j.cell.2006.11.046

Molyneaux, K. A., Schaible, K., & Wylie, C. (2003). GP130, the shared receptor for the LIF/IL6 cytokine family in the mouse, is not required for early germ cell differentiation, but is required cell-autonomously in oocytes for ovulation. *Development, 130*(18), 4287-4294.

Moon, J. H., Hyun, C. S., Lee, S. W., Son, W. Y., Yoon, S. H., & Lim, J. H. (2003). Visualization of the metaphase II meiotic spindle in living human oocytes using the Polscope enables the prediction of embryonic developmental competence after ICSI. *Human Reproduction, 18*(4), 817-820.

Morrison, D. K. (2009). The 14-3-3 proteins: integrators of diverse signaling cues that impact cell fate and cancer development. *Trends Cell Biol, 19*(1), 16-23. doi:10.1016/j.tcb.2008.10.003

Mtango, N. R., Sutovsky, M., Vandevoort, C. A., Latham, K. E., & Sutovsky, P. (2012). Essential role of ubiquitin C-terminal hydrolases UCHL1 and UCHL3 in mammalian oocyte maturation. *J Cell Physiol, 227*(5), 2022-2029. doi:10.1002/jcp.22931

Mu, X. F., Jin, X. L., Farnham, M. M., Li, Y., & O'Neill, C. (2011). DNA damage-sensing kinases mediate the mouse 2-cell embryo's response to genotoxic stress. *Biol Reprod, 85*(3), 524-535. doi:10.1095/biolreprod.110.089334

Nachury, M. V., Maresca, T. J., Salmon, W. C., Waterman-Storer, C. M., Heald, R., & Weis, K. (2001). Importin beta is a mitotic target of the small GTPase Ran in spindle assembly. *Cell, 104*(1), 95-106.

Naito, K., Hawkins, C., Yamashita, M., Nagahama, Y., Aoki, F., Kohmoto, K., . . . Moor, R. M. (1995). Association of p34cdc2 and cyclin B1 during meiotic maturation in porcine oocytes. *Dev Biol, 168*(2), 627-634. doi:10.1006/dbio.1995.1107

Nakamura, Y., Kagami, H., & Tagami, T. (2013). Development, differentiation and manipulation of chicken germ cells. *Dev Growth Differ, 55*(1), 20-40. doi:10.1111/dgd.12026

Nakasato, M., Shirakura, Y., Ooga, M., Iwatsuki, M., Ito, M., Kageyama, S., . . . Aoki, F. (2006). Involvement of the STAT5 signaling pathway in the regulation of mouse preimplantation development. *Biol Reprod, 75*(4), 508-517. doi:10.1095/biolreprod.105.047860

Nishiyama, T., Tachibana, K., Kishimoto, T. (2010). Cytostatic arrest: post-ovulation arrest until fertilization in metazoan oocytes. *Oogenesis: The Universal Process*.

Page, A. W., & Orr-Weaver, T. L. (1997). Activation of the meiotic divisions in Drosophila oocytes. *Dev Biol, 183*(2), 195-207. doi:10.1006/dbio.1997.8506

Pahlavan, G., Polanski, Z., Kalab, P., Golsteyn, R., Nigg, E. A., & Maro, B. (2000). Characterization of polo-like kinase 1 during meiotic maturation of the mouse oocyte. *Dev Biol, 220*(2), 392-400. doi:10.1006/dbio.2000.9656

Palena, A., Mangiacasale, R., Magnano, A. R., Barberi, L., Giordano, R., Spadafora, C., & Lavia, P. (2000). E2F transcription factors are differentially expressed in murine gametes and early embryos. *Mech Dev, 97*(1-2), 211-215.

Parker, L. L., & Piwnica-Worms, H. (1992). Inactivation of the p34cdc2-cyclin B complex by the human WEE1 tyrosine kinase. *Science, 257*(5078), 1955-1957.

Patrizio, P., Fragouli, E., Bianchi, V., Borini, A., & Wells, D. (2007). Molecular methods for selection of the ideal oocyte. *Reprod Biomed Online, 15*(3), 346-353.

Pause, A., Belsham, G. J., Gingras, A. C., Donze, O., Lin, T. A., Lawrence, J. C., Jr., & Sonenberg, N. (1994a). Insulin-dependent stimulation of protein synthesis by phosphorylation of a regulator of 5'-cap function. *Nature, 371*(6500), 762-767. doi:10.1038/371762a0

Pause, A., Belsham, G. J., Gingras, A. C., Donze, O., Lin, T. A., Lawrence, J. C., & Sonenberg, N. (1994b). Insulin-Dependent Stimulation of Protein-Synthesis by Phosphorylation of a Regulator of 5'-Cap Function. *Nature, 371*(6500), 762-767. doi:DOI 10.1038/371762a0

Pause, A., Methot, N., Svitkin, Y., Merrick, W. C., & Sonenberg, N. (1994). Dominant negative mutants of mammalian translation initiation factor eIF-4A define a critical role for eIF-4F in cap-dependent and cap-independent initiation of translation. *Embo Journal, 13*(5), 1205-1215.

Paynton, B. V., & Bachvarova, R. (1994). Polyadenylation and deadenylation of maternal mRNAs during oocyte growth and maturation in the mouse. *Molecular Reproduction and Development, 37*(2), 172-180. doi:10.1002/mrd.1080370208

Paynton, B. V., Rempel, R., & Bachvarova, R. (1988). Changes in state of adenylation and time course of degradation of maternal mRNAs during oocyte maturation and early embryonic development in the mouse. *Dev Biol, 129*(2), 304-314.

Perkins, A. T., Das, T. M., Panzera, L. C., & Bickel, S. E. (2016). Oxidative stress in oocytes during midprophase induces premature loss of cohesion and chromosome segregation errors. *Proc Natl Acad Sci U S A, 113*(44), E6823-E6830. doi:10.1073/pnas.1612047113

Pfender, S., Kuznetsov, V., Pleiser, S., Kerkhoff, E., & Schuh, M. (2011). Spire-type actin nucleators cooperate with Formin-2 to drive asymmetric oocyte division. *Curr Biol, 21*(11), 955-960. doi:10.1016/j.cub.2011.04.029

Phillips, K. P., Petrunewich, M. A., Collins, J. L., Booth, R. A., Liu, X. J., & Baltz, J. M. (2002). Inhibition of MEK or cdc2 kinase parthenogenetically activates mouse eggs and yields the same phenotypes as Mos(-/-) parthenogenotes. *Dev Biol, 247*(1), 210-223. doi:10.1006/dbio.2002.0680

Pickering, S. J., Johnson, M. H., Braude, P. R., & Houliston, E. (1988). Cytoskeletal organization in fresh, aged and spontaneously activated human oocytes. *Human Reproduction, 3*(8), 978-989.

Pincus, G., & Enzmann, E. V. (1935). The Comparative Behavior of Mammalian Eggs in Vivo and in Vitro : I. The Activation of Ovarian Eggs. *J Exp Med, 62*(5), 665-675.

Pitetti, J. L., Torre, D., Conne, B., Papaioannou, M. D., Cederroth, C. R., Xuan, S., . . . Nef, S. (2009). Insulin receptor and IGF1R are not required for oocyte growth, differentiation, and maturation in mice. *Sex Dev, 3*(5), 264-272. doi:10.1159/000252813

Pomerantz, Y., Elbaz, J., Ben-Eliezer, I., Reizel, Y., David, Y., Galiani, D., . . . Dekel, N. (2012). From ubiquitin-proteasomal degradation to CDK1 inactivation: requirements for the first polar body extrusion in mouse oocytes. *Faseb Journal, 26*(11), 4495-4505. doi:10.1096/fj.12-209866

Potireddy, S., Amarnath, D., & Latham, K. E. (2013). Transcription, accumulation, storage, recruitment, and degradation of maternal mRNA in mammalian oocytes. *Biology and Pathology of the Oocyte: Role in Fertility, Medicine, and Nuclear Reprogramming, 2nd Edition*, 154-163. doi:Book_Doi 10.1017/Cbo9781139135030

Potireddy, S., Midic, U., Liang, C. G., Obradovic, Z., & Latham, K. E. (2010a). Positive and negative cis-regulatory elements directing postfertilization maternal mRNA translational control in mouse embryos. *Am J Physiol Cell Physiol, 299*(4), C818-827. doi:10.1152/ajpcell.00166.2010

Potireddy, S., Midic, U., Liang, C. G., Obradovic, Z., & Latham, K. E. (2010b). Positive and negative cis-regulatory elements directing postfertilization maternal mRNA translational control in mouse embryos. *American Journal of Physiology-Cell Physiology, 299*(4), C818-C827. doi:10.1152/ajpcell.00166.2010

Poueymirou, W. T., Conover, J. C., & Schultz, R. M. (1989). Regulation of mouse preimplantation development: differential effects of CZB medium and Whitten's medium on rates and patterns of protein synthesis in 2-cell embryos. *Biol Reprod, 41*(2), 317-322.

Prosser, S. L., & Pelletier, L. (2017). Mitotic spindle assembly in animal cells: a fine balancing act. *Nat Rev Mol Cell Biol, 18*(3), 187-201. doi:10.1038/nrm.2016.162

Rambhatla, L., & Latham, K. E. (1995). Strain-specific progression of alpha-amanitin-treated mouse embryos beyond the two-cell stage. *Molecular Reproduction and Development, 41*(1), 16-19. doi:10.1002/mrd.1080410104

Reik, W., Romer, I., Barton, S. C., Surani, M. A., Howlett, S. K., & Klose, J. (1993). Adult phenotype in the mouse can be affected by epigenetic events in the early embryo. *Development, 119*(3), 933-942.

Renner, A. G., Creancier, L., Dos Santos, C., Fialin, C., Recher, C., Bailly, C., . . . Manenti, S. (2010). A functional link between polo-like kinase 1 and the mammalian target-of-rapamycin pathway? *Cell Cycle, 9*(9), 1690-1696. doi:10.4161/cc.9.9.11295

Reyes, J. M., & Ross, P. J. (2016). Cytoplasmic polyadenylation in mammalian oocyte maturation. *Wiley Interdiscip Rev RNA, 7*(1), 71-89. doi:10.1002/wrna.1316

Reynolds, K. A., Boudoures, A. L., Chi, M. M., Wang, Q., & Moley, K. H. (2015). Adverse effects of obesity and/or high-fat diet on oocyte quality and metabolism are not reversible with resumption of regular diet in mice. *Reprod Fertil Dev, 27*(4), 716-724. doi:10.1071/RD14251

Romasko, E. J., Amarnath, D., Midic, U., & Latham, K. E. (2013). Association of maternal mRNA and phosphorylated EIF4EBP1 variants with the spindle in mouse oocytes: localized translational control supporting female meiosis in mammals. *Genetics, 195*(2), 349-358. doi:10.1534/genetics.113.154005

Ruchaud, S., Carmena, M., & Earnshaw, W. C. (2007). Chromosomal passengers: conducting cell division. *Nat Rev Mol Cell Biol, 8*(10), 798-812. doi:10.1038/nrm2257

Russell, D. L., & Robker, R. L. (2007). Molecular mechanisms of ovulation: co-ordination through the cumulus complex. *Human Reproduction Update, 13*(3), 289-312. doi:10.1093/humupd/dm1062

Sagata, N. (1998). Introduction: meiotic maturation and arrest in animal oocytes. *Semin Cell Dev Biol, 9*(5), 535-537. doi:10.1006/scdb.1998.0247

Sampath, S. C., Ohi, R., Leismann, O., Salic, A., Pozniakovski, A., & Funabiki, H. (2004). The chromosomal passenger complex is required for chromatin-induced microtubule stabilization and spindle assembly. *Cell, 118*(2), 187-202. doi:10.1016/j.cell.2004.06.026

Santoro, S. W., & Dulac, C. (2015). Histone variants and cellular plasticity. *Trends Genet, 31*(9), 516-527. doi:10.1016/j.tig.2015.07.005

Sasanami, T., Matsuzaki, M., Mizushima, S., & Hiyama, G. (2013). Sperm storage in the female reproductive tract in birds. *J Reprod Dev, 59*(4), 334-338.

Saskova, A., Solc, P., Baran, V., Kubelka, M., Schultz, R. M., & Motlik, J. (2008). Aurora kinase A controls meiosis I progression in mouse oocytes. *Cell Cycle, 7*(15), 2368-2376. doi:10.4161/cc.6361

Sauer, G., Korner, R., Hanisch, A., Ries, A., Nigg, E. A., & Sillje, H. H. (2005). Proteome analysis of the human mitotic spindle. *Molecular & Cellular Proteomics, 4*(1), 35-43. doi:10.1074/mcp.M400158-MCP200

Schmidt, A., Duncan, P. I., Rauh, N. R., Sauer, G., Fry, A. M., Nigg, E. A., & Mayer, T. U. (2005). Xenopus polo-like kinase Plx1 regulates XErp1, a novel inhibitor of APC/C activity. *Genes Dev, 19*(4), 502-513. doi:10.1101/gad.320705

Schnakenberg, S. L., Siegal, M. L., & Bloch Qazi, M. C. (2012). Oh, the places they'll go: Female sperm storage and sperm precedence in Drosophila melanogaster. *Spermatogenesis, 2*(3), 224-235. doi:10.4161/spmg.21655

Schneider, C. A., Rasband, W. S., & Eliceiri, K. W. (2012). NIH Image to ImageJ: 25 years of image analysis. *Nat Methods, 9*(7), 671-675.

Schuh, M., & Ellenberg, J. (2007). Self-organization of MTOCs replaces centrosome function during acentrosomal spindle assembly in live mouse oocytes. *Cell, 130*(3), 484-498. doi:10.1016/j.cell.2007.06.025

Schuh, M., & Ellenberg, J. (2008). A new model for asymmetric spindle positioning in mouse oocytes. *Curr Biol, 18*(24), 1986-1992. doi:10.1016/j.cub.2008.11.022

Schultz, R. M., Lamarca, M. J., & Wassarman, P. M. (1978a). Absolute Rates of Protein-Synthesis during Meiotic Maturation of Mammalian Oocytes Invitro. *Proceedings of the National Academy of Sciences of the United States of America, 75*(9), 4160-4164. doi:DOI 10.1073/pnas.75.9.4160

Schultz, R. M., LaMarca, M. J., & Wassarman, P. M. (1978b). Absolute rates of protein synthesis during meiotic maturation of mammalian oocytes in vitro. *Proceedings of the National Academy of Sciences, 75*(9), 4160-4164. doi:10.1073/pnas.75.9.4160

Schwab, M. S., Kim, S. H., Terada, N., Edfjall, C., Kozma, S. C., Thomas, G., & Maller, J. L. (1999). p70(S6K) controls selective mRNA translation during oocyte maturation and early embryogenesis in Xenopus laevis. *Molecular and Cellular Biology, 19*(4), 2485-2494.

Seibel, M. M., Smith, D. M., Levesque, L., Borten, M., & Taymor, M. L. (1982). The temporal relationship between the luteinizing hormone surge and human oocyte maturation. *Am J Obstet Gynecol, 142*(5), 568-572.

Seki, A., Coppinger, J. A., Jang, C. Y., Yates, J. R., & Fang, G. (2008). Bora and the kinase Aurora a cooperatively activate the kinase Plk1 and control mitotic entry. *Science, 320*(5883), 1655-1658. doi:10.1126/science.1157425

Severance, A. L., & Latham, K. E. (2017). PLK1 regulates spindle association of phosphorylated eukaryotic translation initiation factor 4E binding protein, and spindle function in mouse oocytes. *Am J Physiol Cell Physiol*, ajpcell 00075 02017. doi:10.1152/ajpcell.00075.2017

Severson, A. F., von Dassow, G., & Bowerman, B. (2016). Oocyte Meiotic Spindle Assembly and Function. *Curr Top Dev Biol, 116*, 65-98. doi:10.1016/bs.ctdb.2015.11.031

Sha, Q. Q., Dai, X. X., Dang, Y., Tang, F., Liu, J., Zhang, Y. L., & Fan, H. Y. (2017). A MAPK cascade couples maternal mRNA translation and degradation to meiotic cell cycle progression in mouse oocytes. *Development, 144*(3), 452-463. doi:10.1242/dev.144410

Shang, Z. F., Yu, L., Li, B., Tu, W. Z., Wang, Y., Liu, X. D., . . . Zhou, P. K. (2012). 4E-BP1 participates in maintaining spindle integrity and genomic stability via interacting with PLK1. *Cell Cycle, 11*(18), 3463-3471. doi:10.4161/cc.21770

Shimada, M. (2012). Regulation of oocyte meiotic maturation by somatic cells. *Reprod Med Biol, 11*, 177-184.

Shimaoka, T., Nishimura, T., Kano, K., & Naito, K. (2009). Critical effect of pigWee1B on the regulation of meiotic resumption in porcine immature oocytes. *Cell Cycle, 8*(15), 2375-2384. doi:10.4161/cc.8.15.9073

Shinagawa, T., Takagi, T., Tsukamoto, D., Tomaru, C., Huynh, L. M., Sivaraman, P., . . . Ishii, S. (2014). Histone variants enriched in oocytes enhance reprogramming to induced pluripotent stem cells. *Cell Stem Cell, 14*(2), 217-227. doi:10.1016/j.stem.2013.12.015

Shirakawa, J., Fernandez, M., Takatani, T., El Ouaamari, A., Jungtrakoon, P., Okawa, E. R., . . . Kulkarni, R. N. (2017). Insulin Signaling Regulates the FoxM1/PLK1/CENP-A Pathway to Promote Adaptive Pancreatic beta Cell Proliferation. *Cell Metab, 25*(4), 868-882 e865. doi:10.1016/j.cmet.2017.02.004

Shuda, K., Schindler, K., Ma, J., Schultz, R. M., & Donovan, P. J. (2009). Aurora kinase B modulates chromosome alignment in mouse oocytes. *Molecular Reproduction and Development, 76*(11), 1094-1105. doi:10.1002/mrd.21075

Shuda, M., Velasquez, C., Cheng, E., Cordek, D. G., Kwun, H. J., Chang, Y., & Moore, P. S. (2015). CDK1 substitutes for mTOR kinase to activate mitotic cap-dependent protein translation. *Proc Natl Acad Sci U S A, 112*(19), 5875-5882. doi:10.1073/pnas.1505787112

Shulman, J. M., Benton, R., & St Johnston, D. (2000). The Drosophila homolog of C. elegans PAR-1 organizes the oocyte cytoskeleton and directs oskar mRNA localization to the posterior pole. *Cell, 101*(4), 377-388.

Si, H., Verma, S. C., Lampson, M. A., Cai, Q., & Robertson, E. S. (2008). Kaposi's sarcoma-associated herpesvirus-encoded LANA can interact with the nuclear mitotic apparatus protein to regulate genome maintenance and segregation. *J Virol, 82*(13), 6734-6746. doi:10.1128/JVI.00342-08

Skene, P. J., & Henikoff, S. (2013). Histone variants in pluripotency and disease. *Development, 140*(12), 2513-2524. doi:10.1242/dev.091439

Solc, P., Kitajima, T. S., Yoshida, S., Brzakova, A., Kaido, M., Baran, V., . . . Ellenberg, J. (2015a). Multiple requirements of PLK1 during mouse oocyte maturation. *PLoS One, 10*(2), e0116783. doi:10.1371/journal.pone.0116783

Solc, P., Kitajima, T. S., Yoshida, S., Brzakova, A., Kaido, M., Baran, V., . . . Ellenberg, J. (2015b). Multiple Requirements of PLK1 during Mouse Oocyte Maturation. *Plos One, 10*(2). doi:ARTN e0116783 10.1371/journal.pone.0116783

Sousa Martins, J. P., Liu, X., Oke, A., Arora, R., Franciosi, F., Viville, S., . . . Conti, M. (2016). DAZL and CPEB1 regulate mRNA translation synergistically during oocyte maturation. *J Cell Sci, 129*(6), 1271-1282. doi:10.1242/jcs.179218

Stebbins-Boaz, B., Hake, L. E., & Richter, J. D. (1996). CPEB controls the cytoplasmic polyadenylation of cyclin, Cdk2 and c-mos mRNAs and is necessary for oocyte maturation in Xenopus. *Embo Journal, 15*(10), 2582-2592.

Sukarieh, R., Sonenberg, N., & Pelletier, J. (2009). The eIF4E-binding proteins are modifiers of cytoplasmic eIF4E relocalization during the heat shock response. *Am J Physiol Cell Physiol, 296*(5), C1207-1217. doi:10.1152/ajpcell.00511.2008

Sumara, I., Gimenez-Abian, J. F., Gerlich, D., Hirota, T., Kraft, C., de la Torre, C., . . . Peters, J. M. (2004). Roles of polo-like kinase 1 in the assembly of functional mitotic spindles. *Curr Biol, 14*(19), 1712-1722. doi:10.1016/j.cub.2004.09.049

Sun, J., & Spradling, A. C. (2013). Ovulation in Drosophila is controlled by secretory cells of the female reproductive tract. *Elife, 2*, e00415. doi:10.7554/eLife.00415

Sun, Q. Y., Blumenfeld, Z., Rubinstein, S., Goldman, S., Gonen, Y., & Breitbart, H. (1999). Mitogen-activated protein kinase in human eggs. *Zygote, 7*(2), 181-185.

Susor, A., Jansova, D., Cerna, R., Danylevska, A., Anger, M., Toralova, T., . . . Kubelka, M. (2015a). Temporal and spatial regulation of translation in the mammalian oocyte via the mTOR-eIF4F pathway. *Nature Communications, 6*, 6078. doi:10.1038/ncomms7078

Susor, A., Jansova, D., Cerna, R., Danylevska, A., Anger, M., Toralova, T., . . . Kubelka, M. (2015b). Temporal and spatial regulation of translation in the mammalian oocyte via the mTOR-eIF4F pathway. *Nature Communications, 6*. doi:ARTN 6078 10.1038/ncomms7078

Takano, A., Usui, I., Haruta, T., Kawahara, J., Uno, T., Iwata, M., & Kobayashi, M. (2001). Mammalian target of rapamycin pathway regulates insulin signaling via subcellular redistribution of insulin

receptor substrate 1 and integrates nutritional signals and metabolic signals of insulin. *Molecular and Cellular Biology, 21*(15), 5050-5062. doi:10.1128/MCB.21.15.5050-5062.2001

Tanenbaum, M. E., & Medema, R. H. (2010). Mechanisms of centrosome separation and bipolar spindle assembly. *Dev Cell, 19*(6), 797-806. doi:10.1016/j.devcel.2010.11.011

Tatemoto, H., & Muto, N. (2001). Mitogen-activated protein kinase regulates normal transition from metaphase to interphase following parthenogenetic activation in porcine oocytes. *Zygote, 9*(1), 15-23.

Templeman, N. M., Luo, S., Kaletsky, R., Shi, C., Ashraf, J., Keyes, W., & Murphy, C. T. (2018). Insulin Signaling Regulates Oocyte Quality Maintenance with Age via Cathepsin B Activity. *Curr Biol, 28*(5), 753-760 e754. doi:10.1016/j.cub.2018.01.052

Thoreen, C. C., Kang, S. A., Chang, J. W., Liu, Q., Zhang, J., Gao, Y., . . . Gray, N. S. (2009). An ATP-competitive mammalian target of rapamycin inhibitor reveals rapamycin-resistant functions of mTORC1. *J Biol Chem, 284*(12), 8023-8032. doi:10.1074/jbc.M900301200

Till, A., Saito, R., Merkurjev, D., Liu, J. J., Syed, G. H., Kolnik, M., . . . Subramani, S. (2015). Evolutionary trends and functional anatomy of the human expanded autophagy network. *Autophagy, 11*(9), 1652-1667. doi:10.1080/15548627.2015.1059558

Tomek, W., Melo Sterza, F. A., Kubelka, M., Wollenhaupt, K., Torner, H., Anger, M., & Kanitz, W. (2002). Regulation of translation during in vitro maturation of bovine oocytes: the role of MAP kinase, eIF4E (cap binding protein) phosphorylation, and eIF4E-BP1. *Biol Reprod, 66*(5), 1274-1282.

Tong, C., Fan, H. Y., Lian, L., Li, S. W., Chen, D. Y., Schatten, H., & Sun, Q. Y. (2002). Polo-like kinase-1 is a pivotal regulator of microtubule assembly during mouse oocyte meiotic maturation, fertilization, and early embryonic mitosis. *Biol Reprod, 67*(2), 546-554.

Tyrode, M. V. (1910). The mode of action of some purgative salts. *Archives Internationales De Pharmacodynamie Et De Therapie, 20*, 205-223.

van Vugt, M. A., & Medema, R. H. (2005). Getting in and out of mitosis with Polo-like kinase-1. *Oncogene, 24*(17), 2844-2859. doi:10.1038/sj.onc.1208617

Verlhac, M. H., Lefebvre, C., Guillaud, P., Rassinier, P., & Maro, B. (2000). Asymmetric division in mouse oocytes: with or without Mos. *Curr Biol, 10*(20), 1303-1306.

Von Stetina, J. R., & Orr-Weaver, T. L. (2011). Developmental control of oocyte maturation and egg activation in metazoan models. *Cold Spring Harb Perspect Biol, 3*(10), a005553. doi:10.1101/cshperspect.a005553

Von Stetina, J. R., Tranguch, S., Dey, S. K., Lee, L. A., Cha, B., & Drummond-Barbosa, D. (2008). alpha-Endosulfine is a conserved protein required for oocyte meiotic maturation in Drosophila. *Development, 135*(22), 3697-3706. doi:10.1242/dev.025114

Wakayama, T., & Yanagimachi, R. (2001). Mouse cloning with nucleus donor cells of different age and type. *Molecular Reproduction and Development, 58*(4), 376-383. doi:10.1002/1098-2795(20010401)58:4<376::AID-MRD4>3.0.CO;2-L

Walczak, C. E., & Heald, R. (2008). Mechanisms of mitotic spindle assembly and function. *Int Rev Cytol, 265*, 111-158. doi:10.1016/S0074-7696(07)65003-7

Wang, H., Luo, Y., Lin, Z., Lee, I. W., Kwon, J., Cui, X. S., & Kim, N. H. (2015). Effect of ATM and HDAC Inhibition on Etoposide-Induced DNA Damage in Porcine Early Preimplantation Embryos. *PLoS One, 10*(11), e0142561. doi:10.1371/journal.pone.0142561

Wang, L., Guo, Q., Fisher, L. A., Liu, D., & Peng, A. (2015). Regulation of polo-like kinase 1 by DNA damage and PP2A/B55alpha. *Cell Cycle, 14*(1), 157-166. doi:10.4161/15384101.2014.986392

Wang, Q., Ratchford, A. M., Chi, M. M., Schoeller, E., Frolova, A., Schedl, T., & Moley, K. H. (2009). Maternal diabetes causes mitochondrial dysfunction and meiotic defects in murine oocytes. *Mol Endocrinol, 23*(10), 1603-1612. doi:10.1210/me.2009-0033

Wang, Q., & Sun, Q. Y. (2007). Evaluation of oocyte quality: morphological, cellular and molecular predictors. *Reprod Fertil Dev, 19*(1), 1-12.

Wang, X., Li, W., Parra, J. L., Beugnet, A., & Proud, C. G. (2003). The C terminus of initiation factor 4E-binding protein 1 contains multiple regulatory features that influence its function and phosphorylation. *Mol Cell Biol, 23*(5), 1546-1557.

Weaver, L. N., & Walczak, C. E. (2015). Spatial gradients controlling spindle assembly. *Biochem Soc Trans, 43*(1), 7-12. doi:10.1042/BST20140243

Wen, D., Banaszynski, L. A., Liu, Y., Geng, F., Noh, K. M., Xiang, J., . . . Rafii, S. (2014). Histone variant H3.3 is an essential maternal factor for oocyte reprogramming. *Proc Natl Acad Sci U S A, 111*(20), 7325-7330. doi:10.1073/pnas.1406389111

Wiese, C., Wilde, A., Moore, M. S., Adam, S. A., Merdes, A., & Zheng, Y. (2001). Role of importin-beta in coupling Ran to downstream targets in microtubule assembly. *Science, 291*(5504), 653-656.

Xu, Y., Ashley, T., Brainerd, E. E., Bronson, R. T., Meyn, M. S., & Baltimore, D. (1996). Targeted disruption of ATM leads to growth retardation, chromosomal fragmentation during meiosis, immune defects, and thymic lymphoma. *Genes Dev, 10*(19), 2411-2422.

Yalu, R., Oyesiji, A. E., Eisenberg, I., Imbar, T., & Meidan, R. (2015). HIF1A-dependent increase in endothelin 2 levels in granulosa cells: role of hypoxia, LH/cAMP, and reactive oxygen species. *Reproduction, 149*(1), 11-20. doi:10.1530/REP-14-0409

Yamamoto, A., Mizushima, N., & Tsukamoto, S. (2014). Fertilization-induced autophagy in mouse embryos is independent of mTORC1. *Biol Reprod, 91*(1), 7. doi:10.1095/biolreprod.113.115816

Yamamoto, I., Kosinski, M. E., & Greenstein, D. (2006). Start me up: cell signaling and the journey from oocyte to embryo in C. elegans. *Dev Dyn, 235*(3), 571-585. doi:10.1002/dvdy.20662

Yang, D. Q., & Kastan, M. B. (2000). Participation of ATM in insulin signalling through phosphorylation of eIF-4E-binding protein 1. *Nat Cell Biol, 2*(12), 893-898. doi:10.1038/35046542

Yang, P., Wu, W., & Macfarlan, T. S. (2015). Maternal histone variants and their chaperones promote paternal genome activation and boost somatic cell reprogramming. *Bioessays, 37*(1), 52-59. doi:10.1002/bies.201400072

Yang, Y. F., Han, S. M., & Miller, M. A. (2010). MSP hormonal control of the oocyte MAP kinase cascade and reactive oxygen species signaling. *Developmental Biology, 342*(1), 96-107. doi:10.1016/j.ydbio.2010.03.026

Yi, K., Rubinstein, B., Unruh, J. R., Guo, F., Slaughter, B. D., & Li, R. (2013). Sequential actin-based pushing forces drive meiosis I chromosome migration and symmetry breaking in oocytes. *Journal of Cell Biology, 200*(5), 567-576. doi:10.1083/jcb.201211068

Yi, K., Unruh, J. R., Deng, M., Slaughter, B. D., Rubinstein, B., & Li, R. (2011). Dynamic maintenance of asymmetric meiotic spindle position through Arp2/3-complex-driven cytoplasmic streaming in mouse oocytes. *Nat Cell Biol, 13*(10), 1252-1258. doi:10.1038/ncb2320

Yokoo, M., Shimizu, T., Kimura, N., Tunjung, W. A., Matsumoto, H., Abe, H., . . . Sato, E. (2007). Role of the hyaluronan receptor CD44 during porcine oocyte maturation. *J Reprod Dev, 53*(2), 263-270.

Yoon, M. S. (2017). The Role of Mammalian Target of Rapamycin (mTOR) in Insulin Signaling. *Nutrients, 9*(11). doi:10.3390/nu9111176

Yu, C., Ji, S. Y., Dang, Y. J., Sha, Q. Q., Yuan, Y. F., Zhou, J. J., . . . Fan, H. Y. (2016). Oocyte-expressed yes-associated protein is a key activator of the early zygotic genome in mouse. *Cell Res, 26*(3), 275-287. doi:10.1038/cr.2016.20

Yuan, J., Li, M., Wei, L., Yin, S., Xiong, B., Li, S., . . . Sun, Q. Y. (2009). Astrin regulates meiotic spindle organization, spindle pole tethering and cell cycle progression in mouse oocytes. *Cell Cycle, 8*(20), 3384-3395. doi:10.4161/cc.8.20.9885

Zhang, L., Han, L., Ma, R., Hou, X., Yu, Y., Sun, S., . . . Wang, Q. (2015). Sirt3 prevents maternal obesity-associated oxidative stress and meiotic defects in mouse oocytes. *Cell Cycle, 14*(18), 2959-2968. doi:10.1080/15384101.2015.1026517

Zhang, R. N., Pang, B., Xu, S. R., Wan, P. C., Guo, S. C., Ji, H. Z., . . . Yang, Q. E. (2018). The CXCL12-CXCR4 signaling promotes oocyte maturation by regulating cumulus expansion in sheep. *Theriogenology, 107*, 85-94. doi:10.1016/j.theriogenology.2017.10.039

Zhang, X. Q., Jafari, N., Barnes, R. B., Confino, E., Milad, M., & Kazer, R. R. (2005). Studies of gene expression in human cumulus cells indicate pentraxin 3 as a possible marker for oocyte quality. *Fertility and Sterility, 83*, 1169-1179. doi:10.1016/j.fertnstert.2004.11.030

Zhong, Z. S., Huo, L. J., Liang, C. G., Chen, D. Y., & Sun, Q. Y. (2005). Small GTPase RhoA is required for ooplasmic segregation and spindle rotation, but not for spindle organization and chromosome separation during mouse oocyte maturation, fertilization, and early cleavage. *Molecular Reproduction and Development, 71*(2), 256-261. doi:10.1002/mrd.20253

Zhou, Y., & King, M. L. (2004). Sending RNAs into the future: RNA localization and germ cell fate. *Iubmb Life, 56*(1), 19-27. doi:10.1080/15216540310001658886

Zhu, Z. Y., Chen, D. Y., Li, J. S., Lian, L., Lei, L., Han, Z. M., & Sun, Q. Y. (2003). Rotation of meiotic spindle is controlled by microfilaments in mouse oocytes. *Biol Reprod, 68*(3), 943-946.